

The electron-ion collider

Charlotte Van Hulse
University of Alcalá

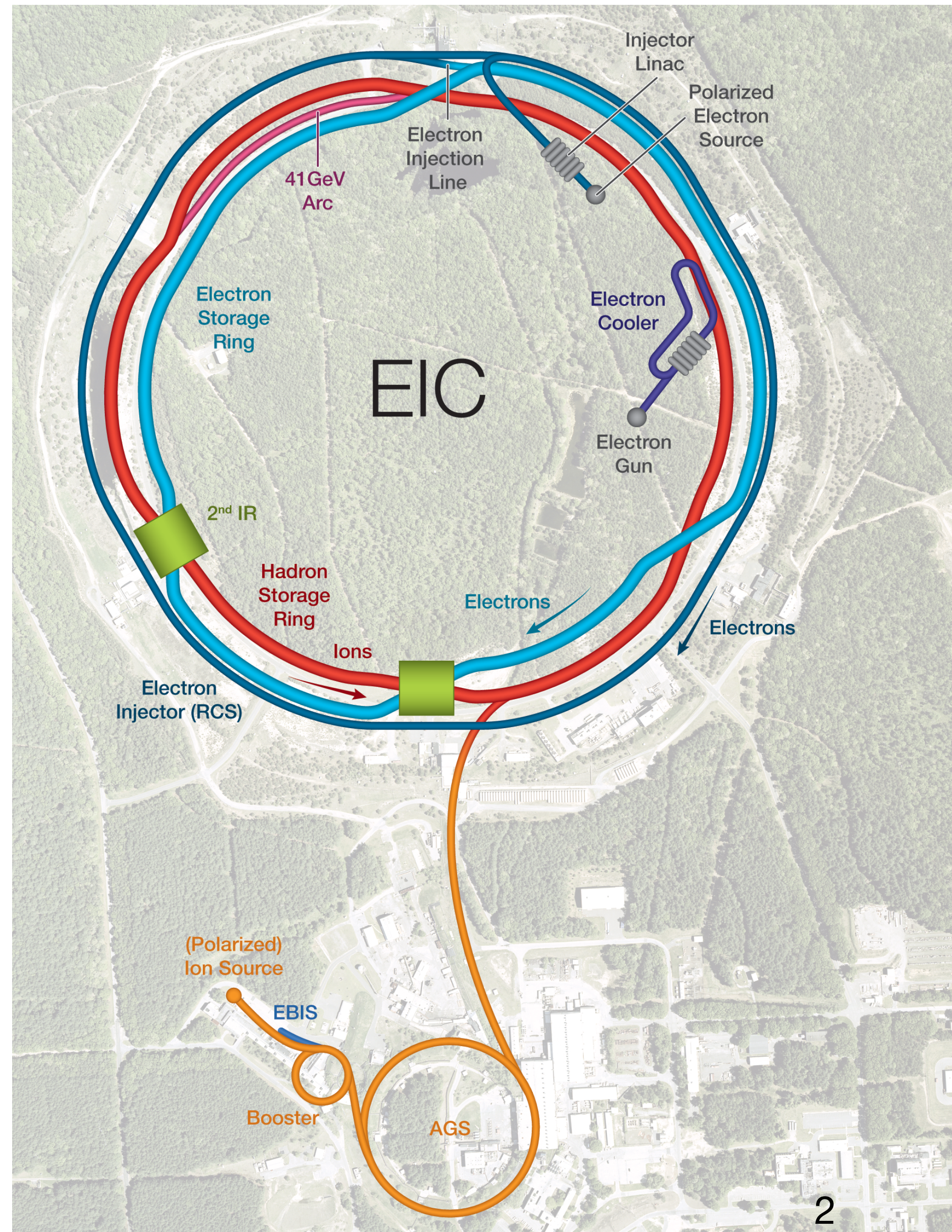
AdT



**Comunidad
de Madrid**

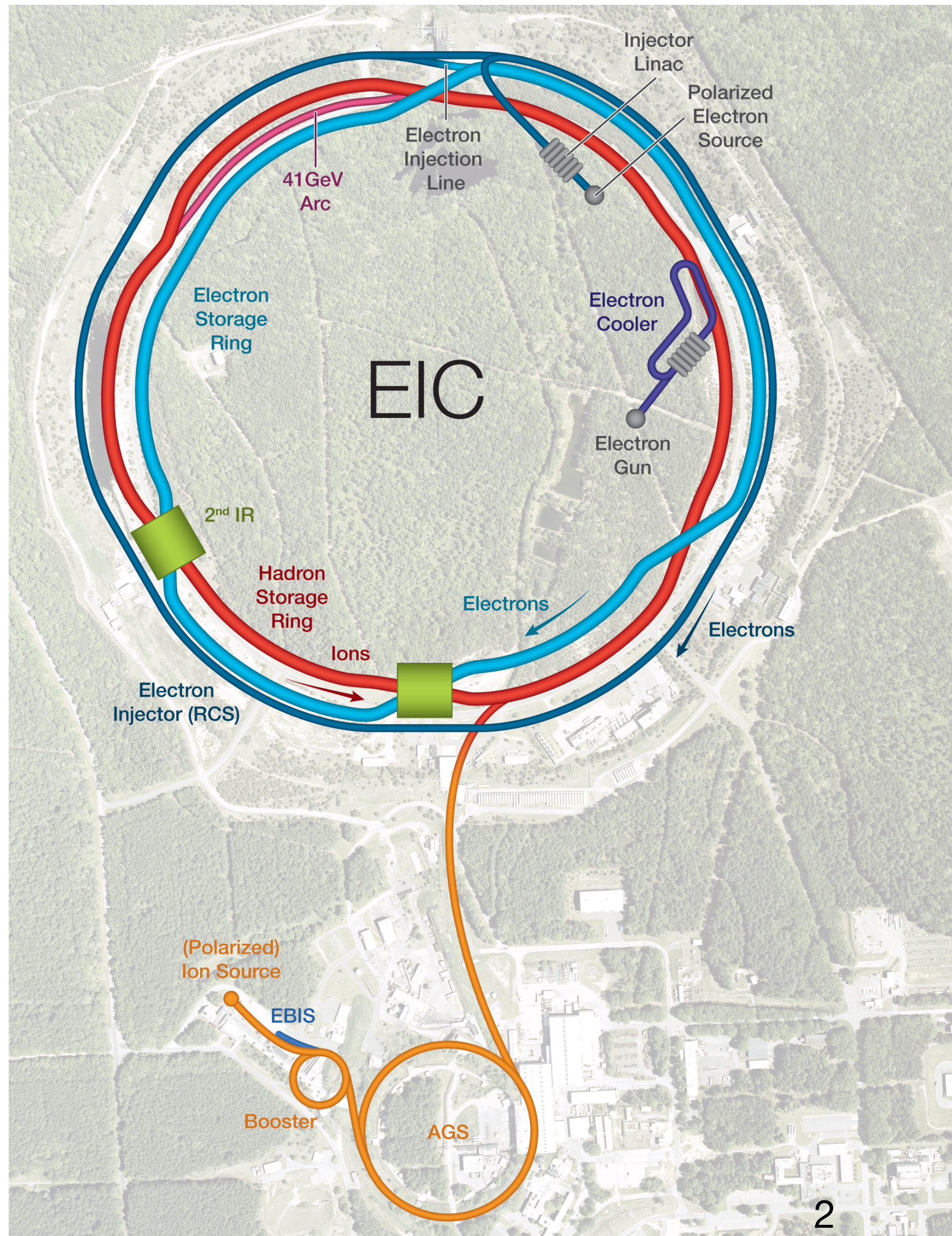
Towards improved hadron femtography with hard exclusive reactions 2024
ECT*, Trento, Italy
August 5–9, 2024

The electron-ion collider (EIC)



- Based on RHIC:
 - use existing hadron storage ring energy: 41–275 GeV
 - add electron storage ring in RHIC tunnel energy: 5–18 GeV

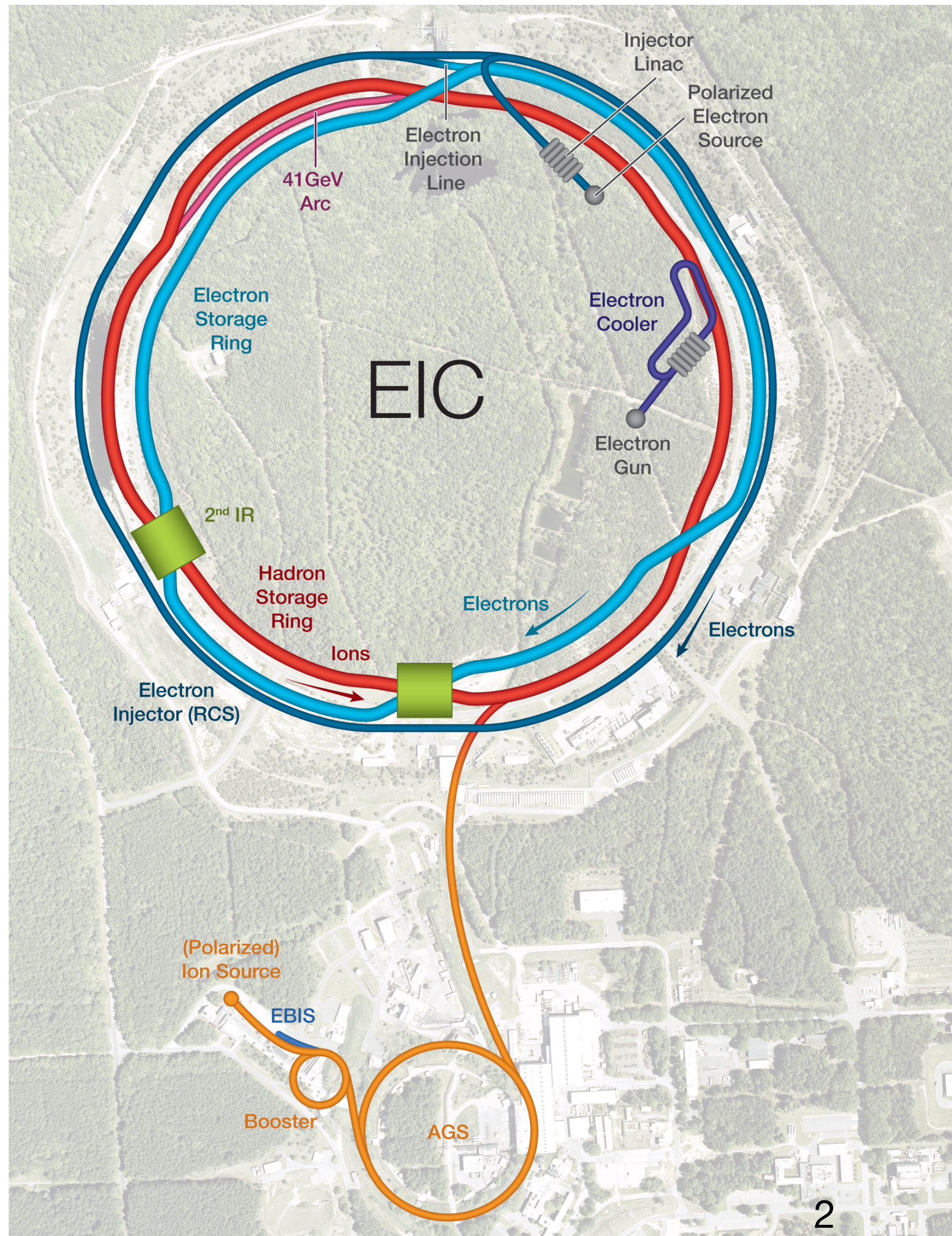
The electron-ion collider (EIC)



- Based on RHIC:
 - use existing hadron storage ring energy: 41–275 GeV
 - add electron storage ring in RHIC tunnel energy: 5–18 GeV

- $\vec{e} + \vec{p}^\uparrow, \vec{d}^\uparrow, \vec{He}^\uparrow$, unpolarised ions up to U
~ 70% polarisation

The electron-ion collider (EIC)



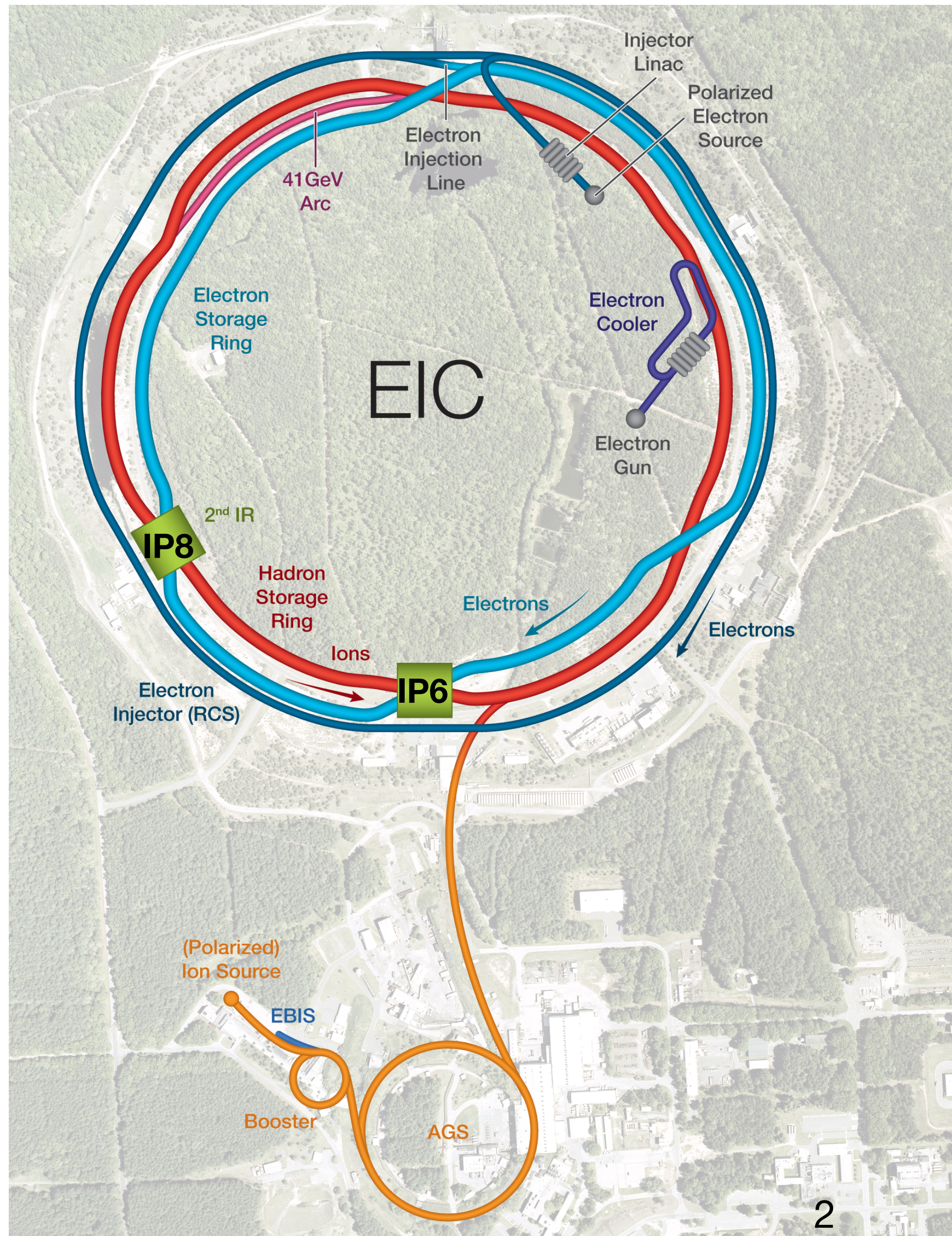
- Based on RHIC:
 - use existing hadron storage ring energy: 41–275 GeV
 - add electron storage ring in RHIC tunnel energy: 5–18 GeV

• $\vec{e} + \vec{p}^\uparrow, \vec{d}^\uparrow, \vec{He}^\uparrow$, unpolarised ions up to U
 ~ 70% polarisation

• $\mathcal{L} = 10^{33-34} \text{ cm}^{-2} \text{ s}^{-1}$

$\leftrightarrow \mathcal{L}_{\text{int}} = 10 - 100 \text{ fb}^{-1}/\text{year}$

The electron-ion collider (EIC)



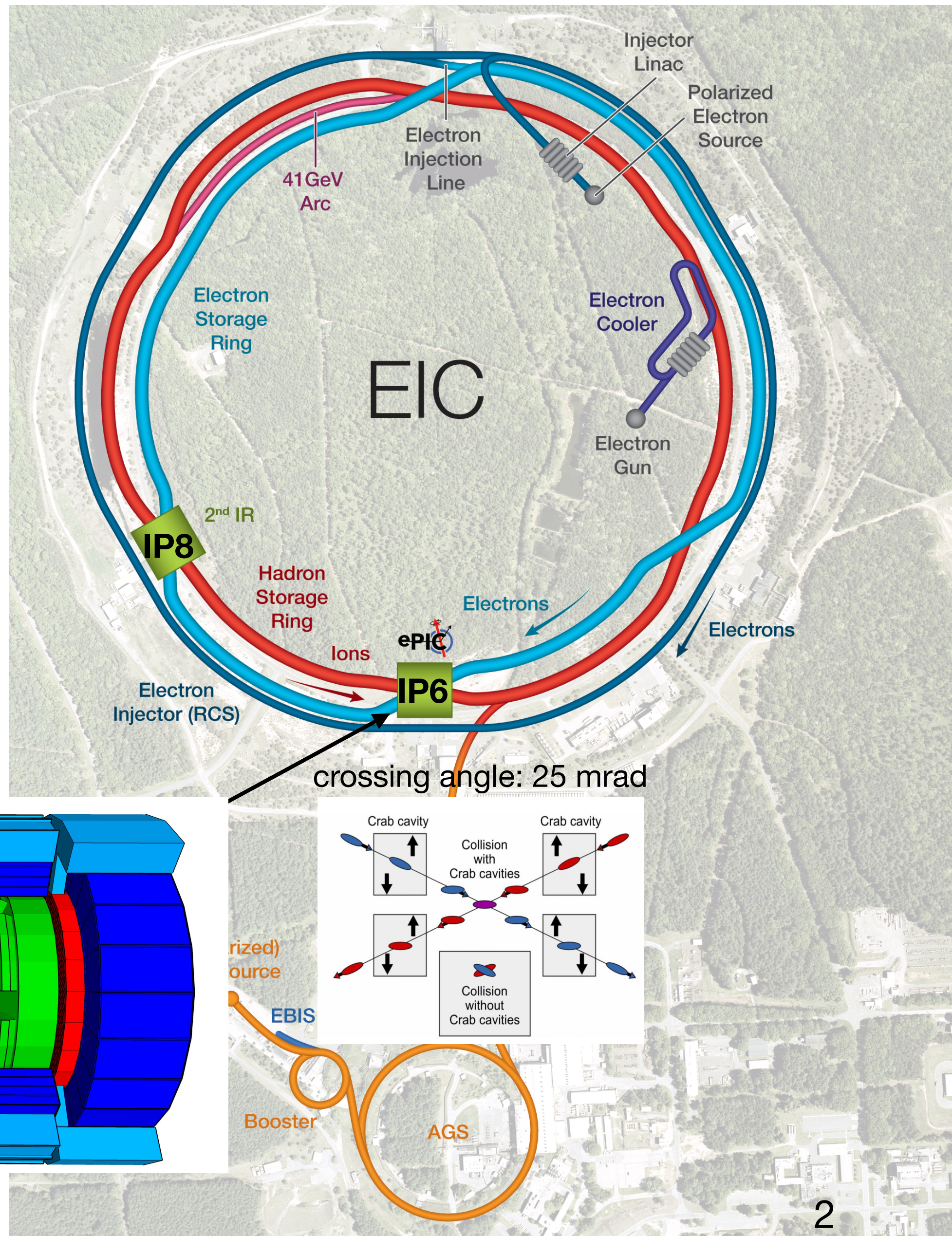
- Based on RHIC:
 - use existing hadron storage ring energy: 41–275 GeV
 - add electron storage ring in RHIC tunnel energy: 5–18 GeV

- $\vec{e} + \vec{p}^\uparrow, \vec{d}^\uparrow, \vec{He}^\uparrow$, unpolarised ions up to U
 ~ 70% polarisation

- $\mathcal{L} = 10^{33-34} \text{ cm}^{-2} \text{ s}^{-1}$

- $\leftrightarrow \mathcal{L}_{\text{int}} = 10 - 100 \text{ fb}^{-1}/\text{year}$

The electron-ion collider (EIC)



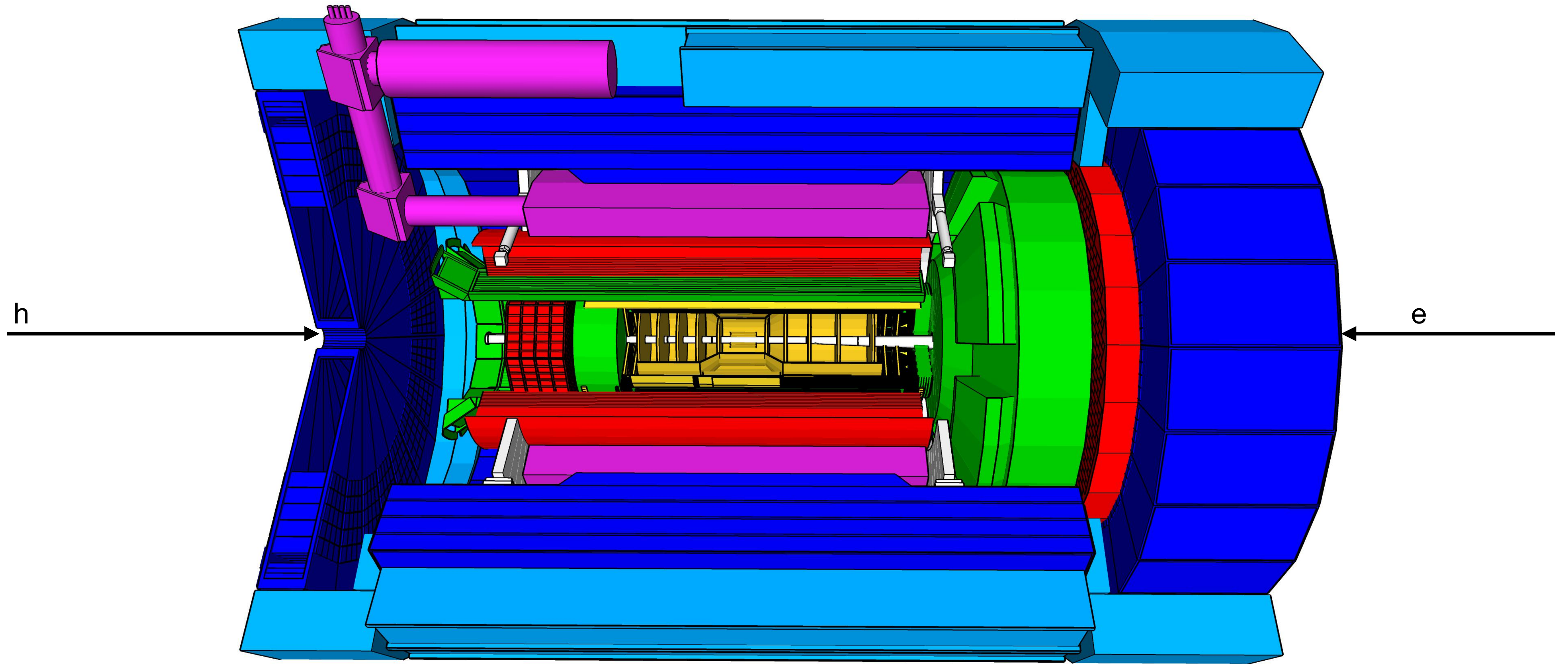
- Based on RHIC:
 - use existing hadron storage ring energy: 41–275 GeV
 - add electron storage ring in RHIC tunnel energy: 5–18 GeV

• $\vec{e} + \vec{p}^\uparrow, \vec{d}^\uparrow, \vec{He}^\uparrow$, unpolarised ions up to U
 ~ 70% polarisation

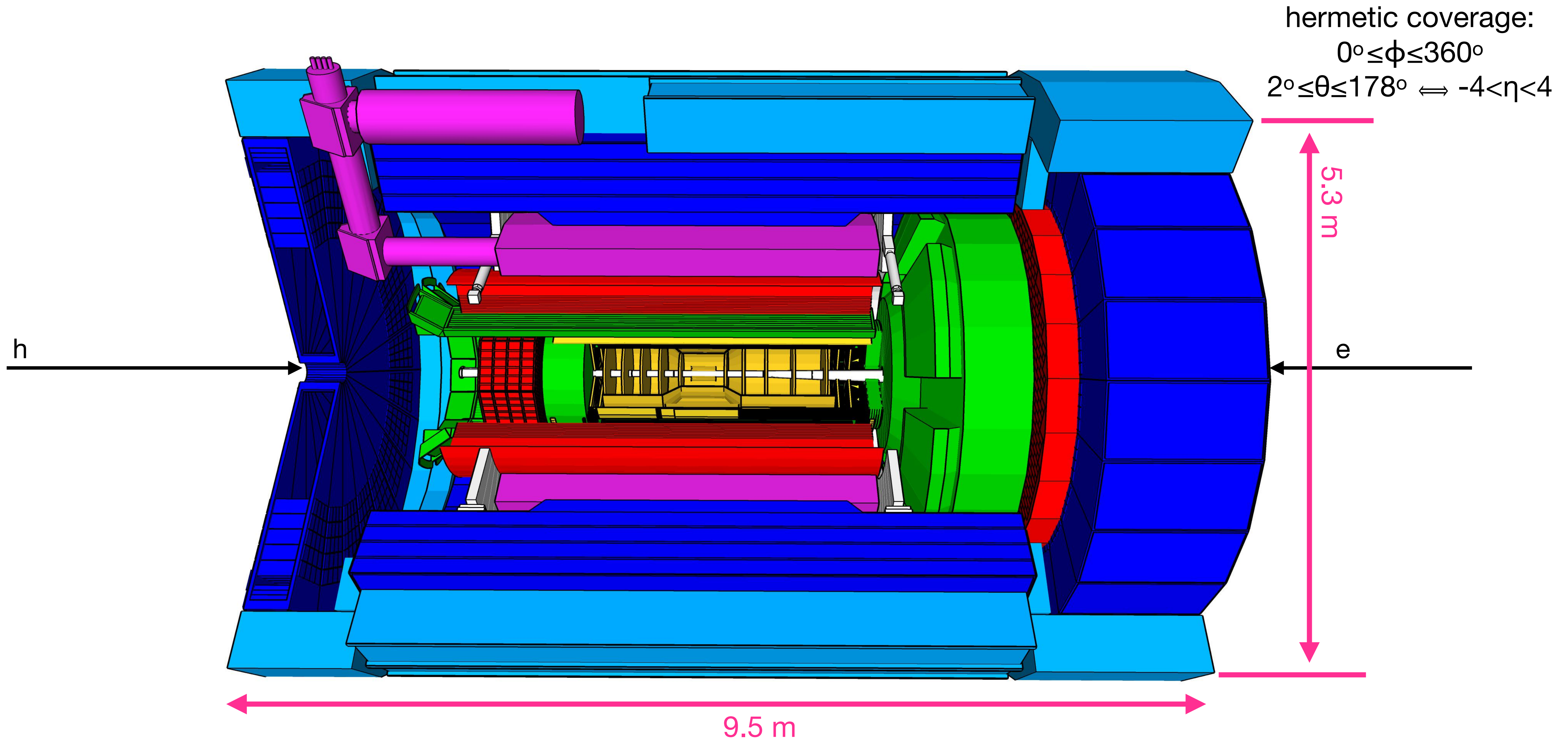
• $\mathcal{L} = 10^{33-34} \text{ cm}^{-2} \text{ s}^{-1}$

$\leftrightarrow \mathcal{L}_{\text{int}} = 10 - 100 \text{ fb}^{-1}/\text{year}$

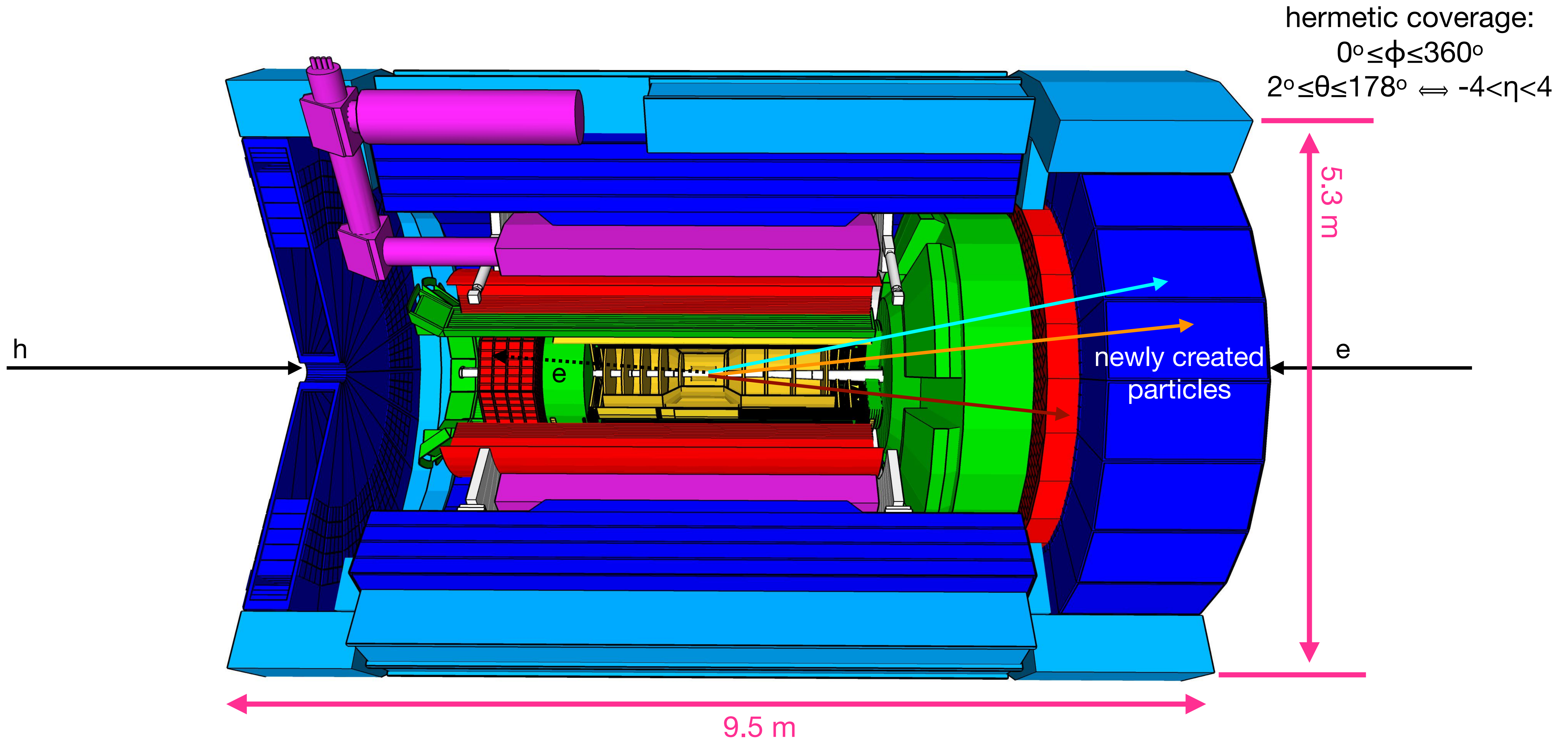
The electron-proton/ion collider (ePIC) detector



The electron-proton/ion collider (ePIC) detector

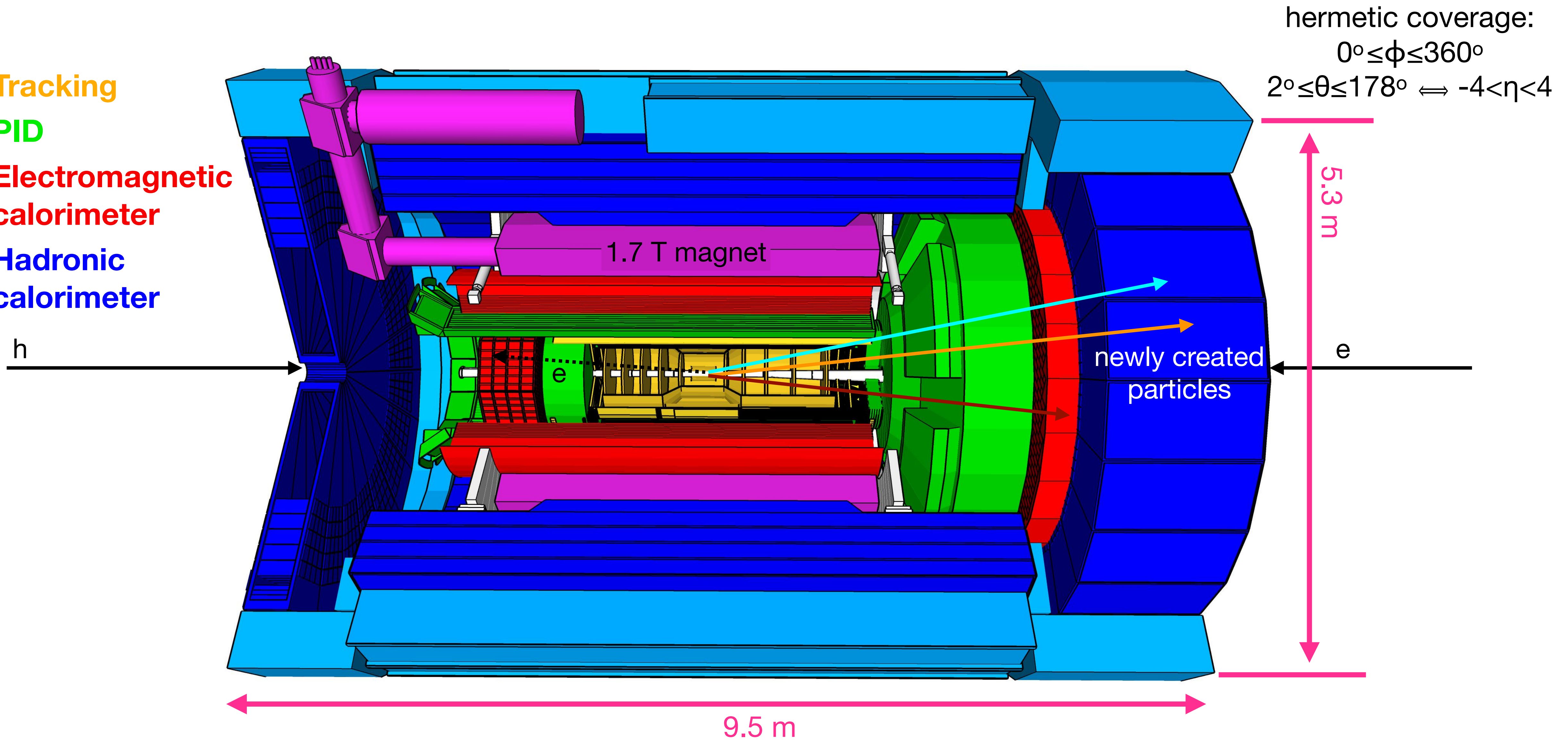


The electron-proton/ion collider (ePIC) detector

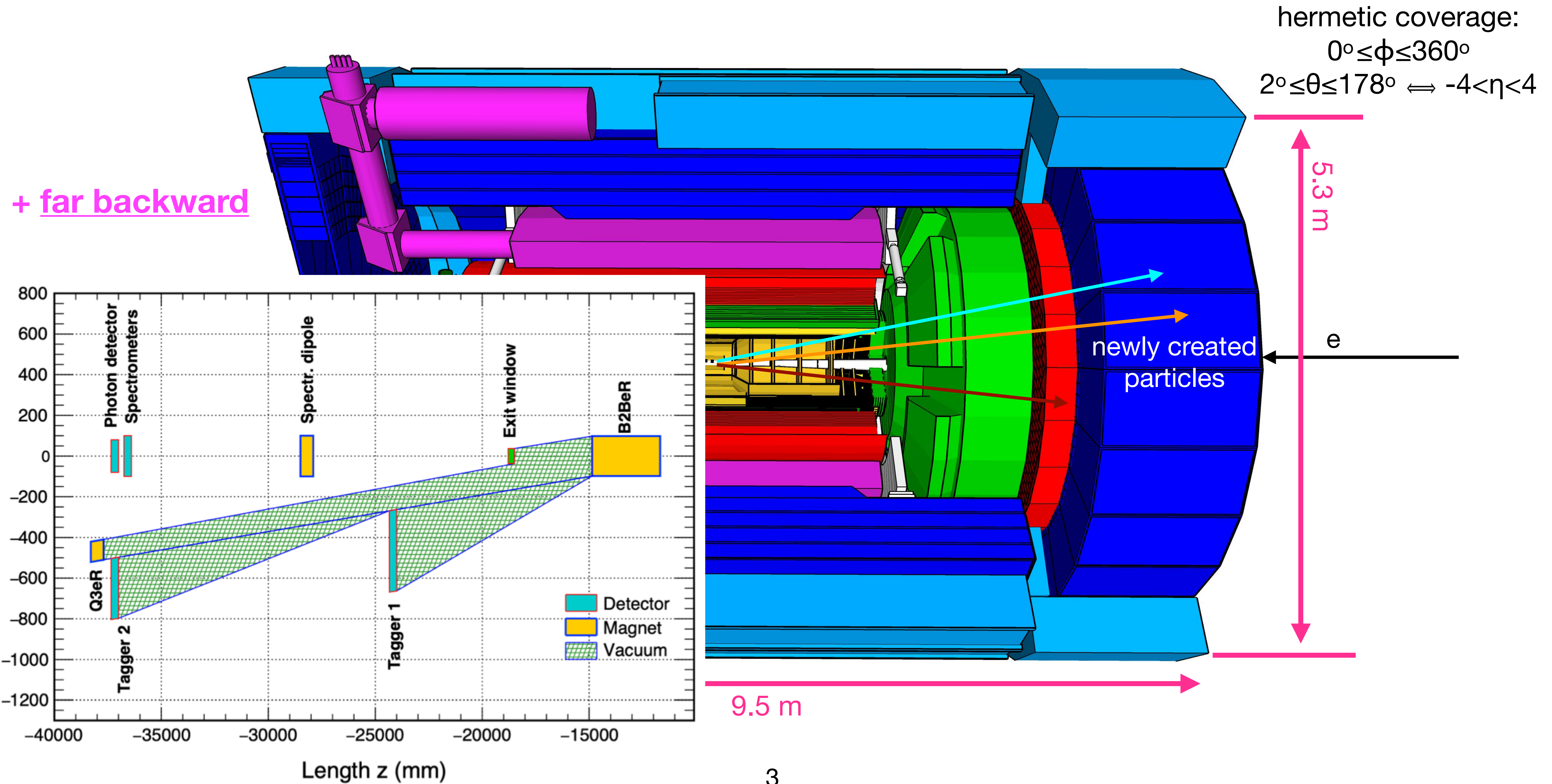


The electron-proton/ion collider (ePIC) detector

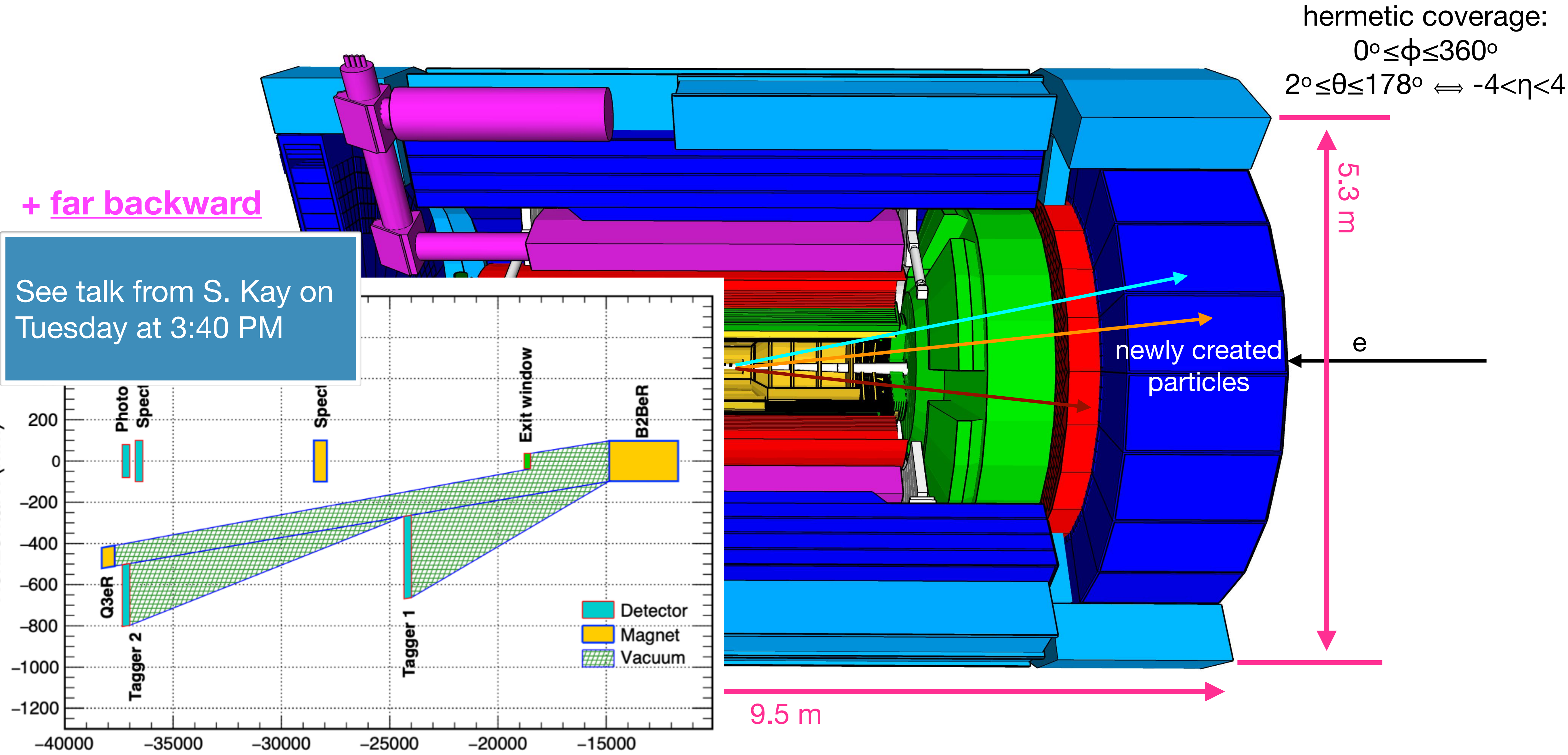
- Tracking
- PID
- Electromagnetic calorimeter
- Hadronic calorimeter



The electron-proton/ion collider (ePIC) detector

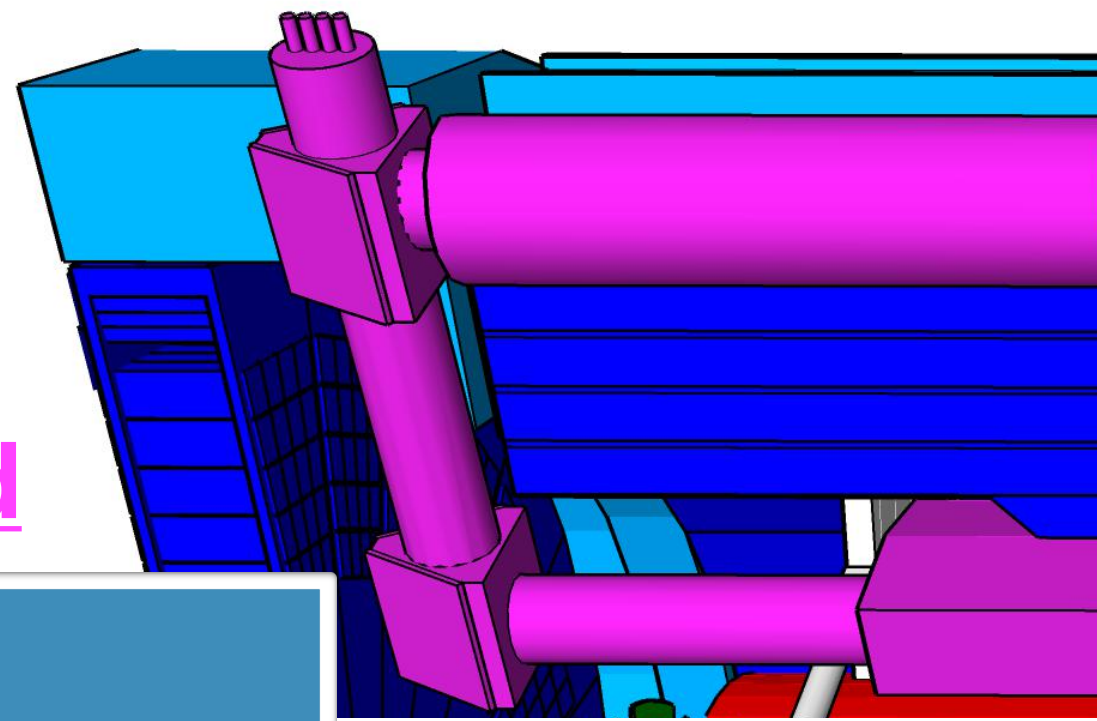


The electron-proton/ion collider (ePIC) detector

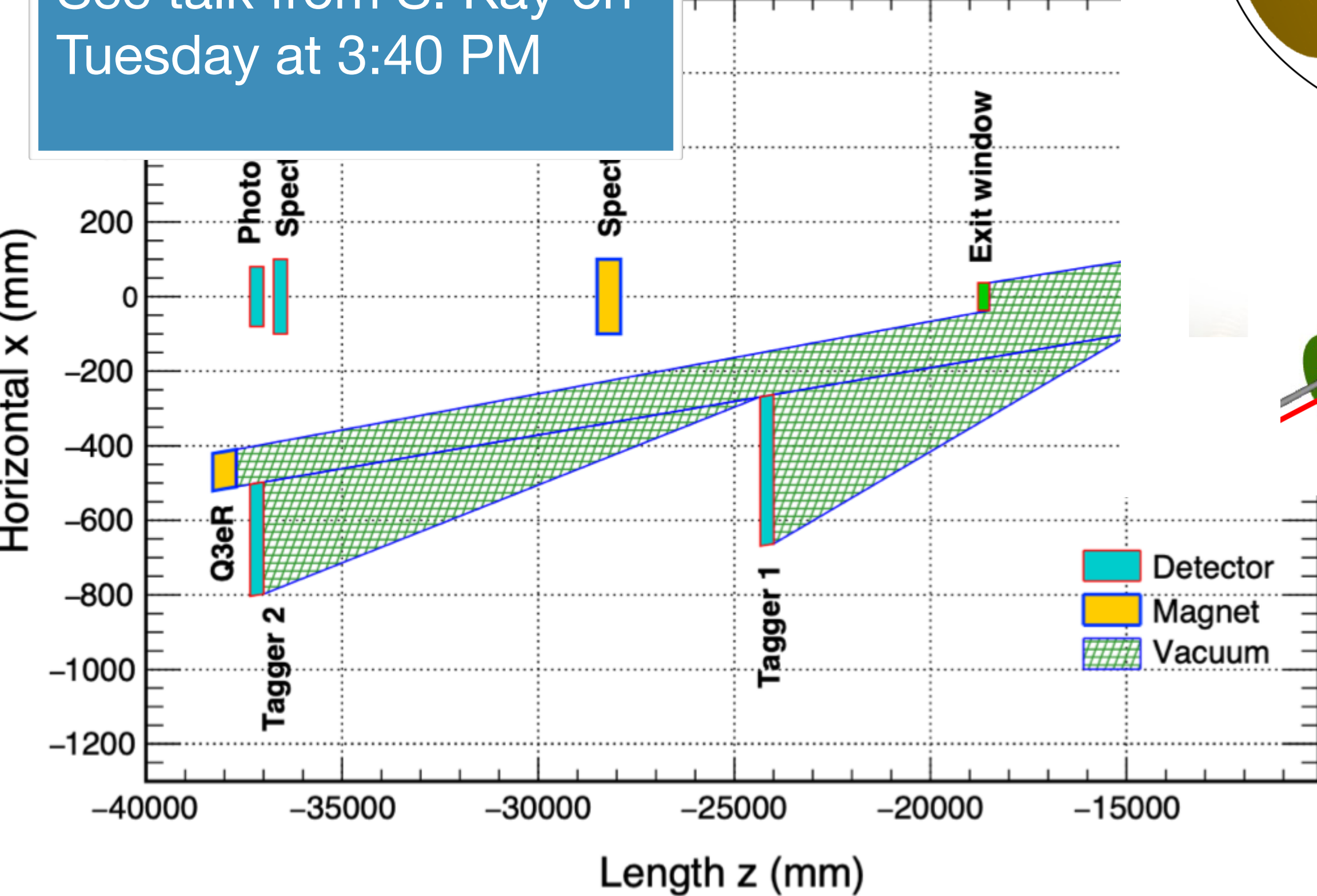


The electron-proton/ion collider (ePIC) detector

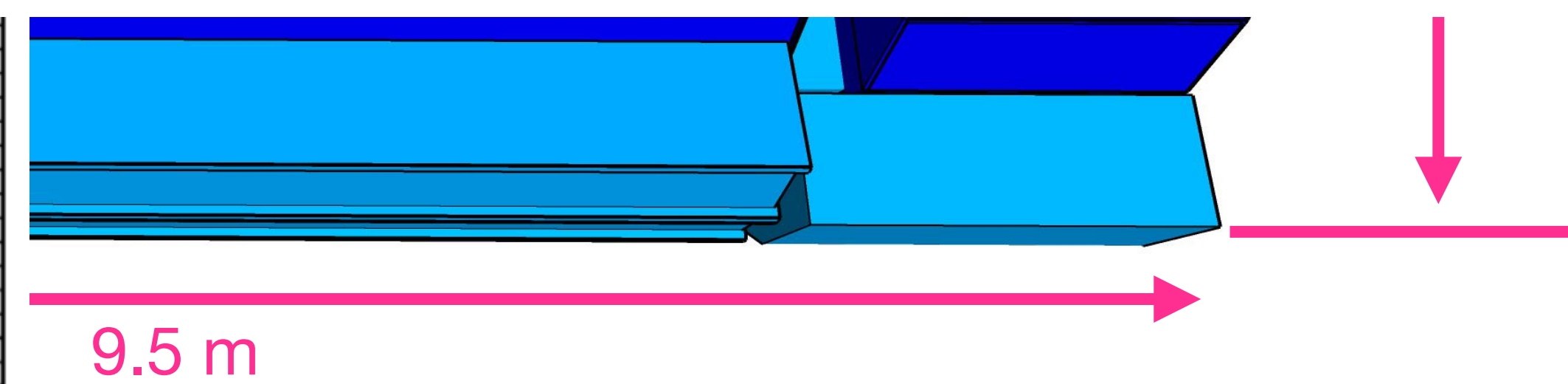
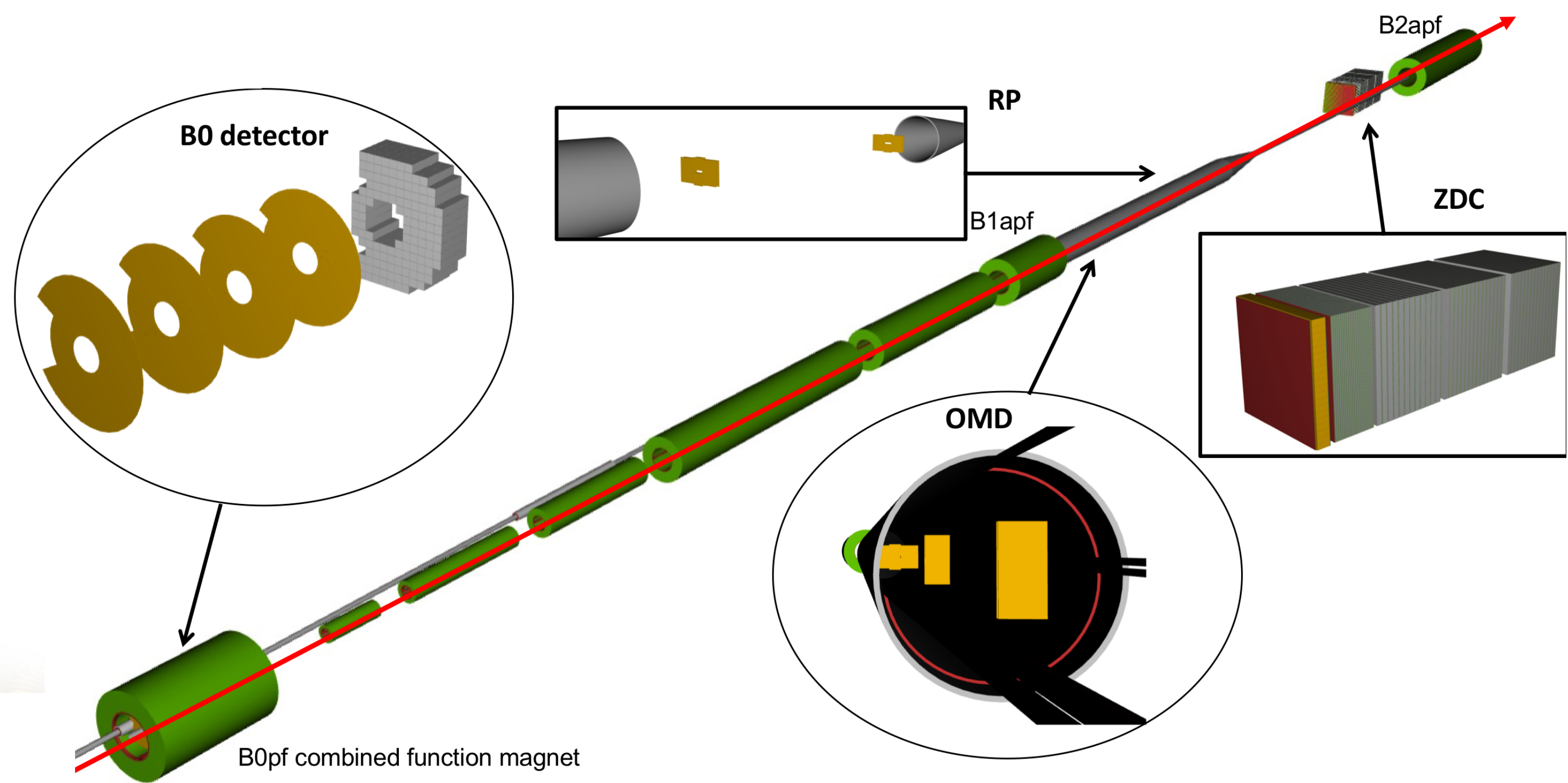
+ far backward



See talk from S. Kay on Tuesday at 3:40 PM

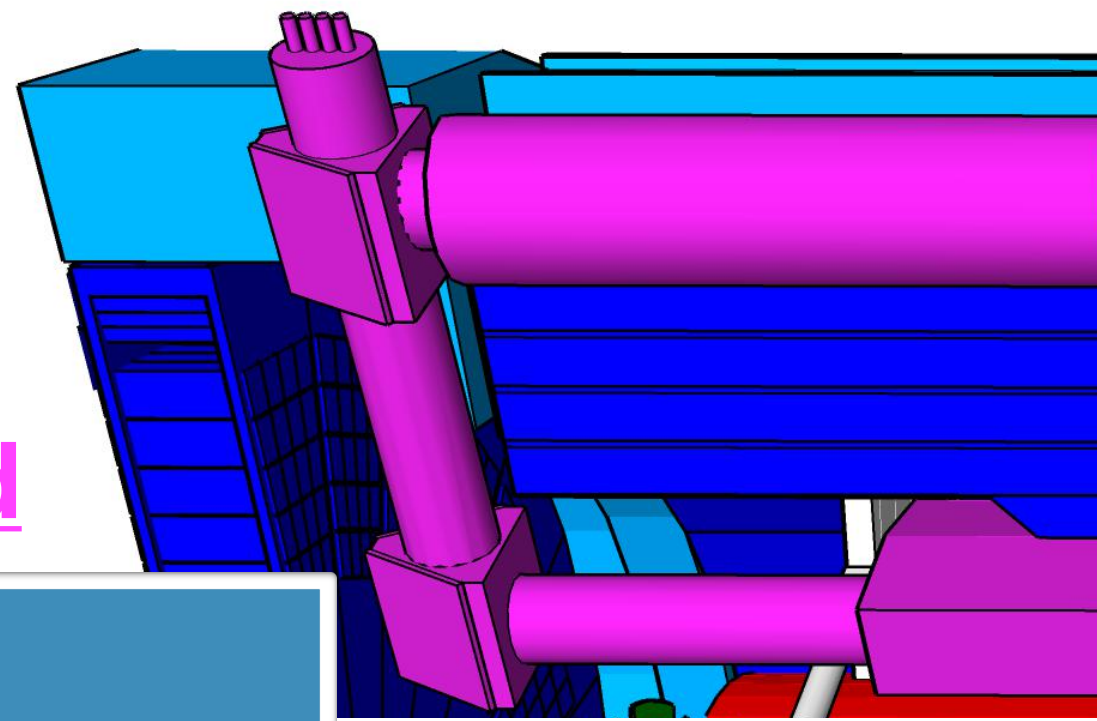


+ far forward

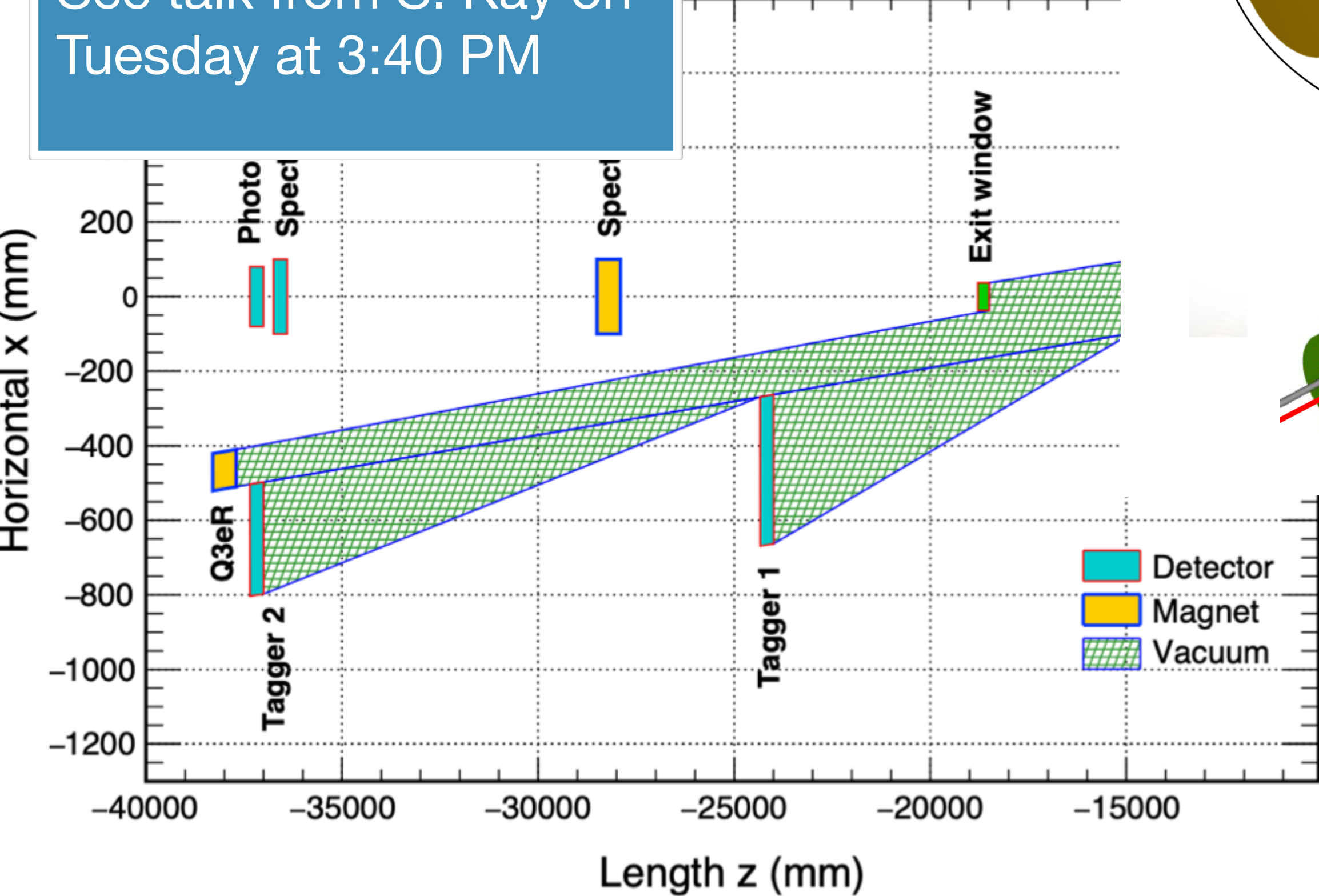


The electron-proton/ion collider (ePIC) detector

+ far backward

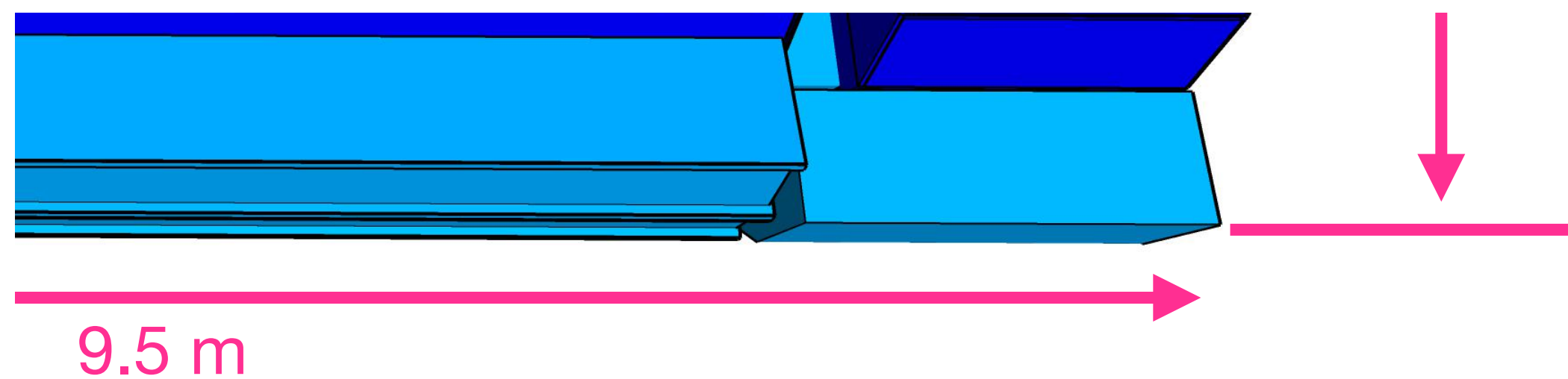
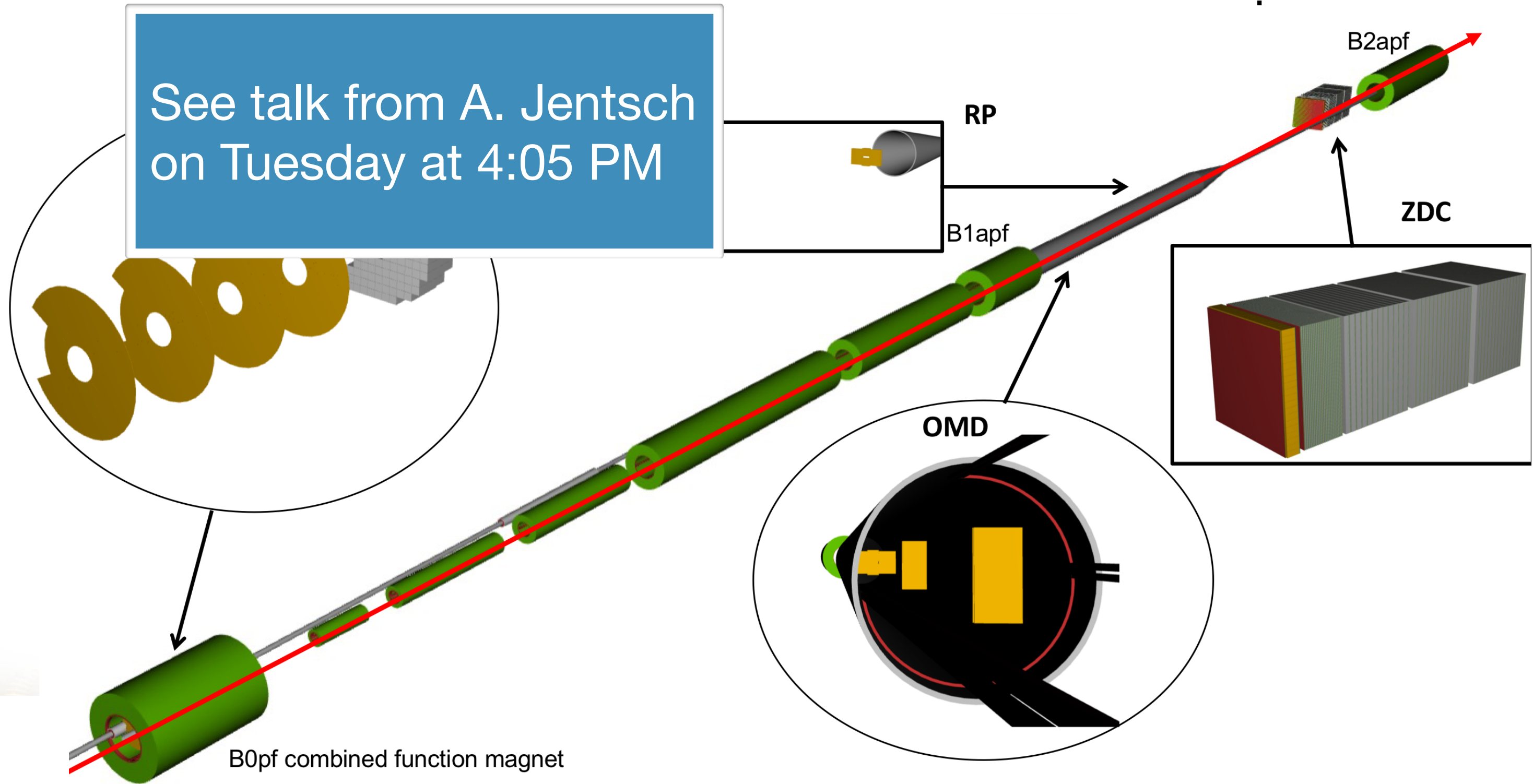


See talk from S. Kay on Tuesday at 3:40 PM

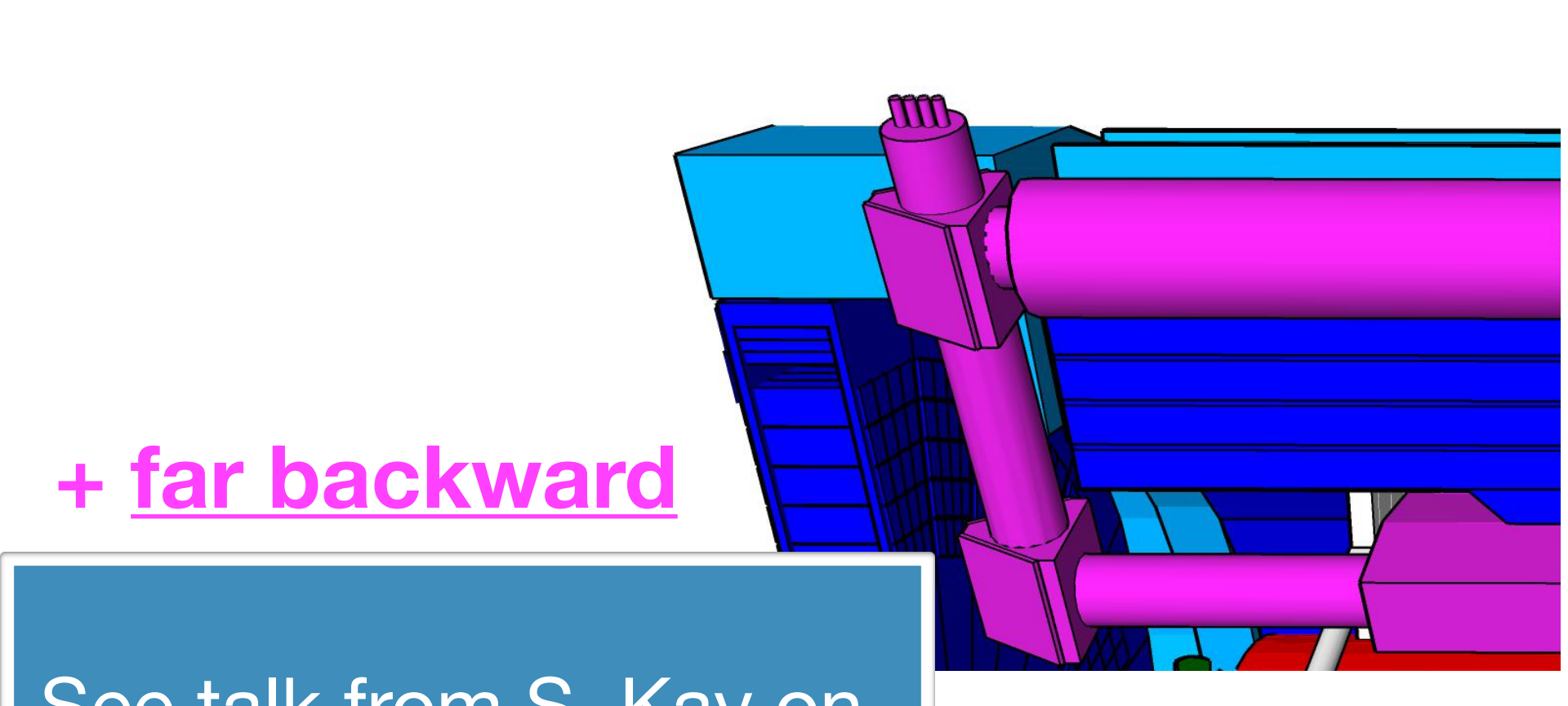


+ far forward

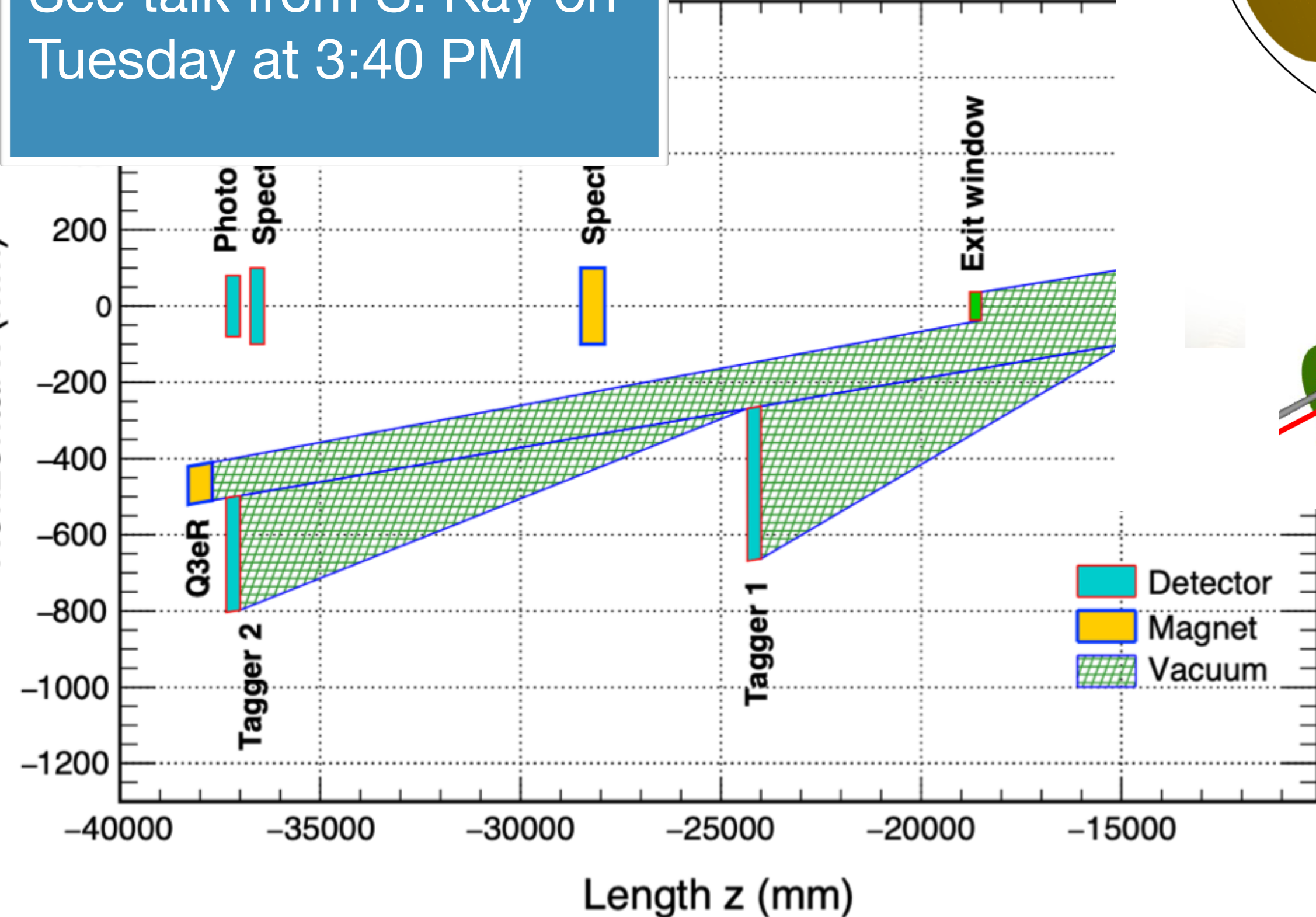
See talk from A. Jentsch on Tuesday at 4:05 PM



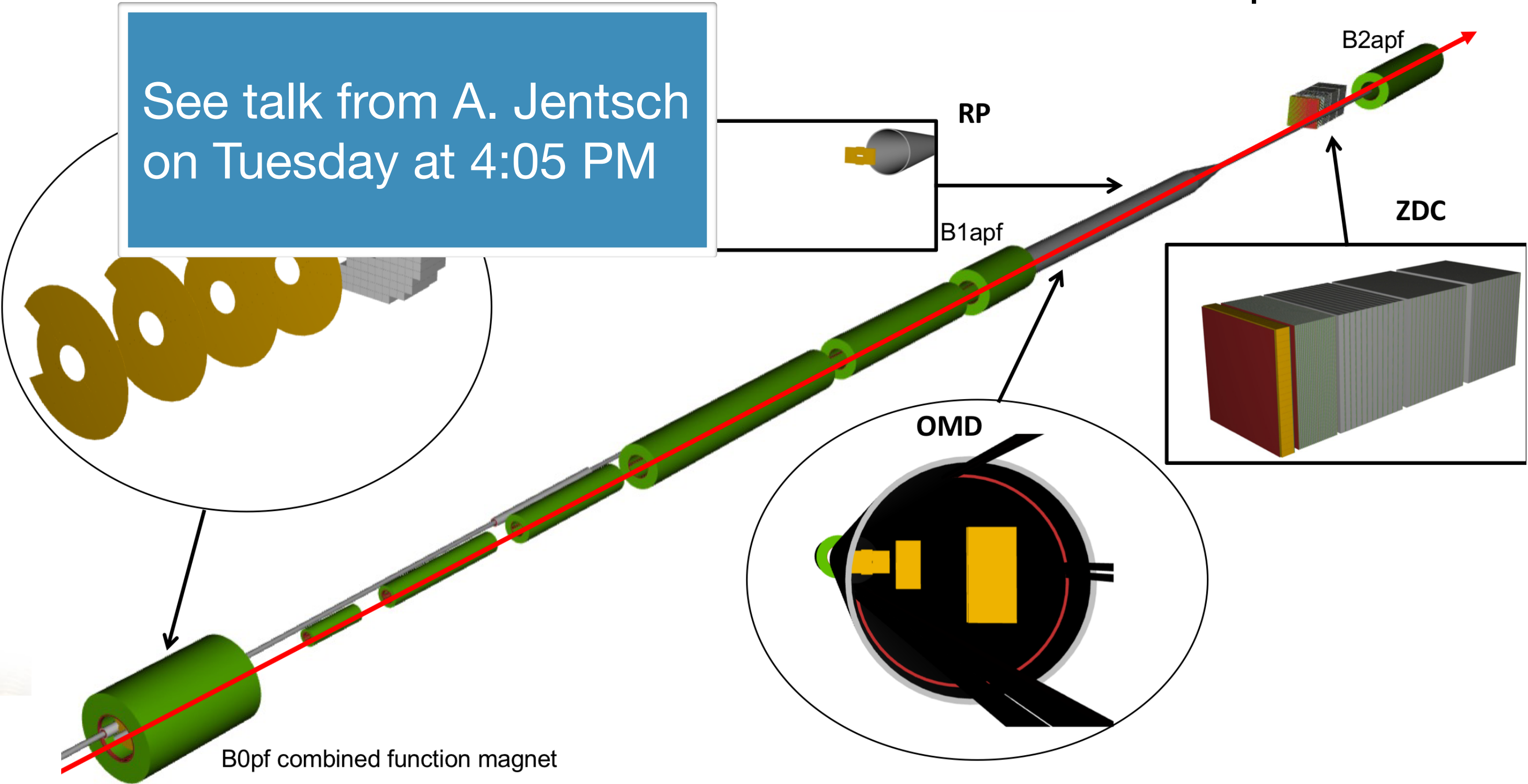
The electron-proton/ion collider (ePIC) detector



See talk from S. Kay on Tuesday at 3:40 PM



+ far forward

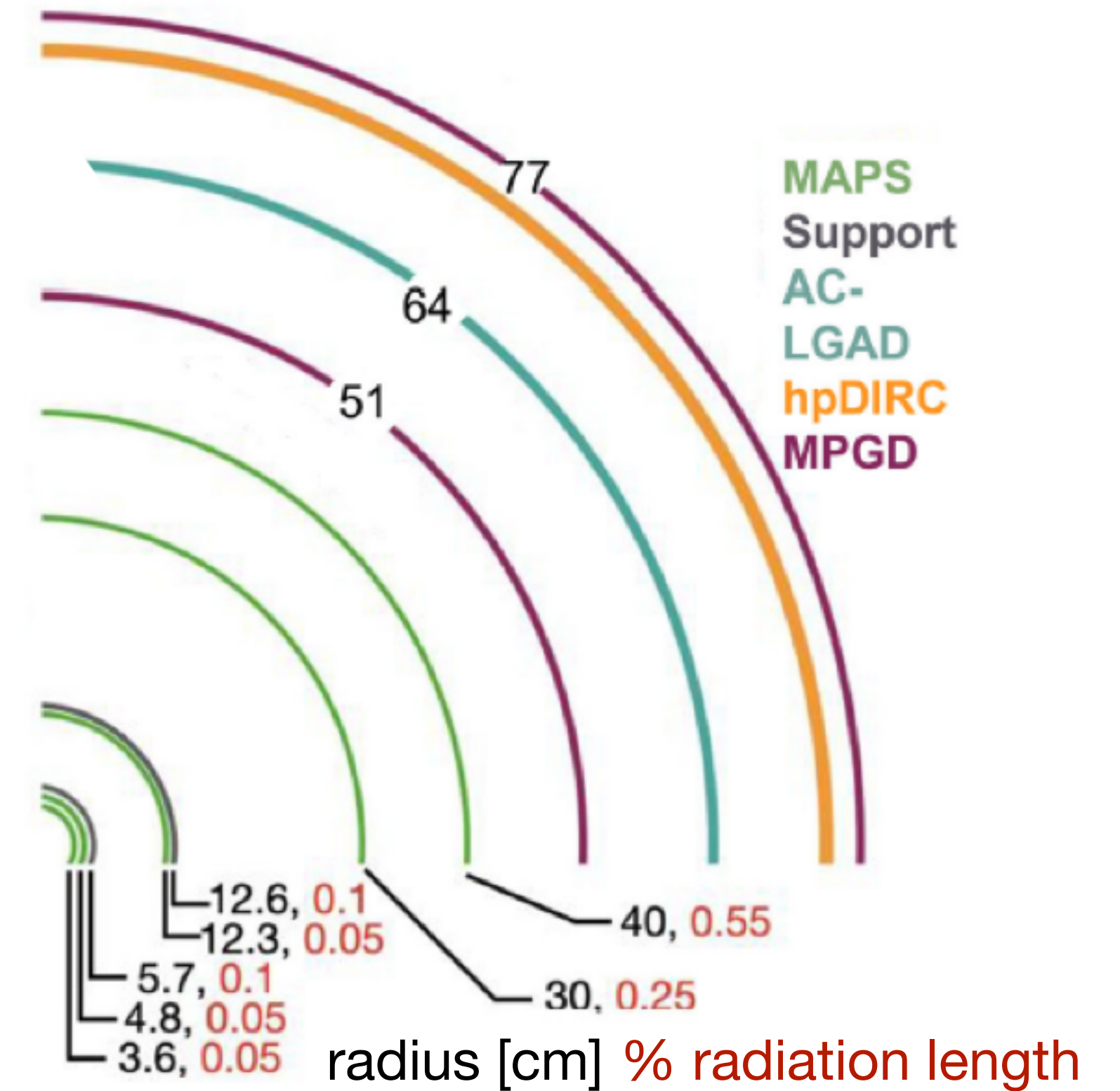
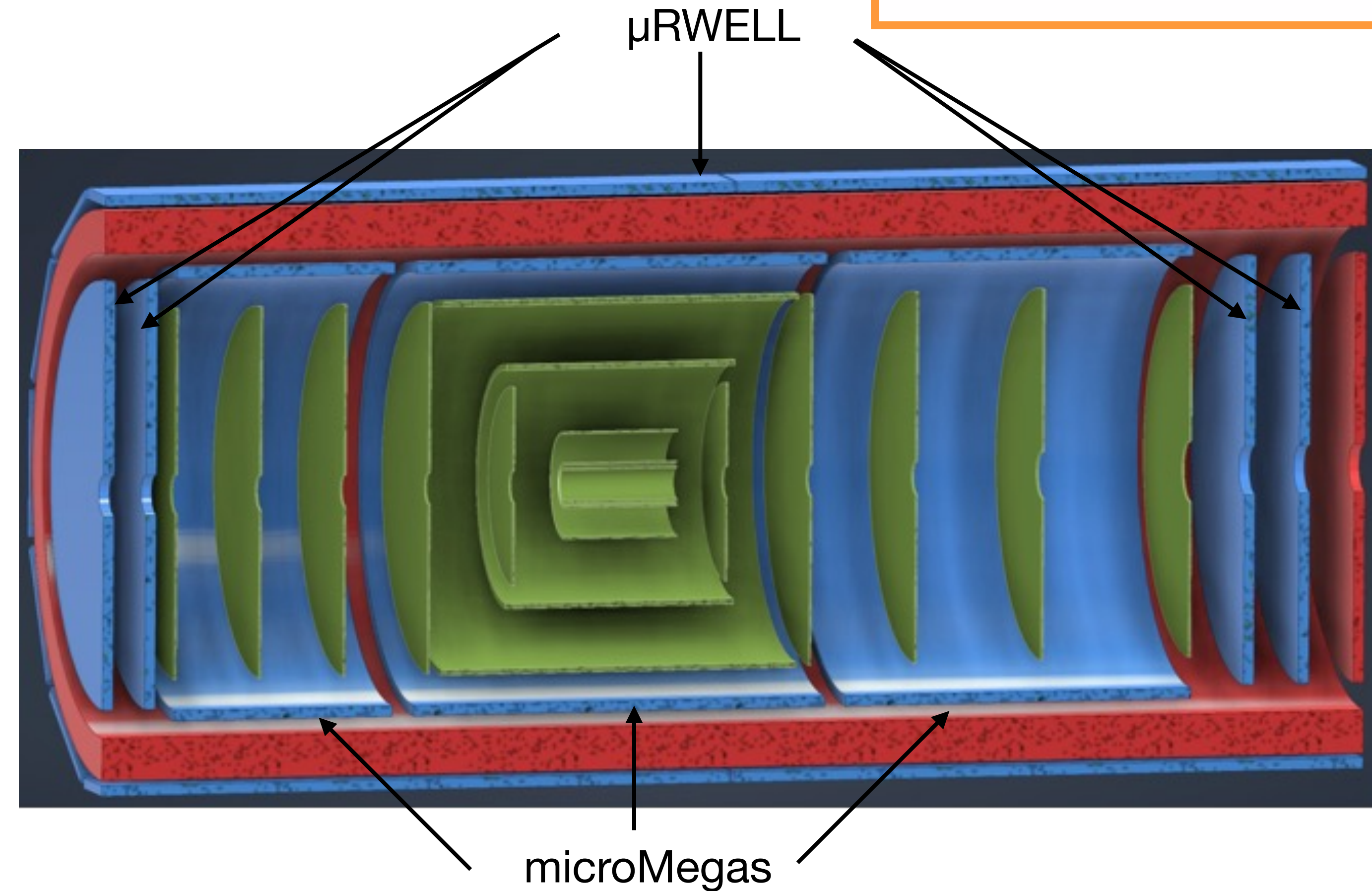
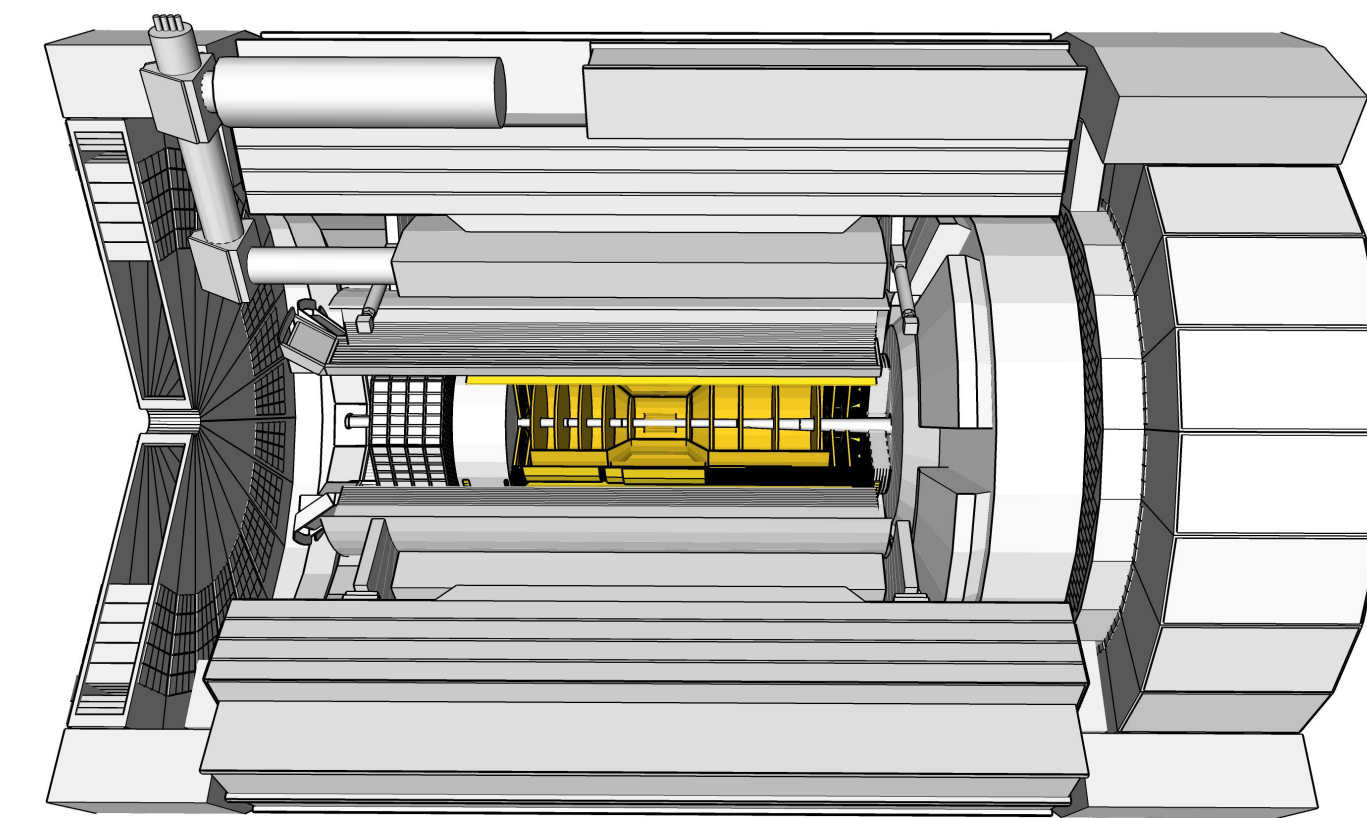


9.5 m

Data acquisition:
no trigger
all collision data is digitised
with strong zero-suppression at front-end electronics

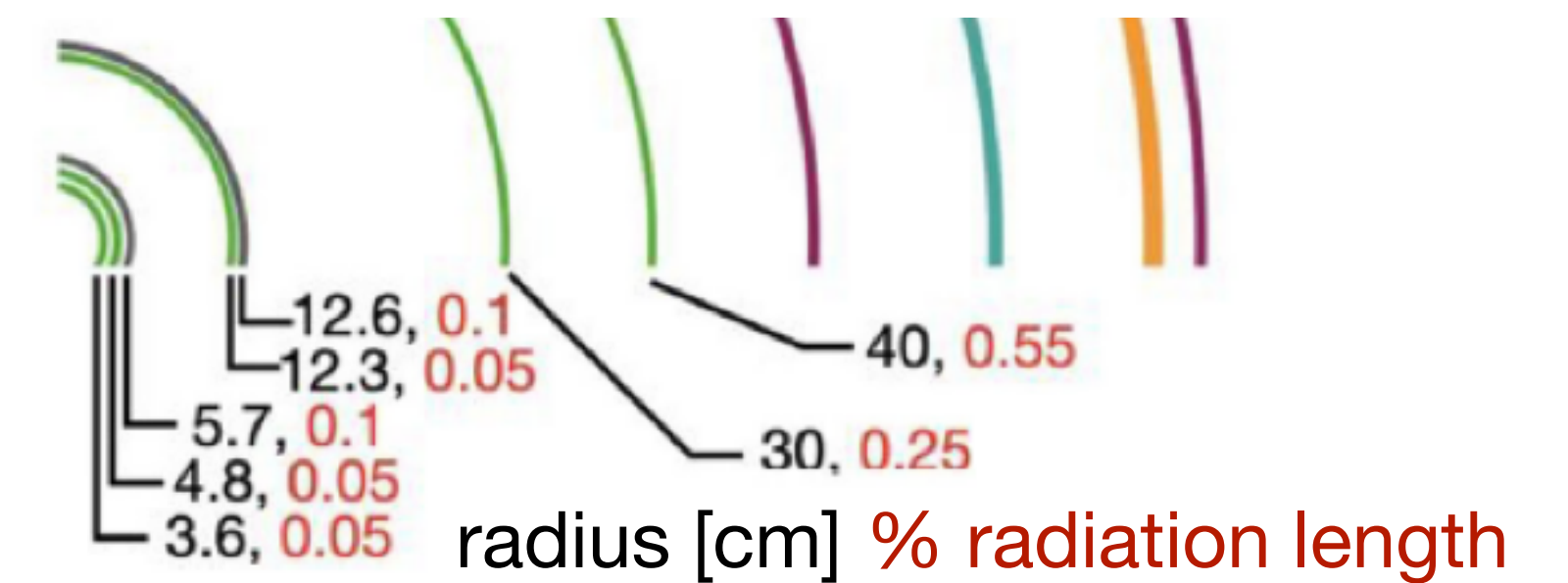
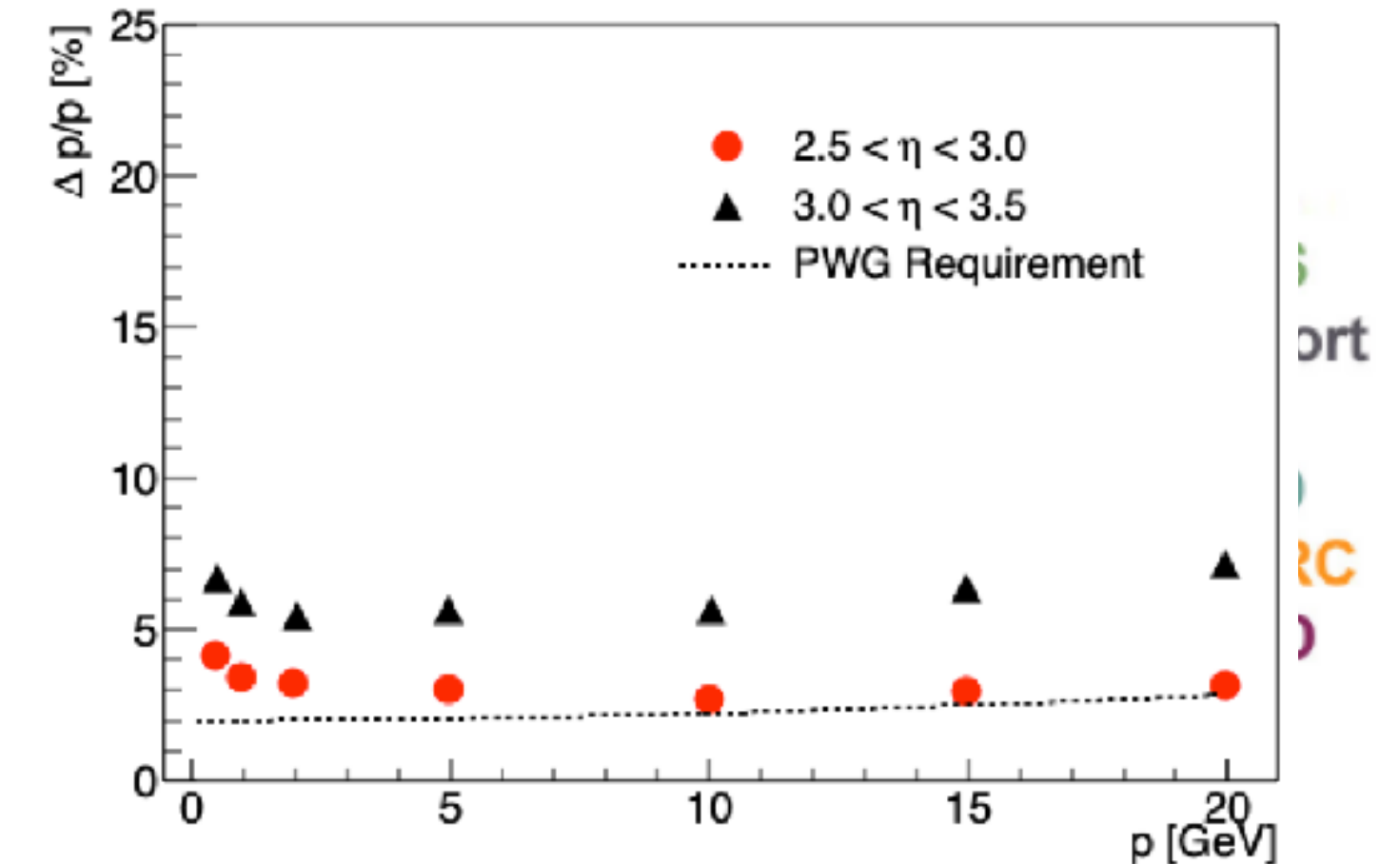
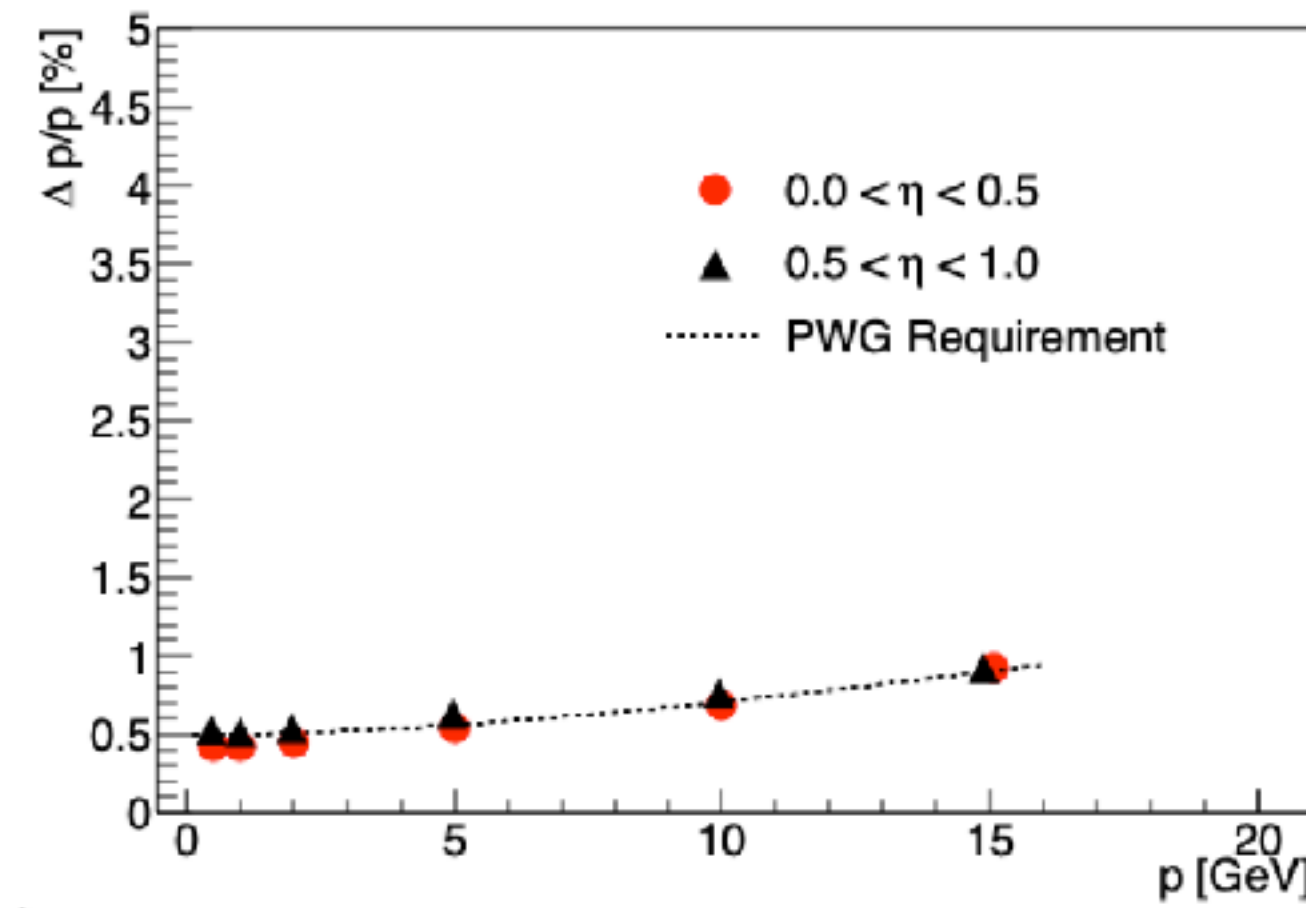
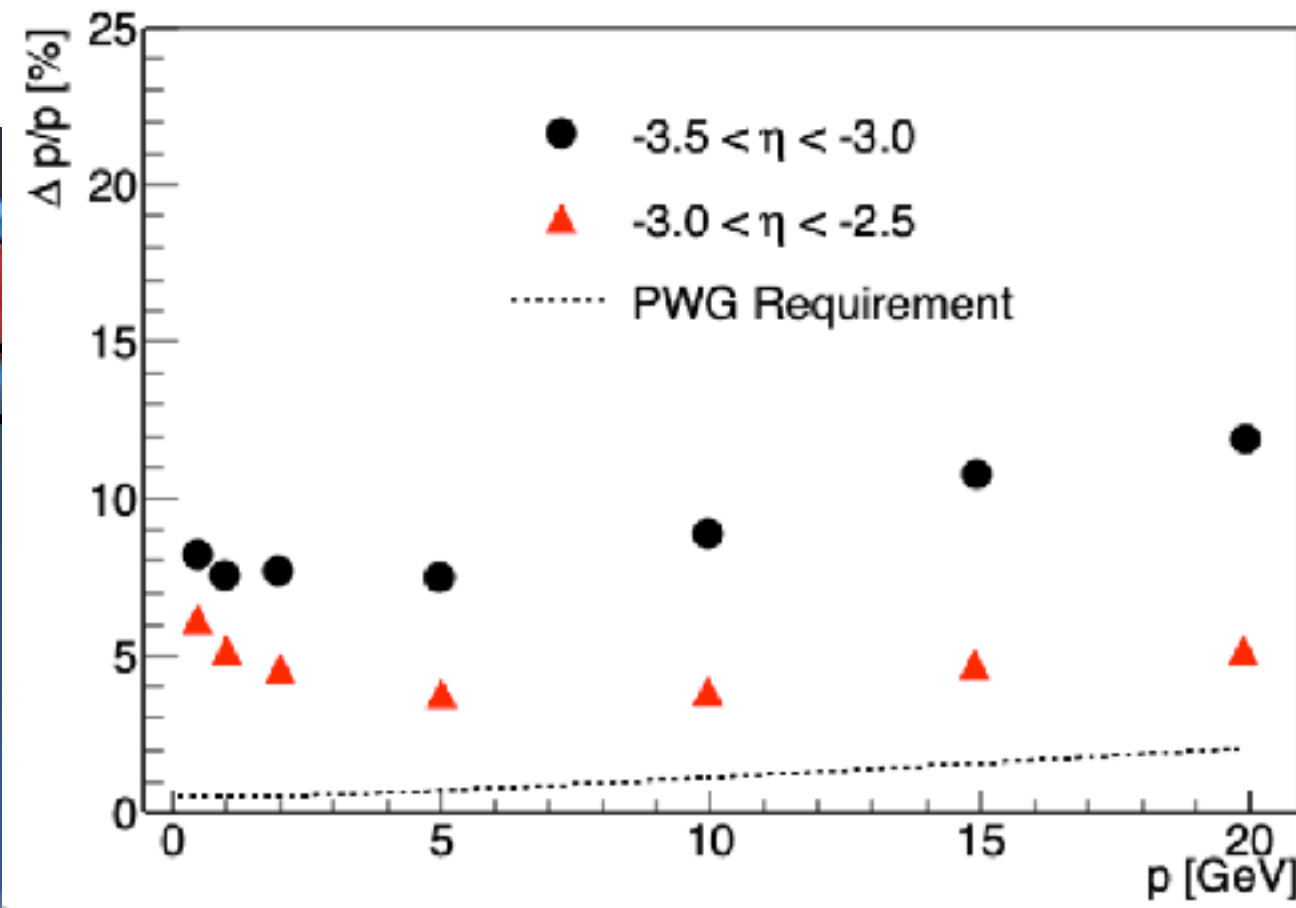
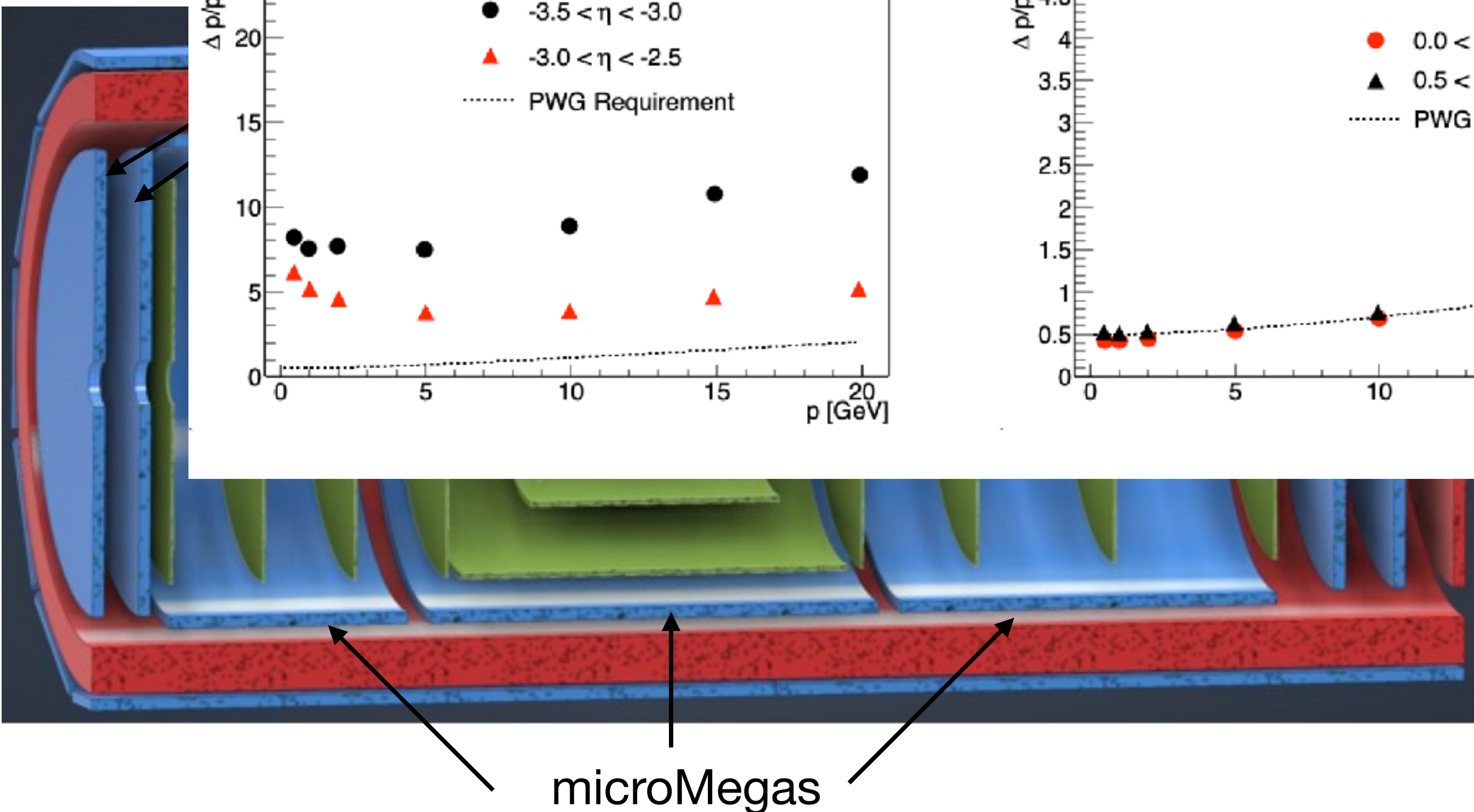
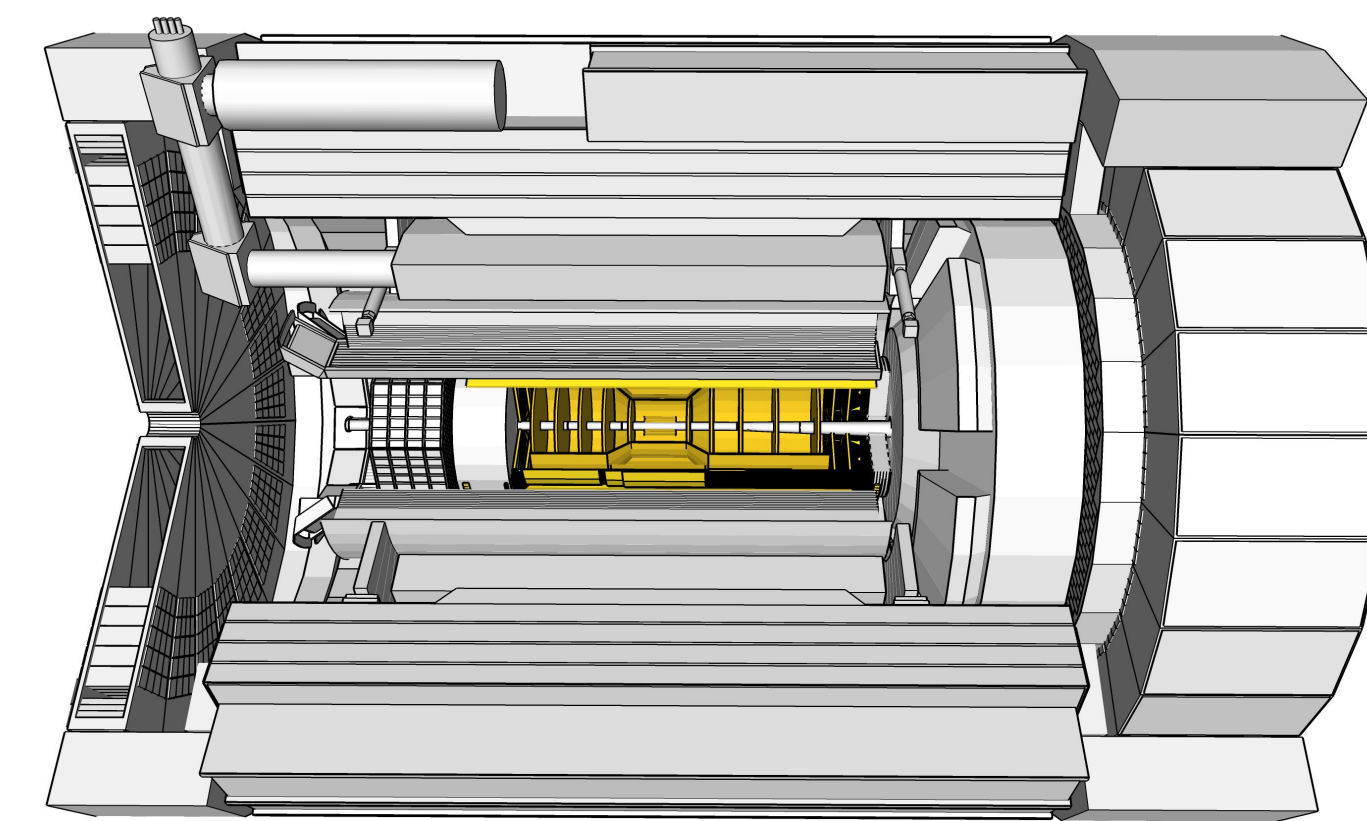
Tracking system

- 1.7 T magnet
- Monolithic Active Pixel Sensor (MAPS)
Silicon vertexing/inner tracker
- Micro-pattern gaseous detectors
 μ RWELL/microMegas:
timing & pattern recognition
- AC-LGAD based TOF:
PID & additional tracking point



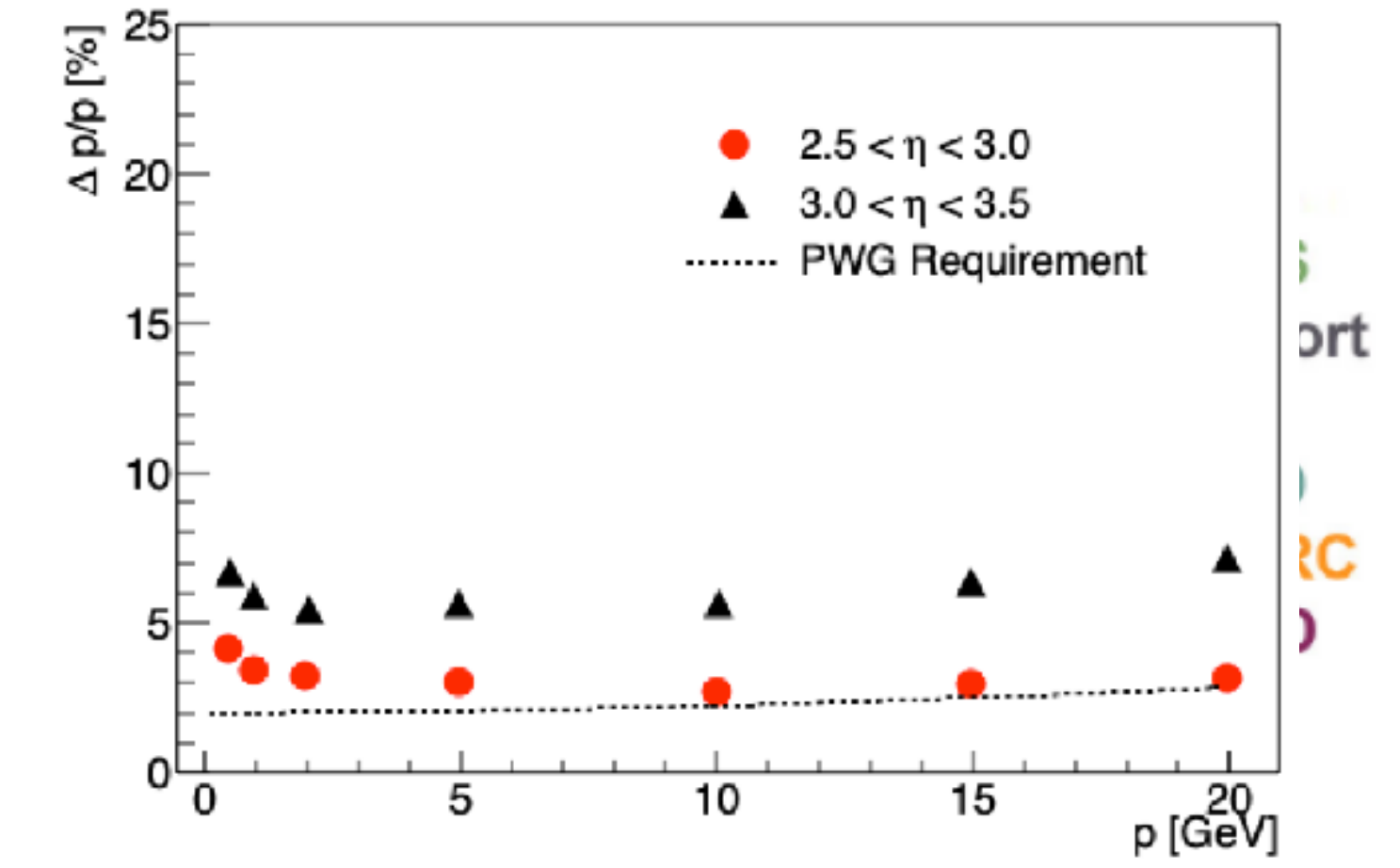
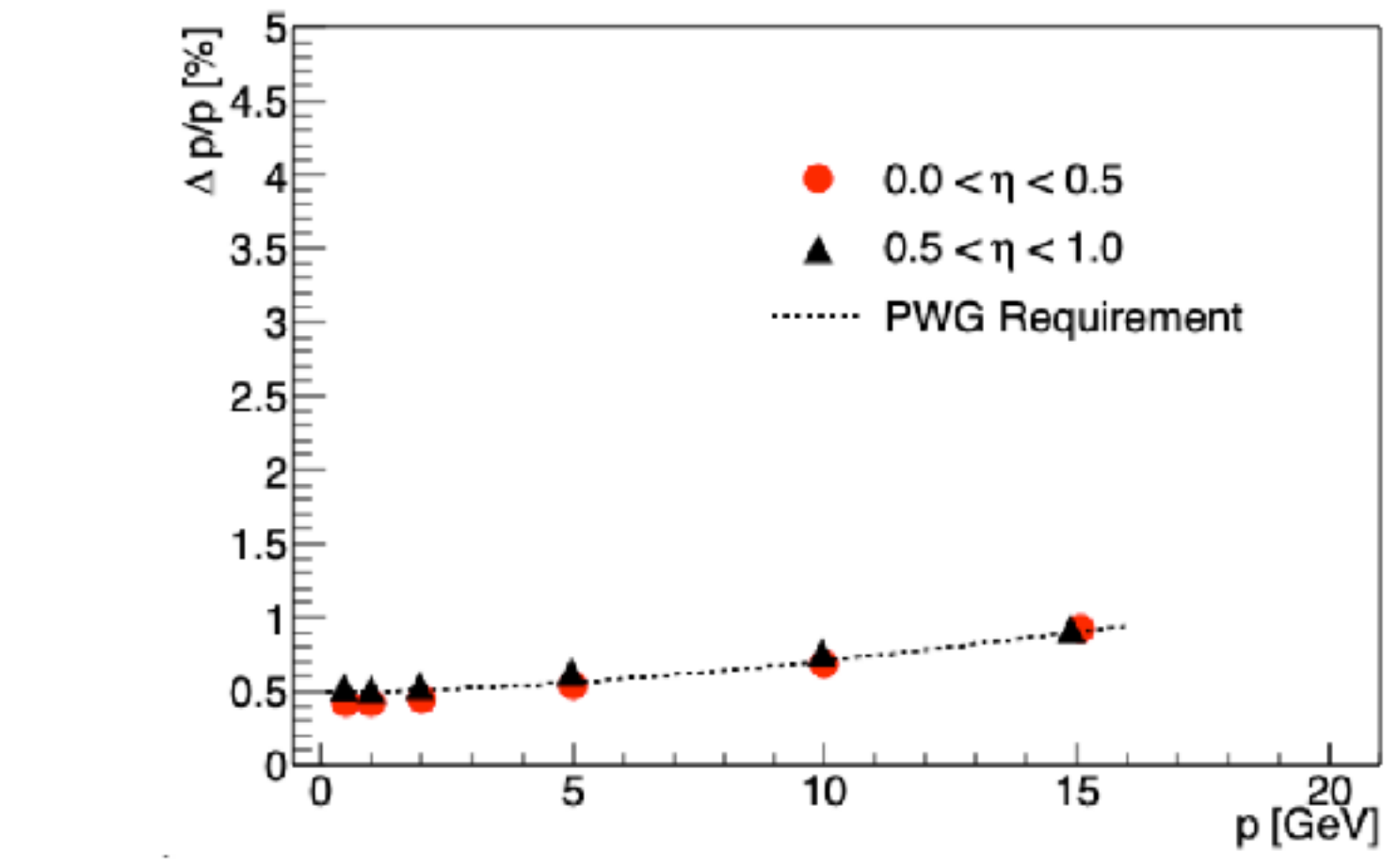
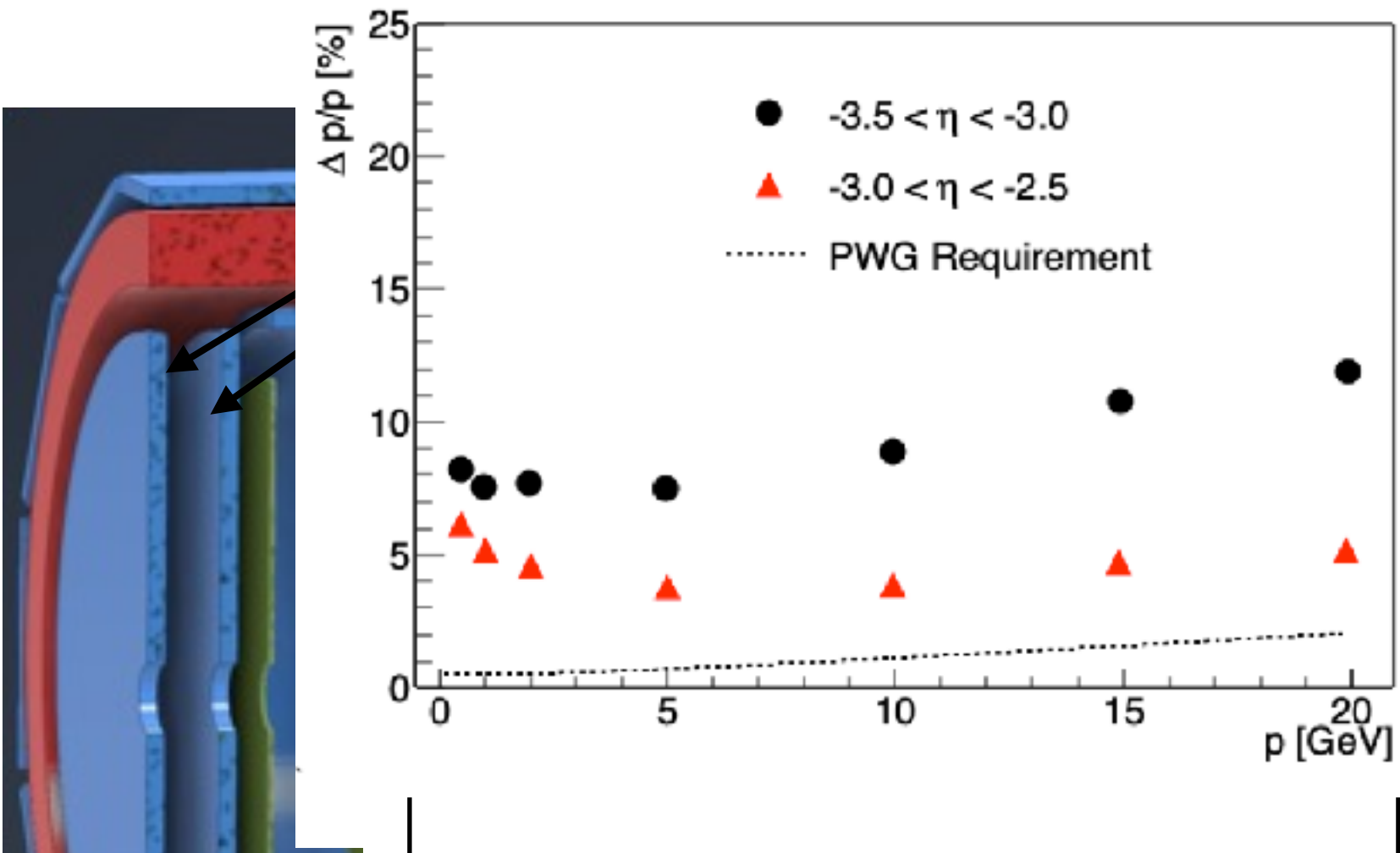
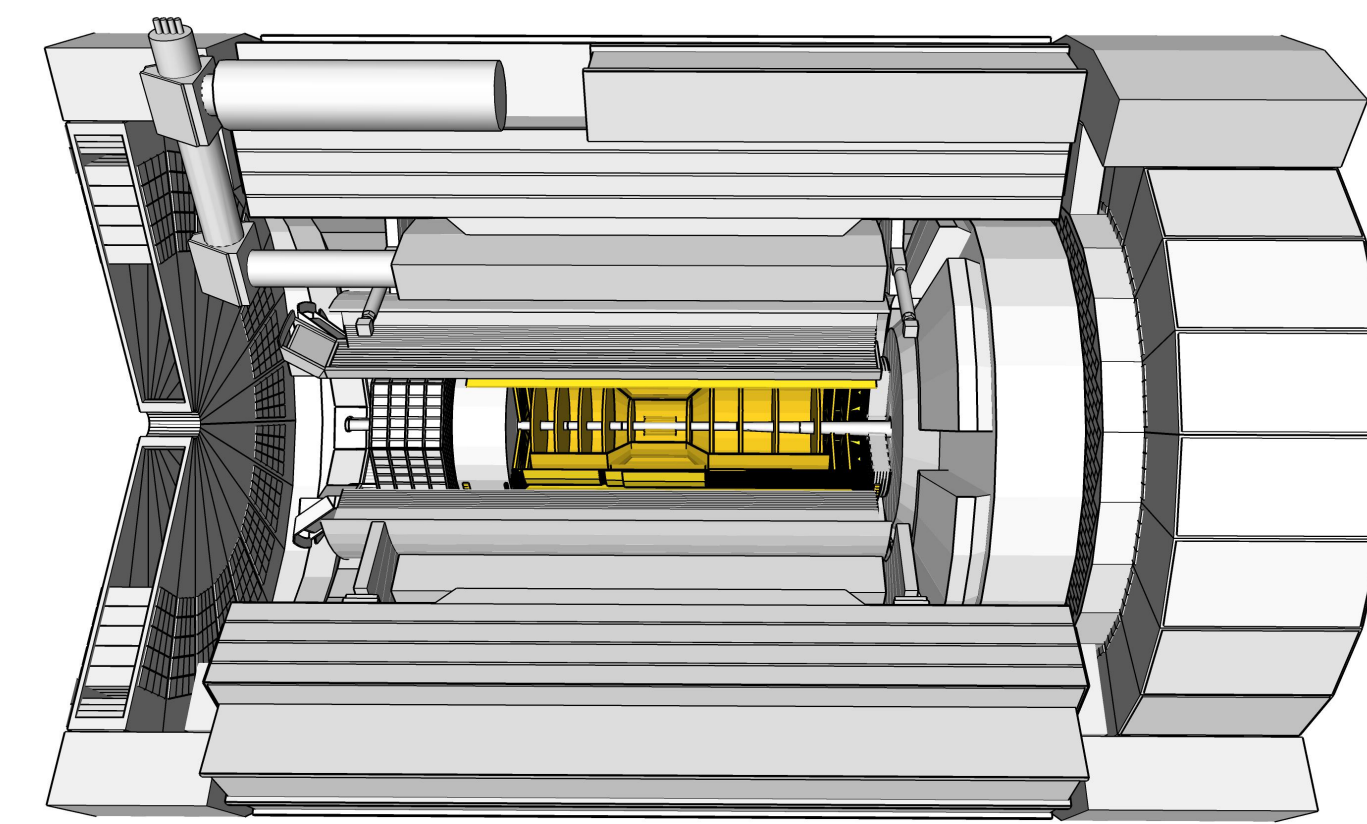
Tracking system

- 1.7 T magnet
- Monolithic Active Pixel Sensor (MAPS)
Silicon vertexing/inner tracker
- Micro-pattern gaseous detectors
 μ RWELL/microMegas:
timing & pattern recognition
- AC-LGAD based TOF:
PID & additional tracking point
momentum resolution



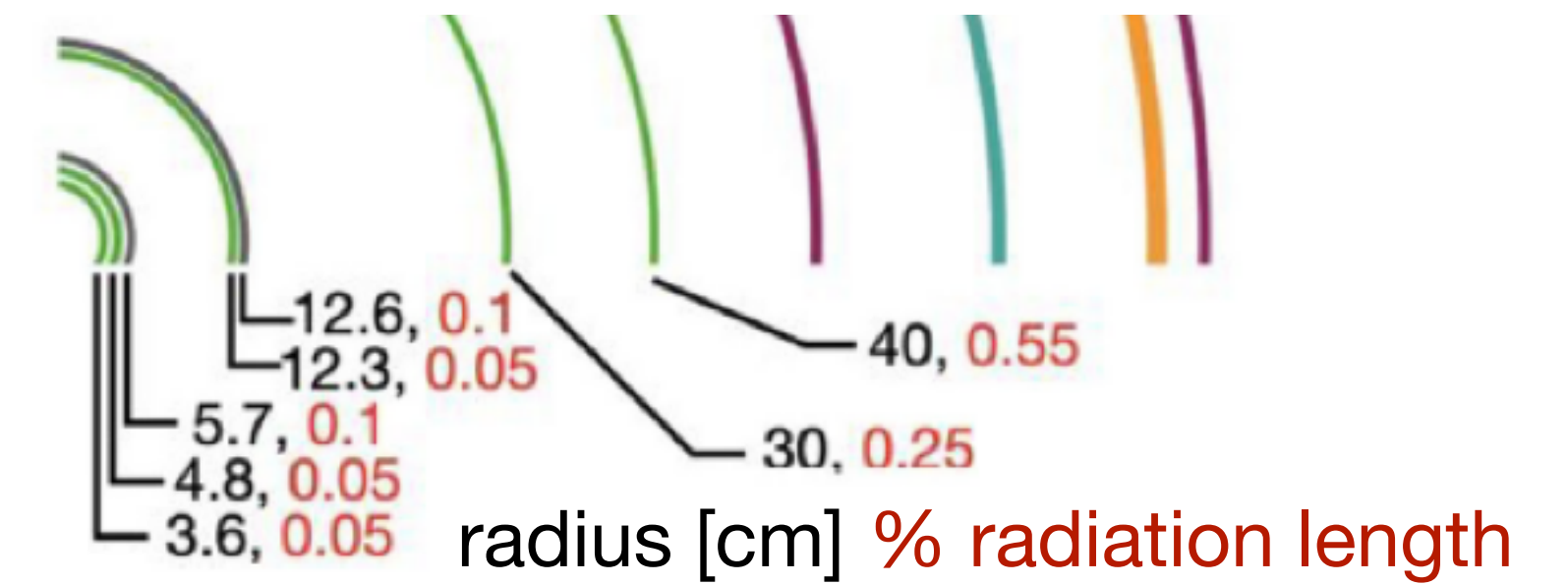
Tracking system

- 1.7 T magnet
- Monolithic Active Pixel Sensor (MAPS)
Silicon vertexing/inner tracker
- Micro-pattern gaseous detectors
 μ RWELL/microMegas:
timing & pattern recognition
- AC-LGAD based TOF:
PID & additional tracking point
momentum resolution

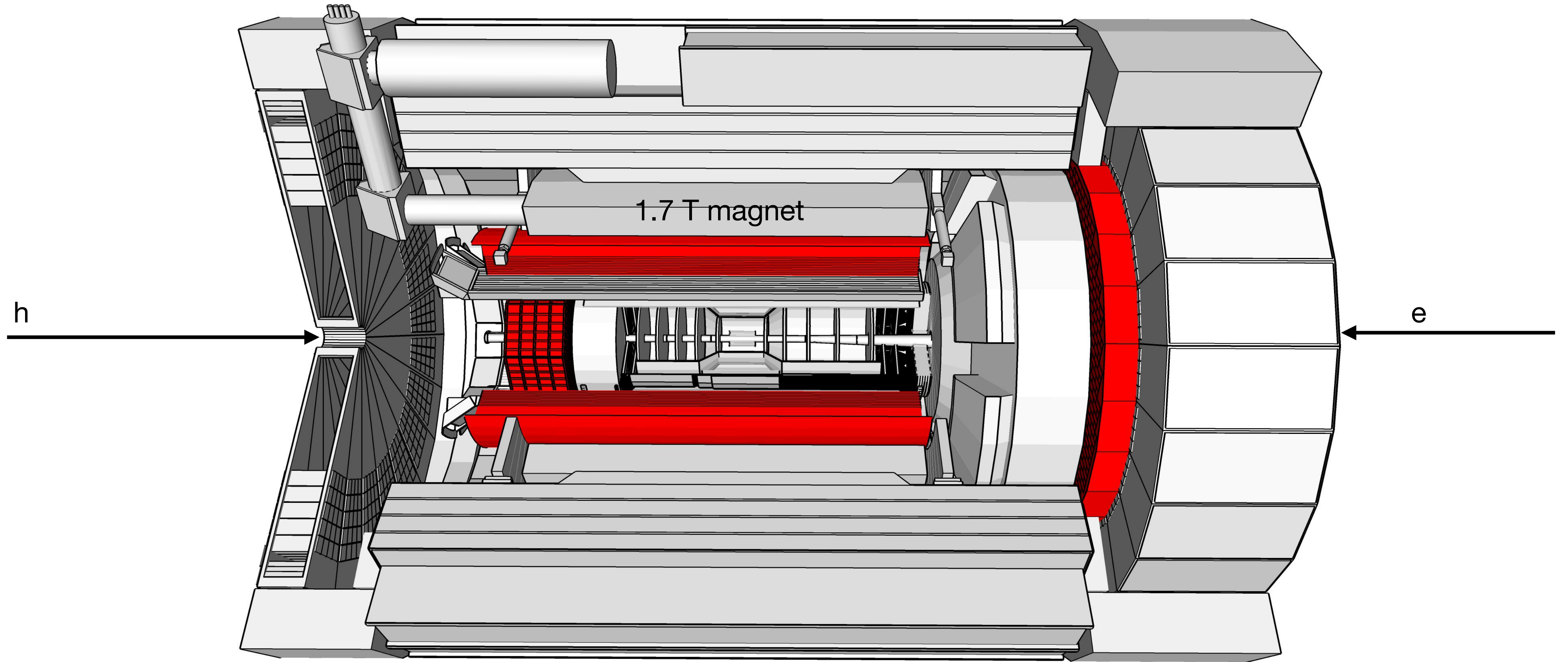


complemented with
electromagnetic calorimeter

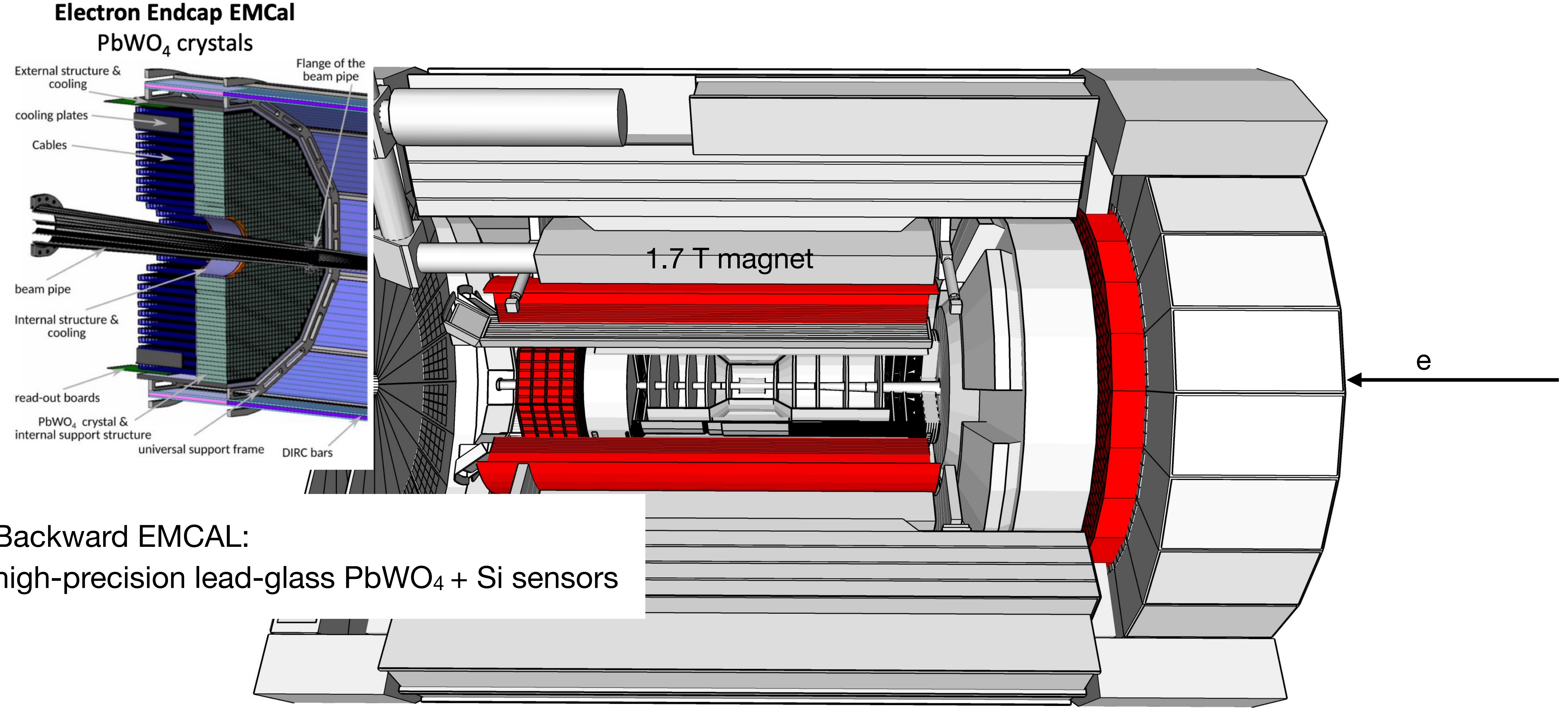
microMegas



Electromagnetic calorimeter

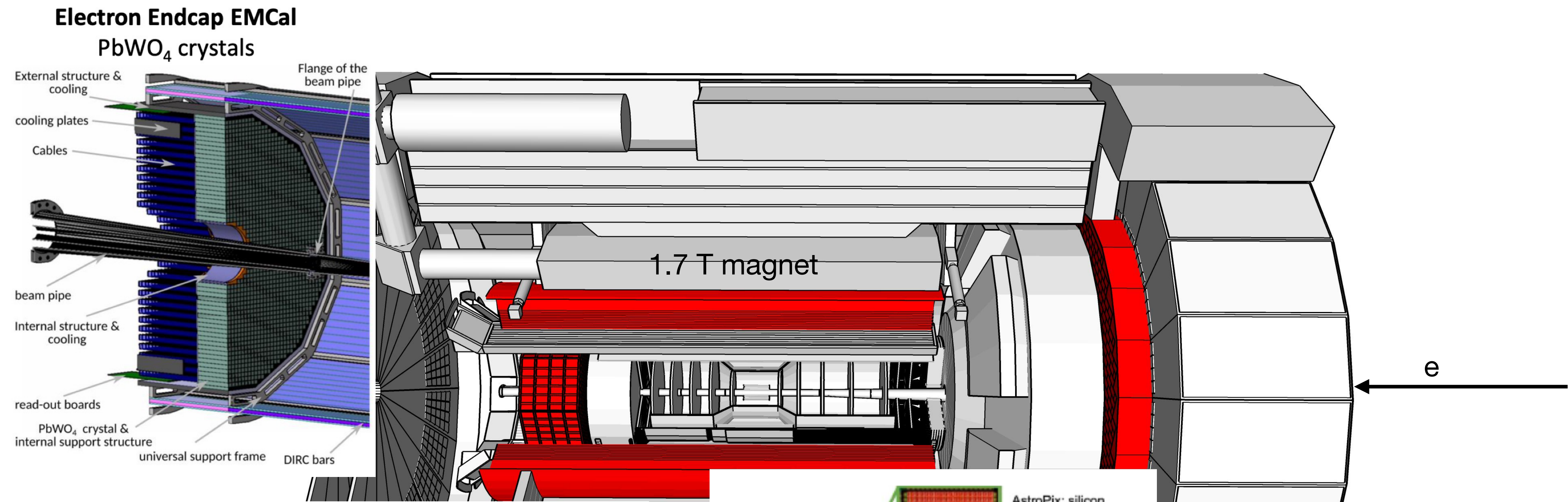


Electromagnetic calorimeter

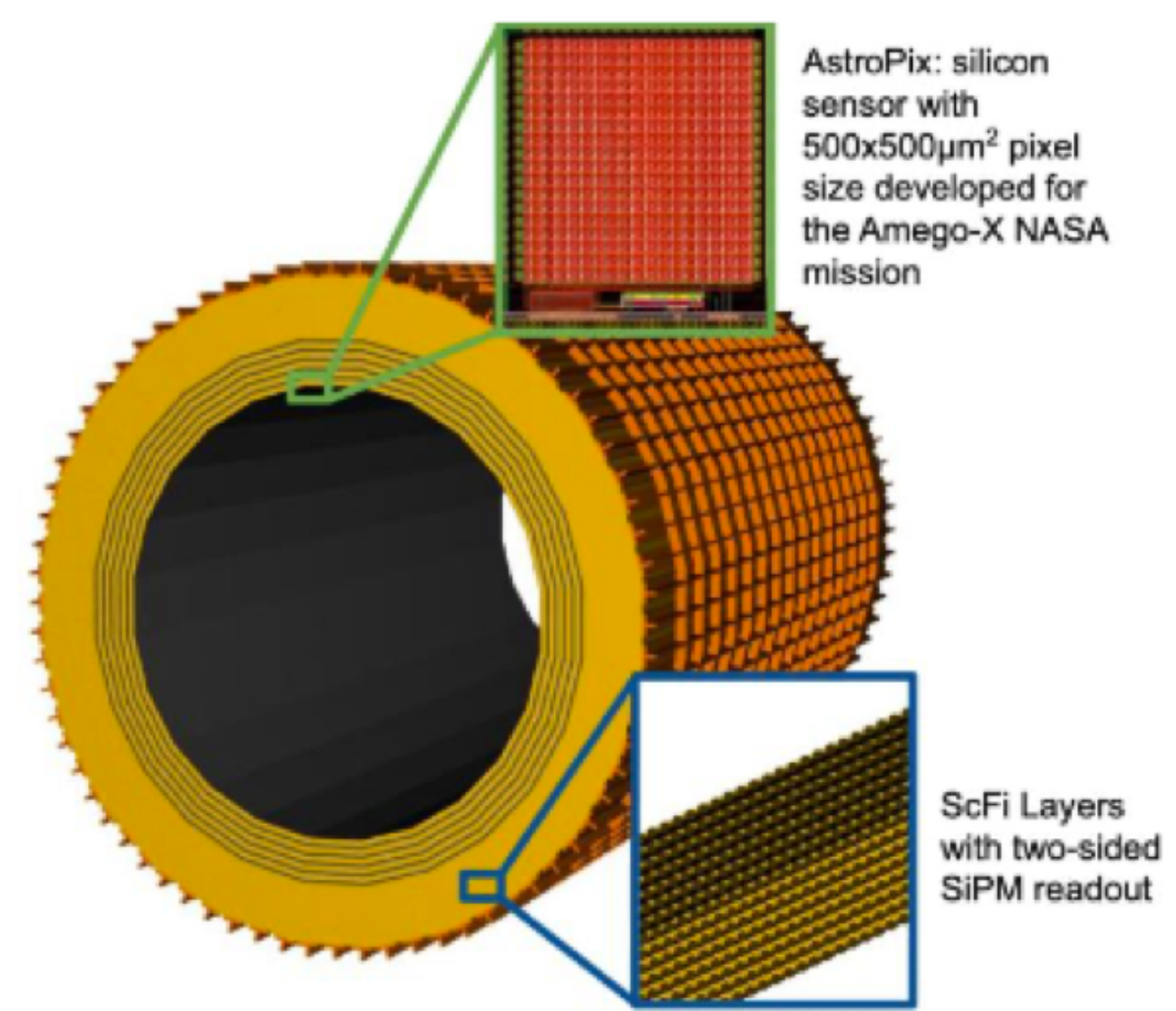


- Backward EMCAL:
high-precision lead-glass PbWO₄ + Si sensors

Electromagnetic calorimeter

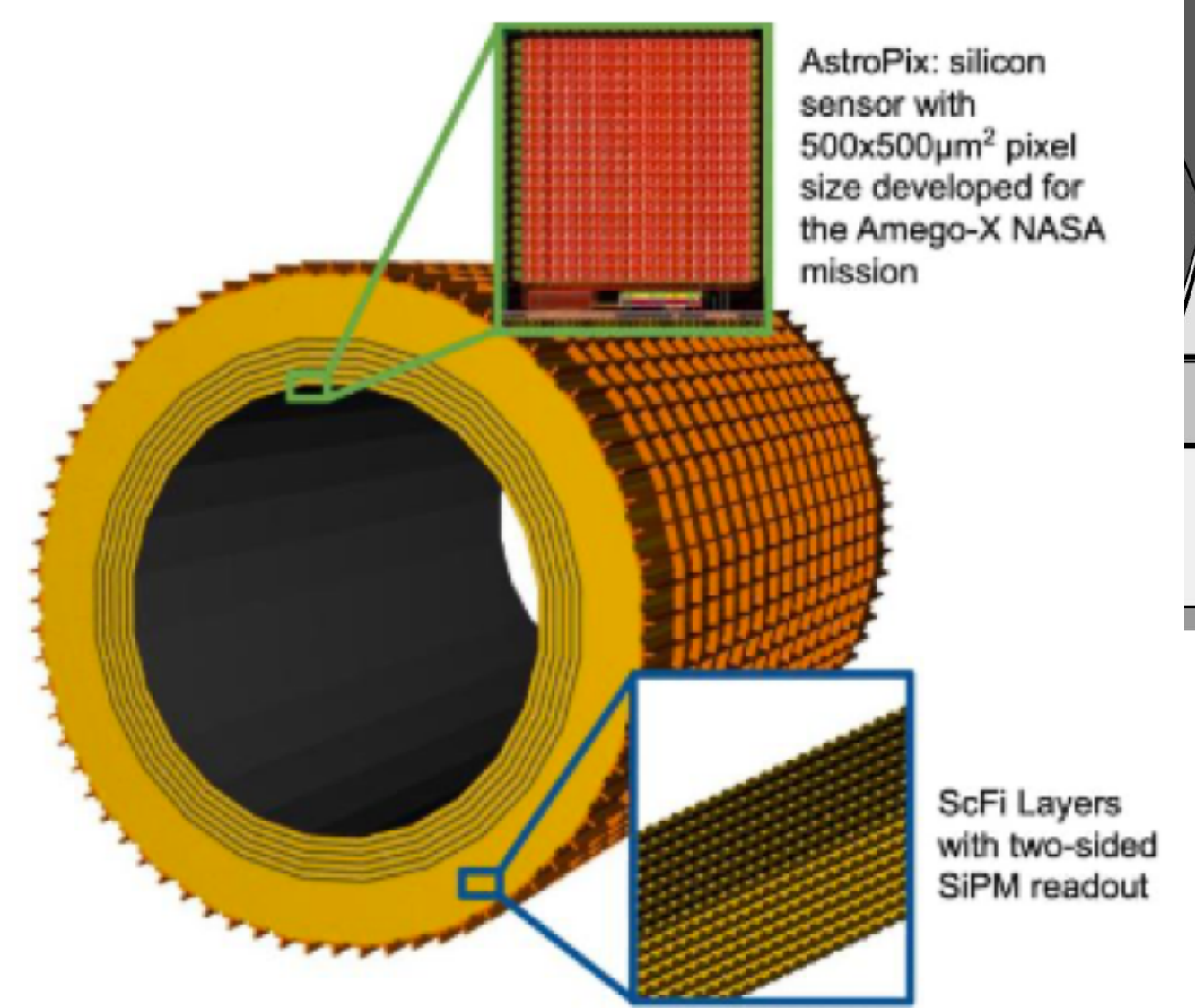
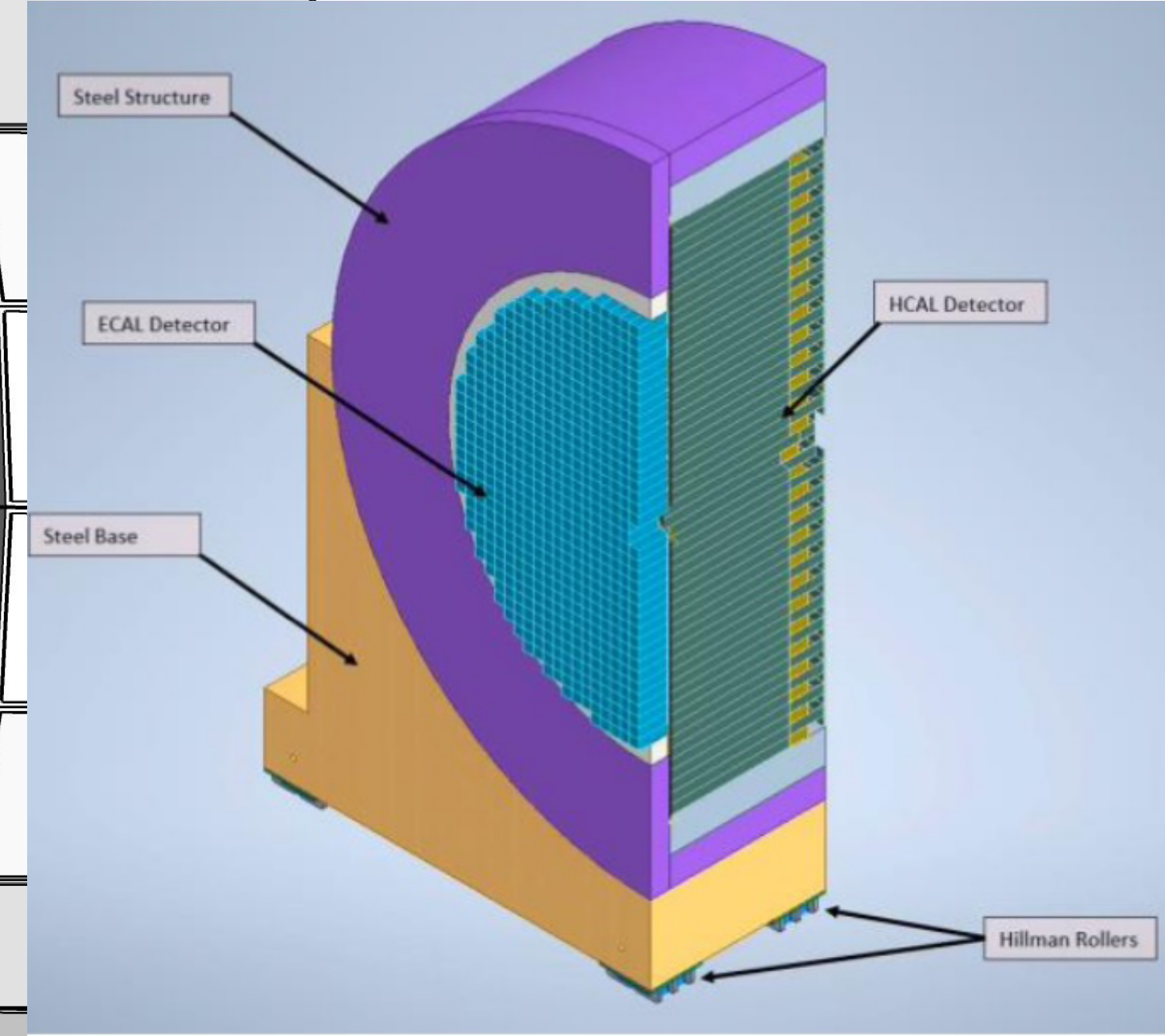
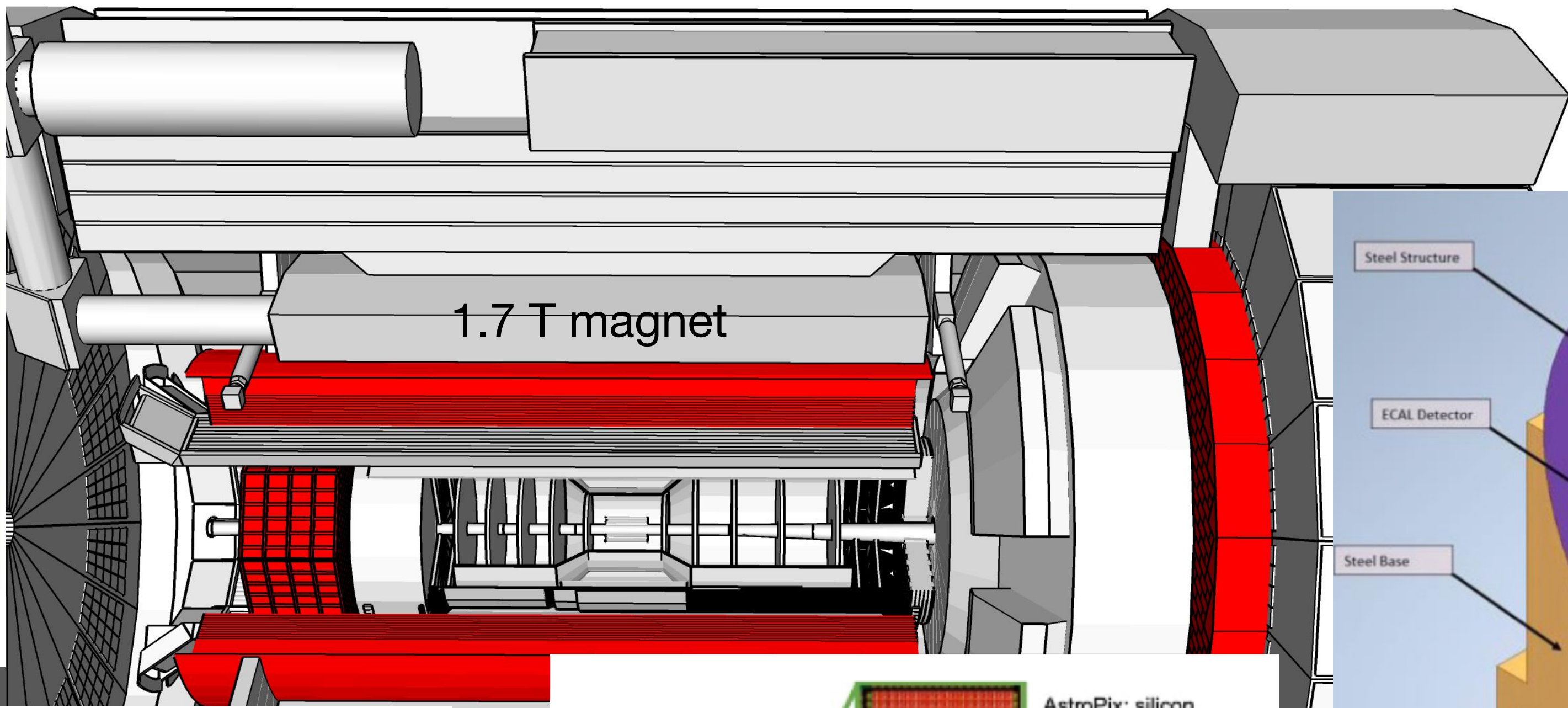
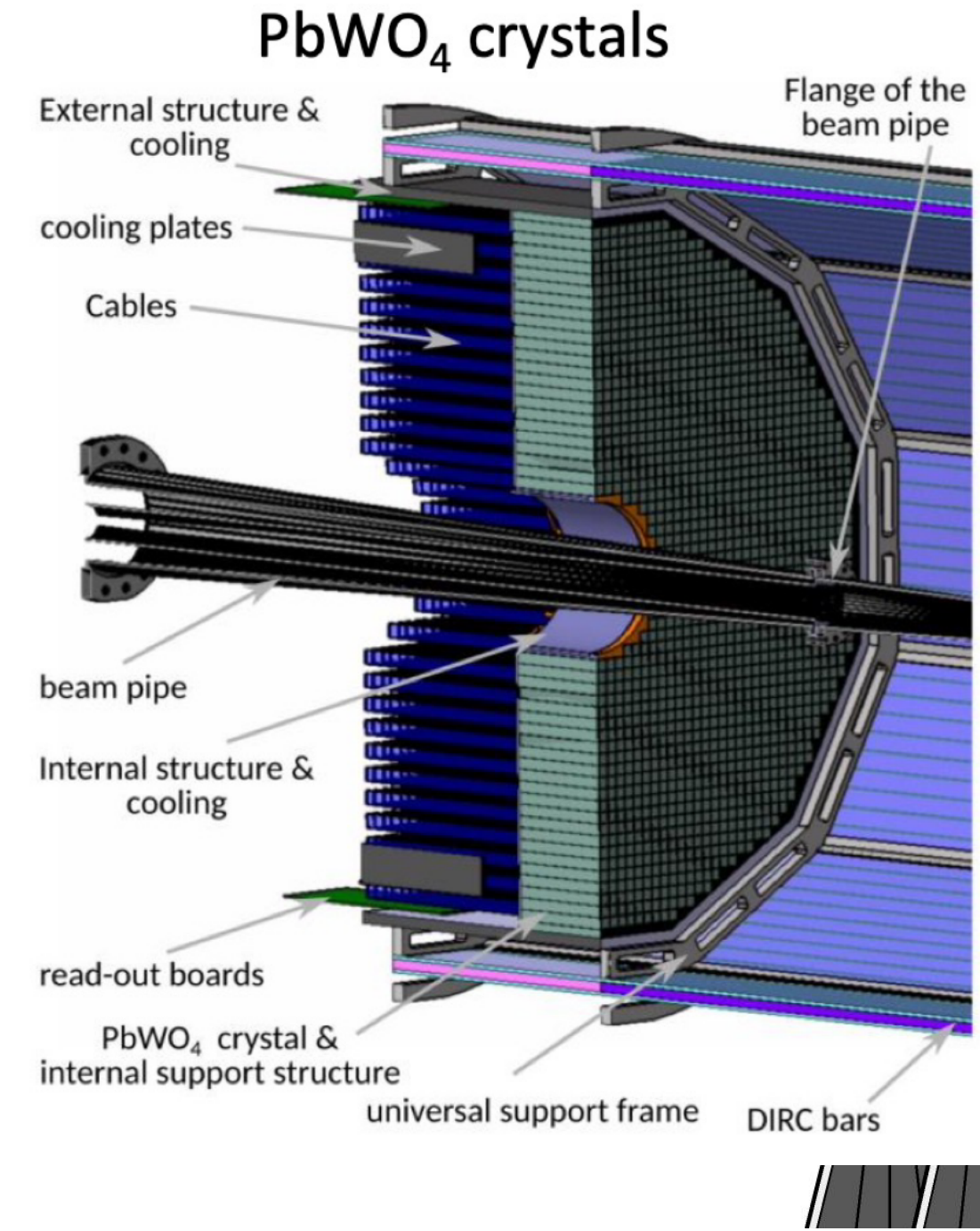


- Backward EMCAL:
high-precision lead-glass PbWO_4 + Si sensors
- Barrel EMCAL:
3D imaging with MAPS and sampling Pb/
scintillating fibres with Si sensors



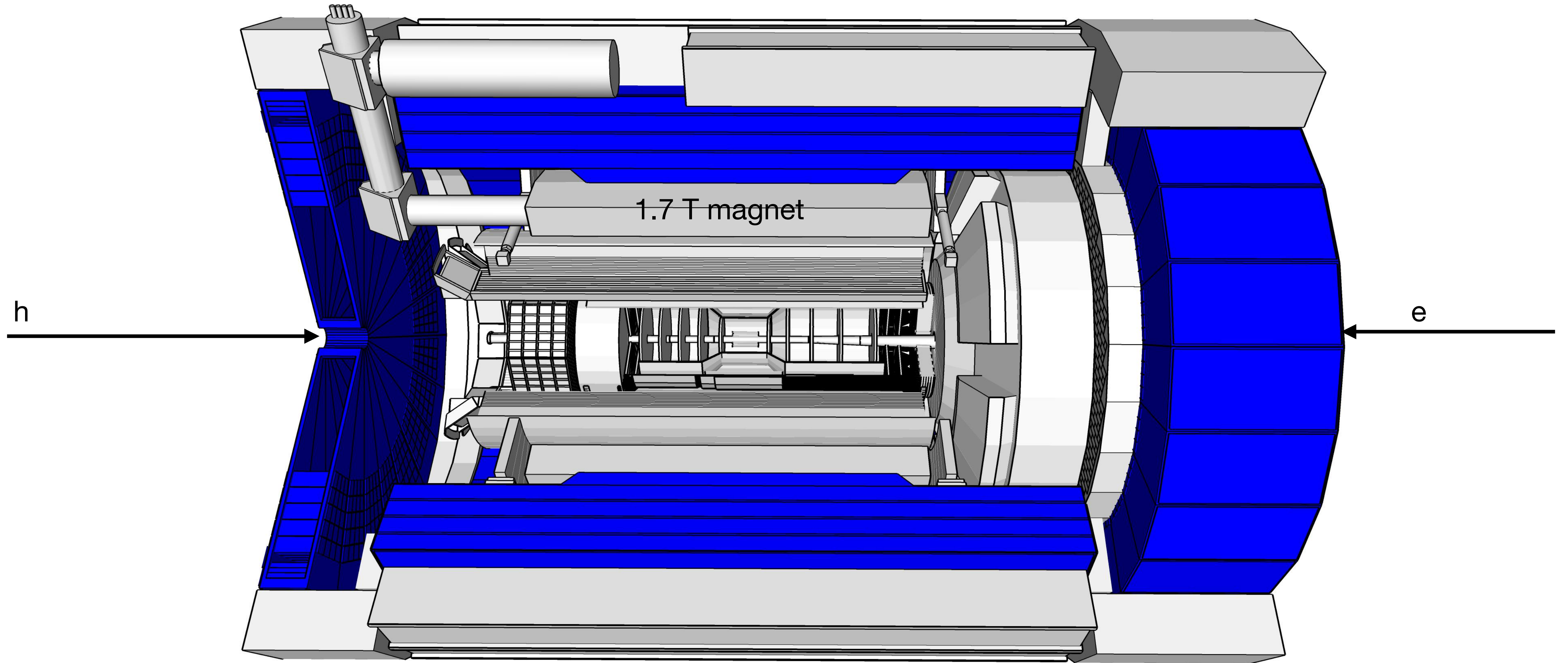
Electromagnetic calorimeter

Electron Endcap EMCal

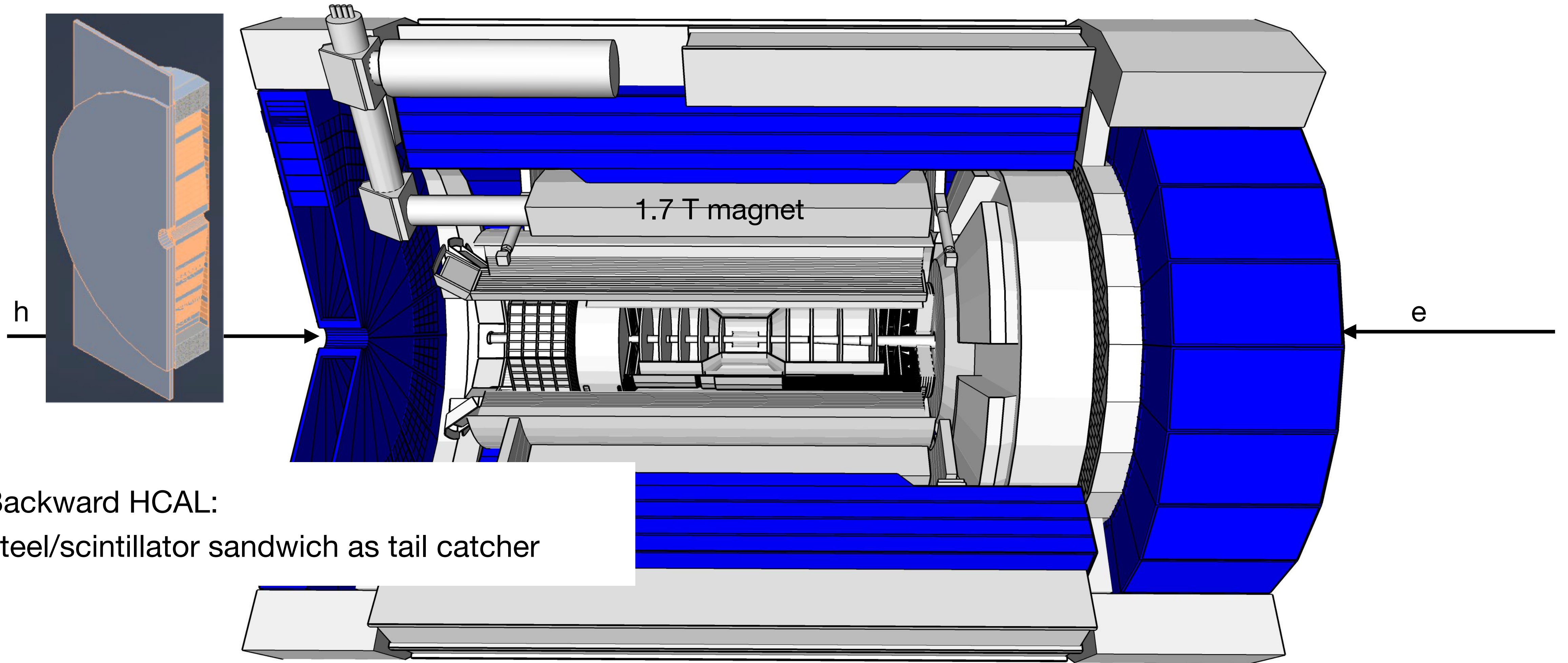


- Backward EMCAL: high-precision PbWO₄ + Si sensors
- Barrel EMCAL: 3D imaging with MAPS and sampling Pb/scintillating fibres with Si sensors
- Forward EMCAL: finely segmented W powder/scintillating fibres

Hadronic calorimeter

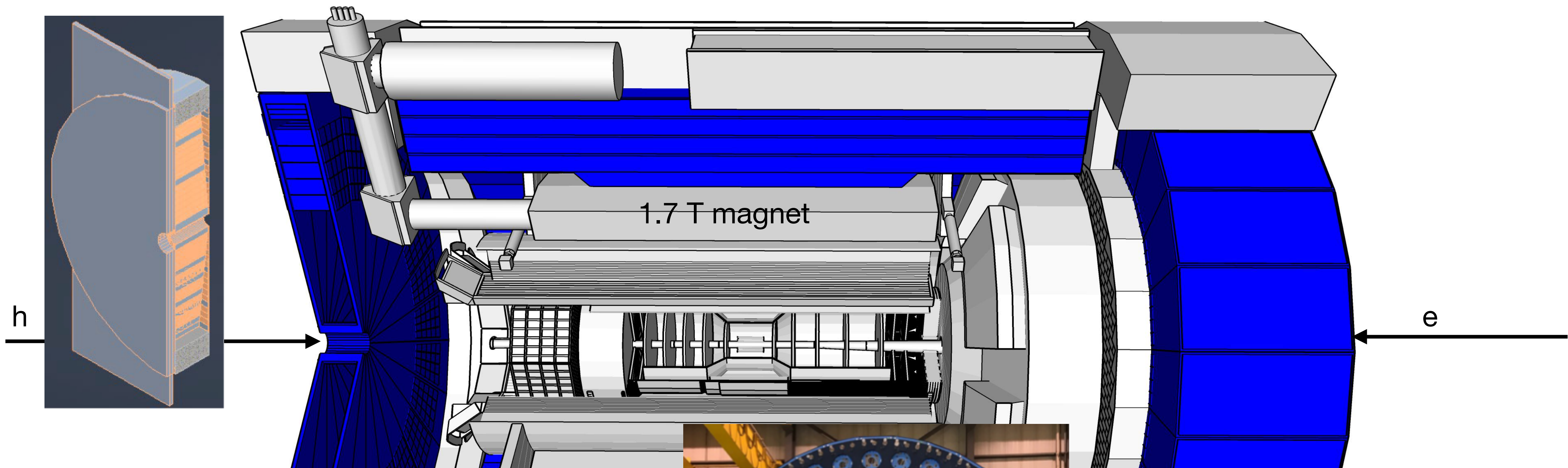


Hadronic calorimeter



- Backward HCAL:
steel/scintillator sandwich as tail catcher

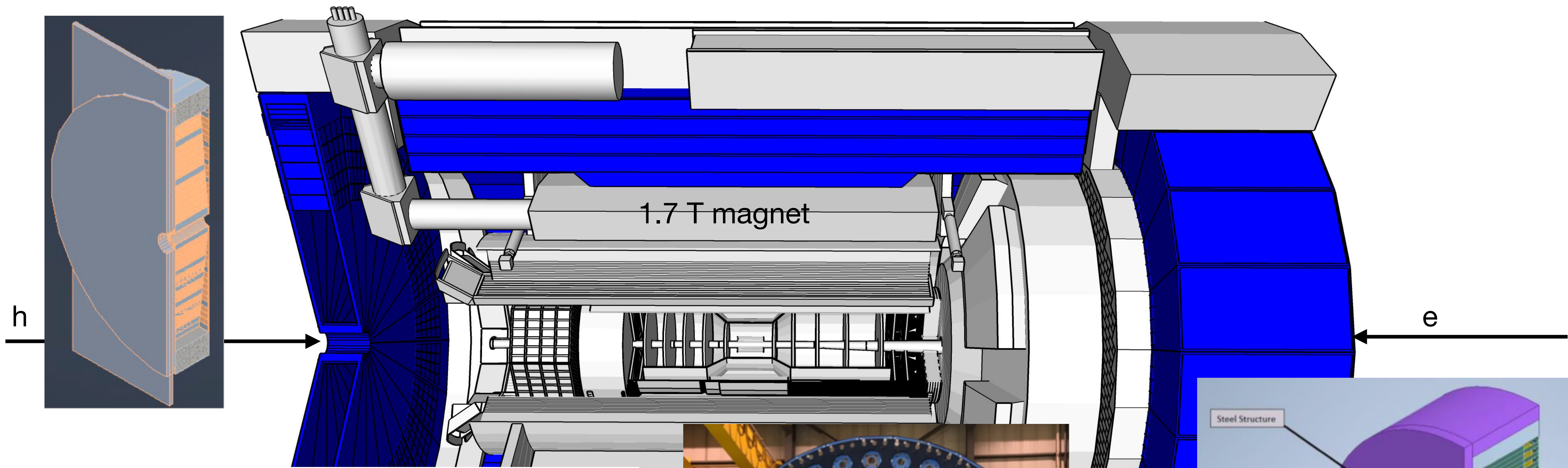
Hadronic calorimeter



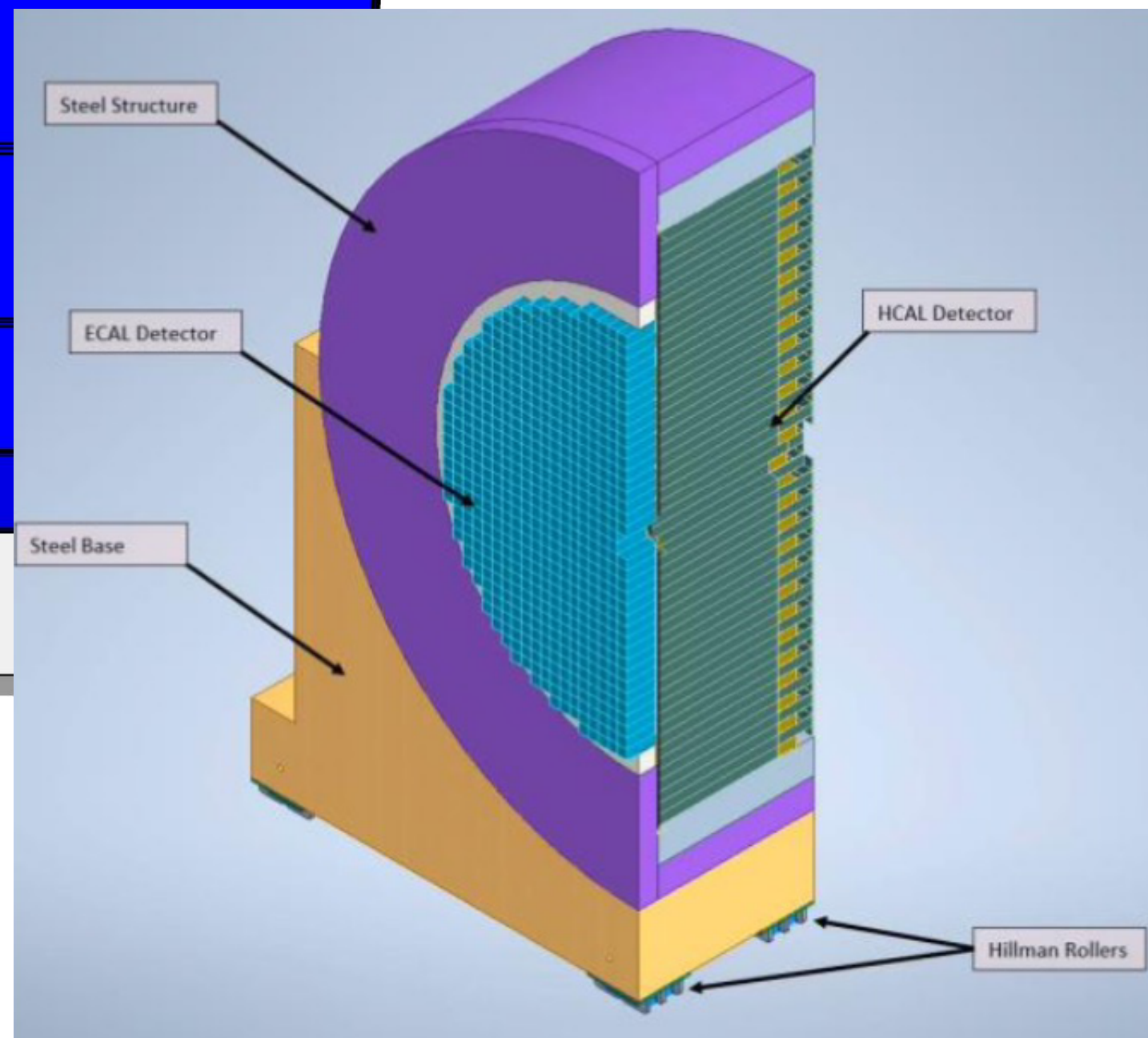
- Backward HCAL:
steel/scintillator sandwich as tail catcher
- Barrel HCAL:
Fe/scintillator sandwich: detection of neutrals



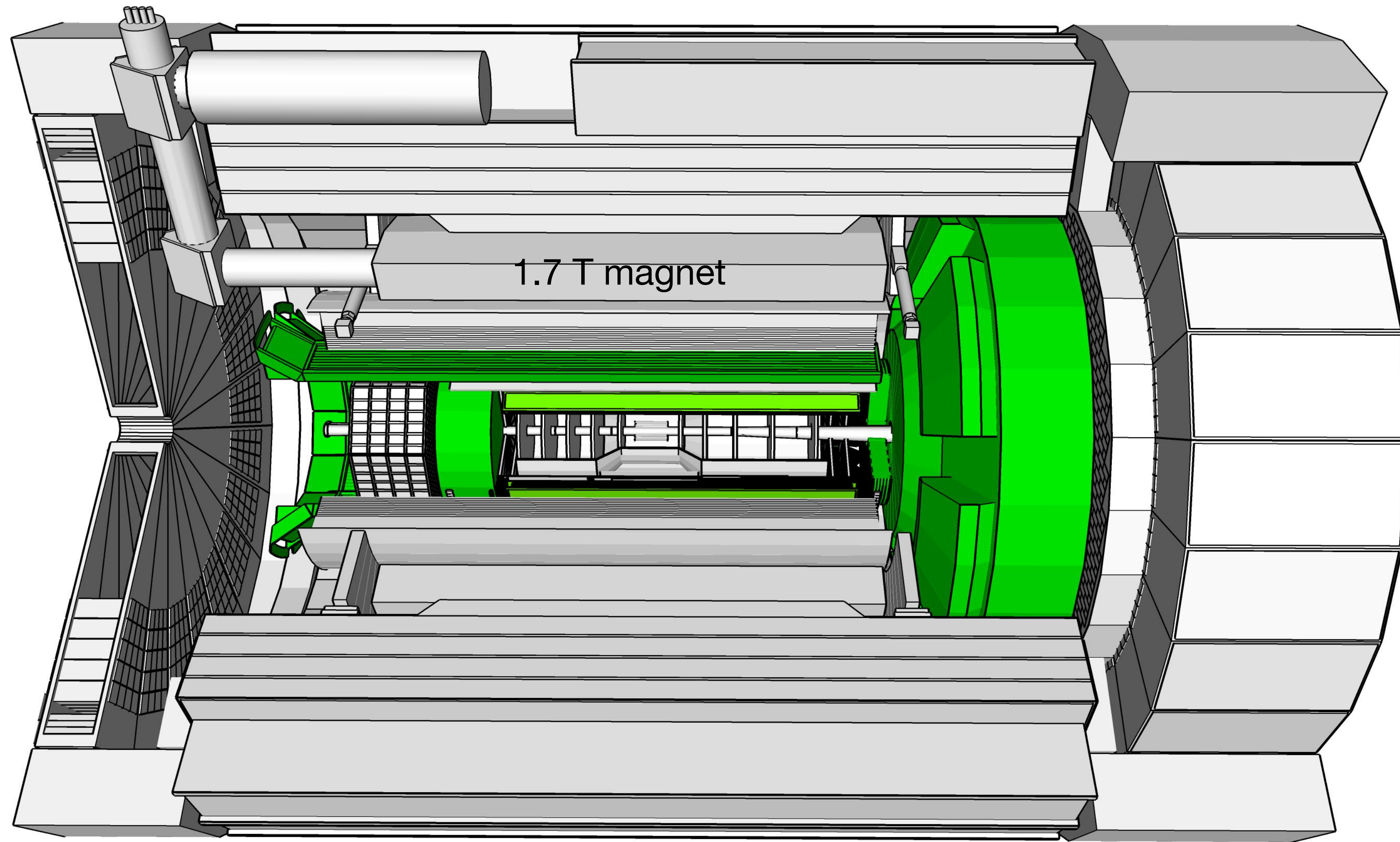
Hadronic calorimeter



- Backward HCAL:
steel/scintillator sandwich as tail catcher
- Barrel HCAL:
Fe/scintillator sandwich: detection of neutrals
- Forward HCAL:
W/scintillator sandwich longitudinally segmented, high granularity: good E resolution

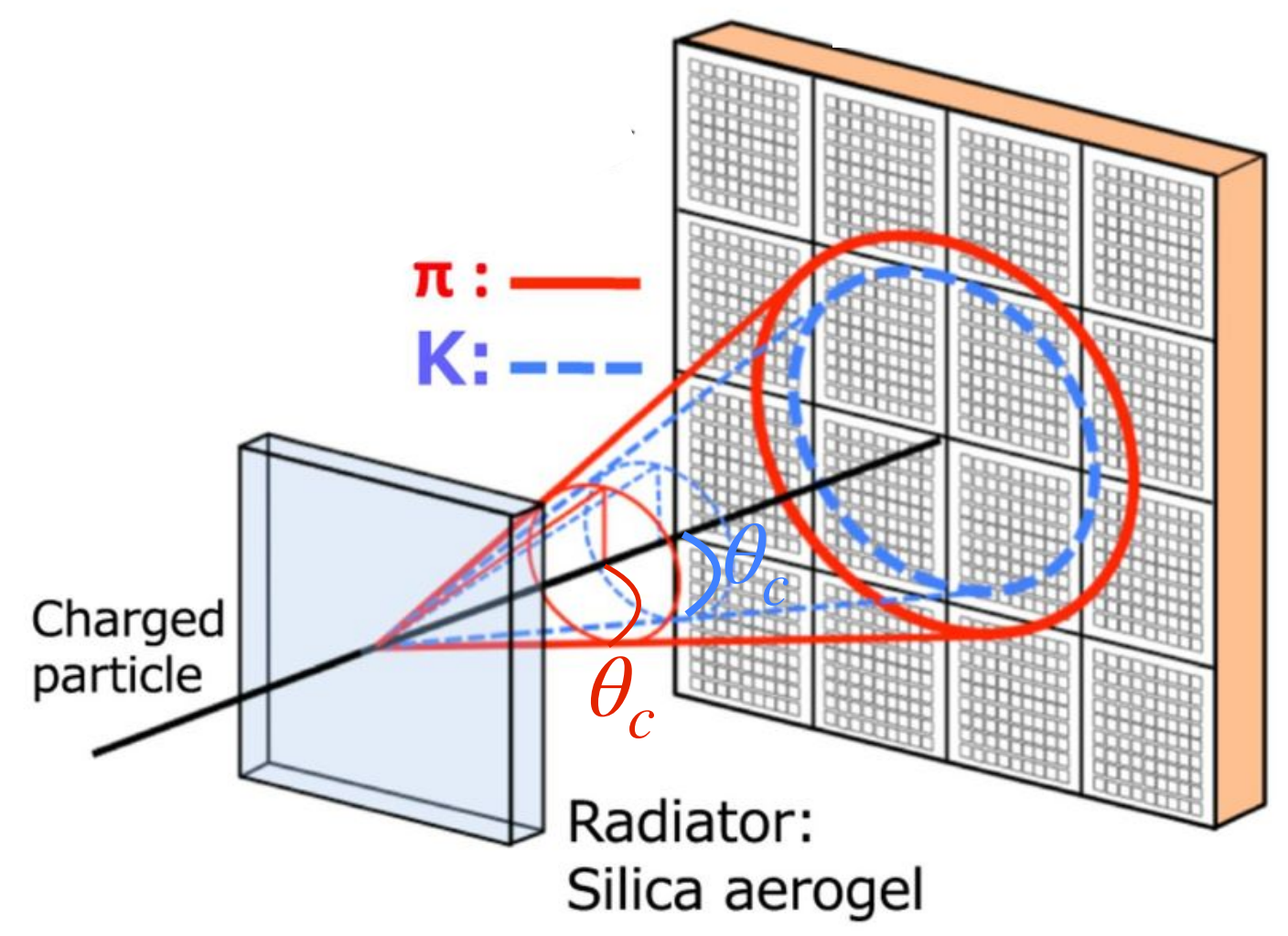
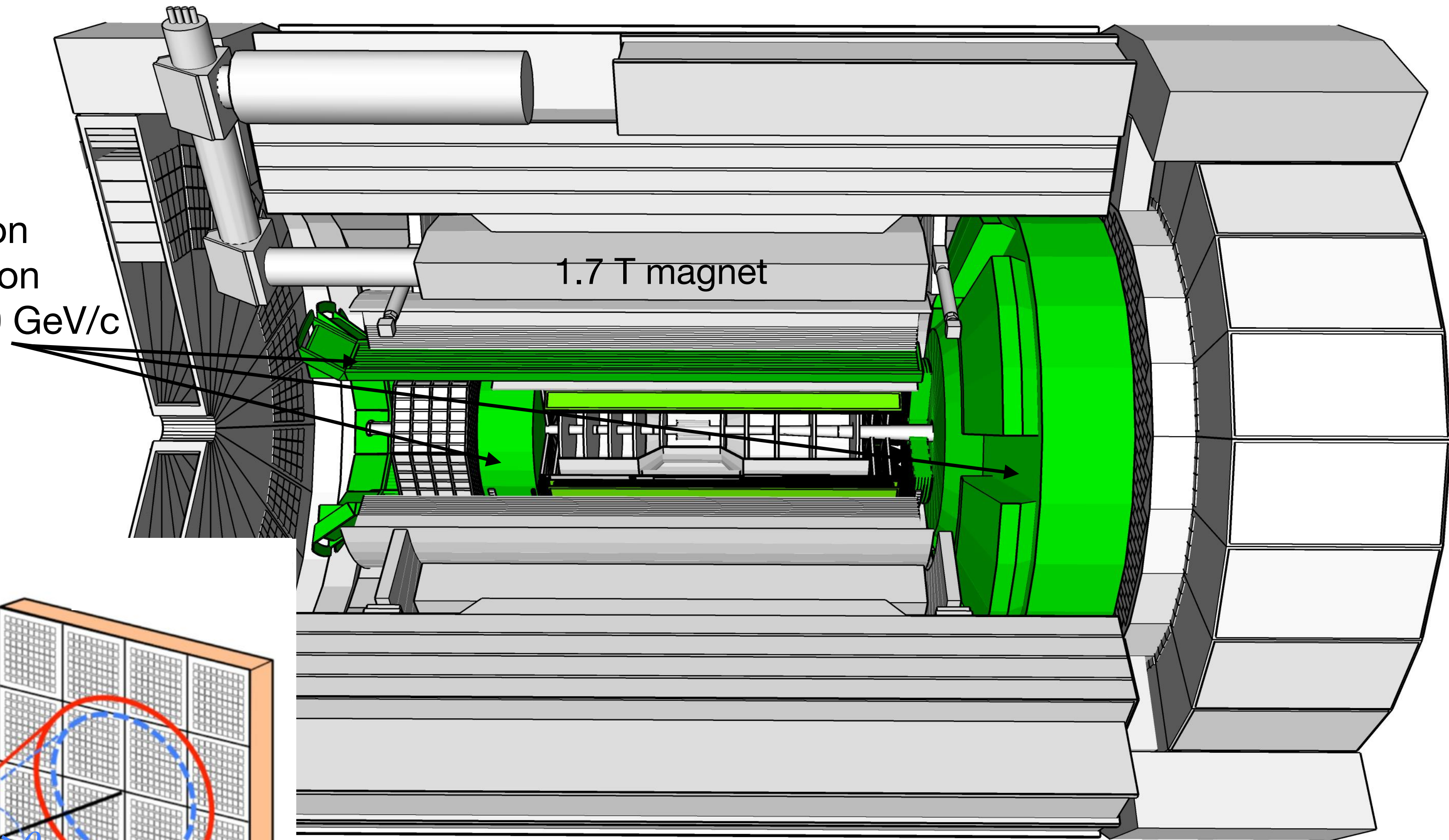


Particle identification



Particle identification

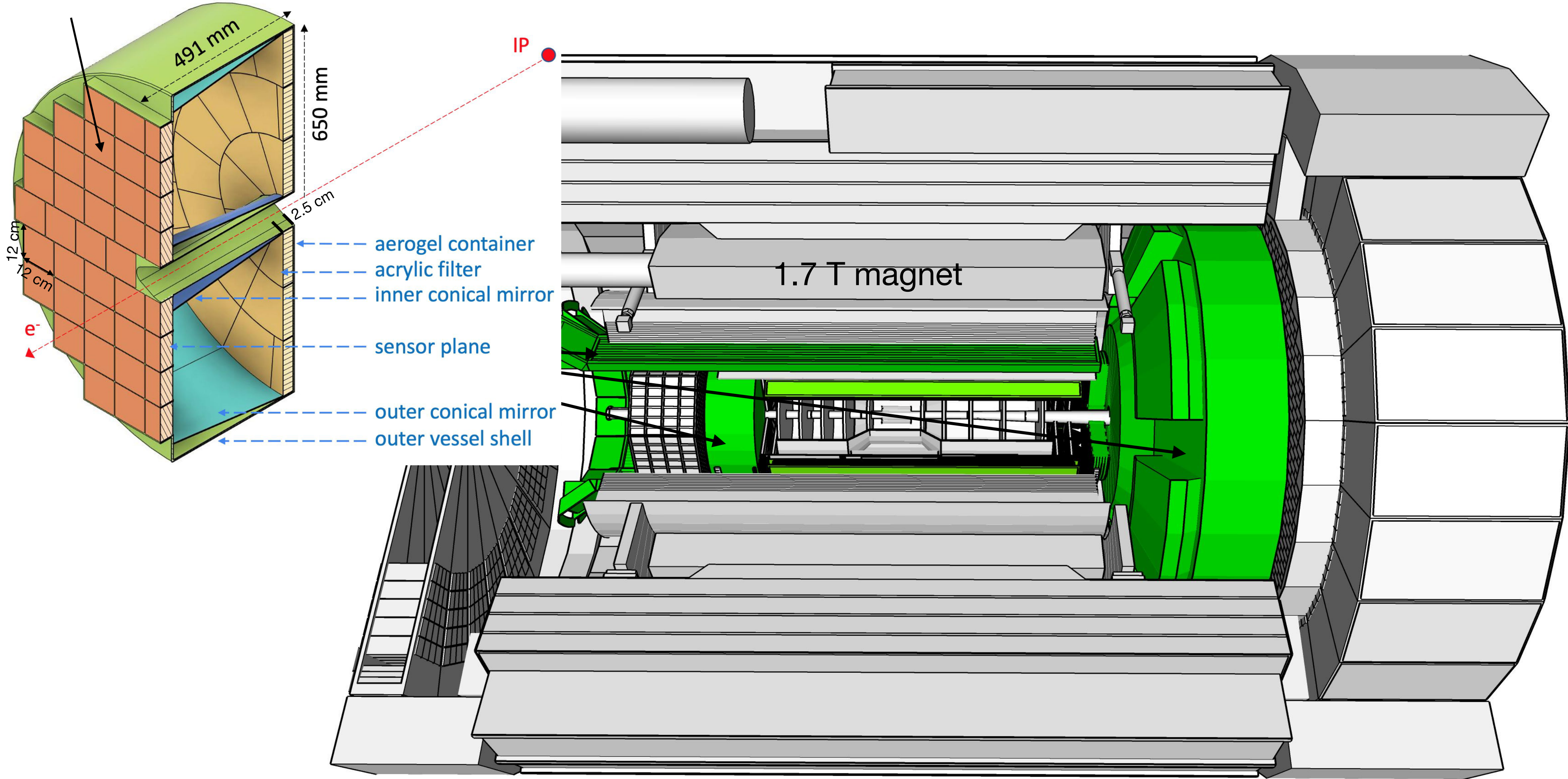
detectors based on Cherenkov radiation for $1 \text{ GeV}/c < p < 50 \text{ GeV}/c$



$$\cos \theta_c \propto \frac{1}{\gamma}$$

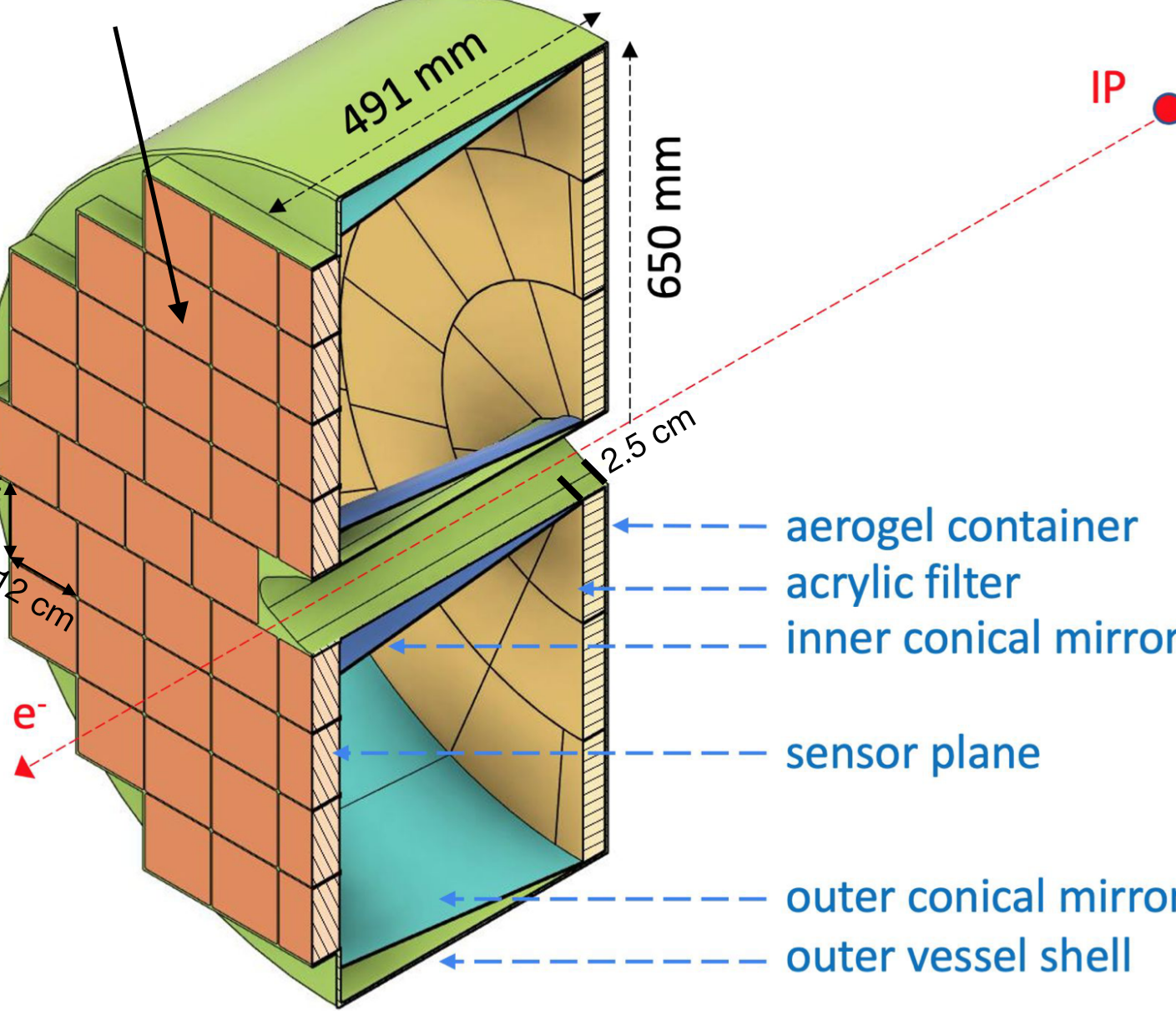
Particle identification

HRPPD photosensors,
include TOF

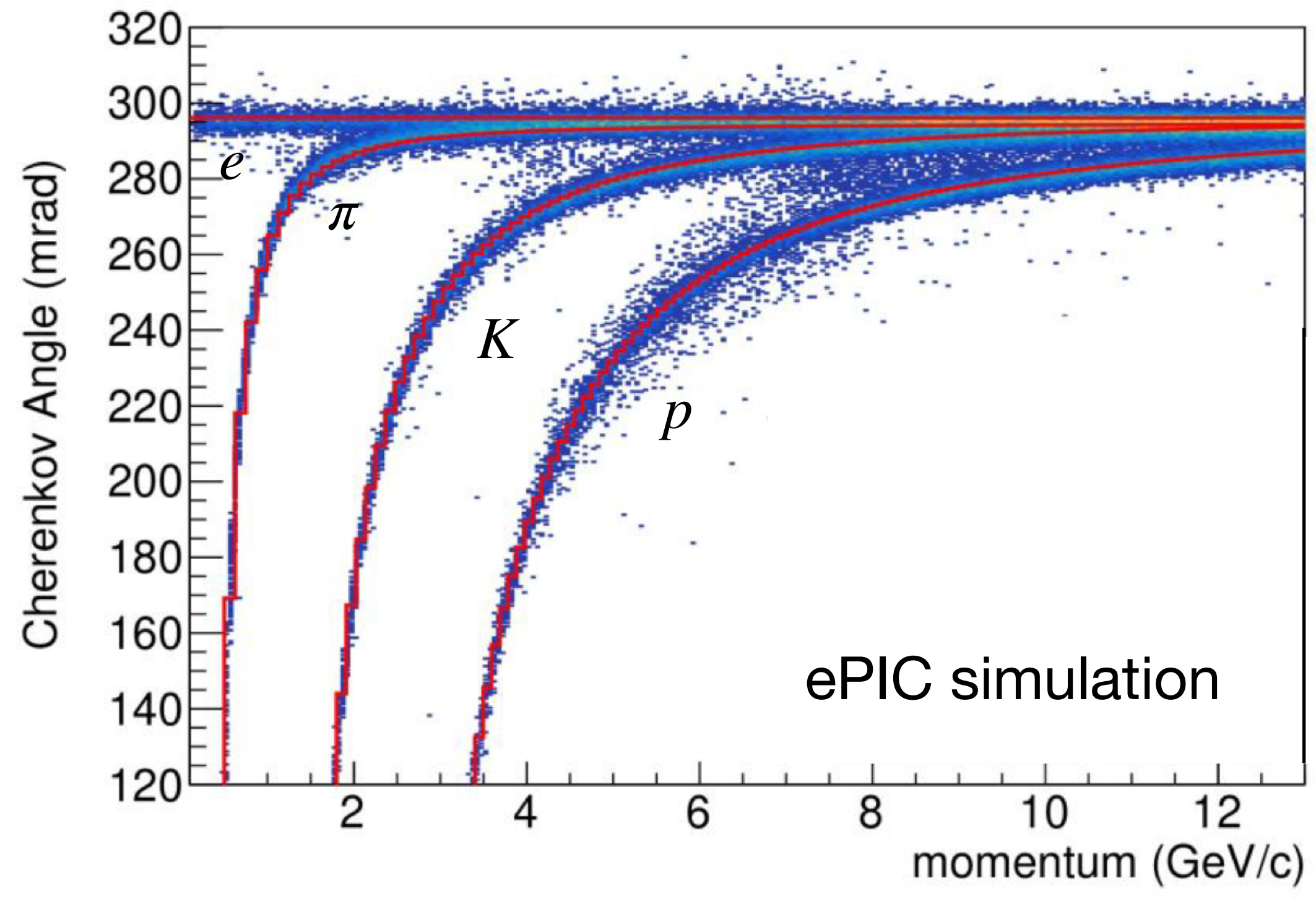
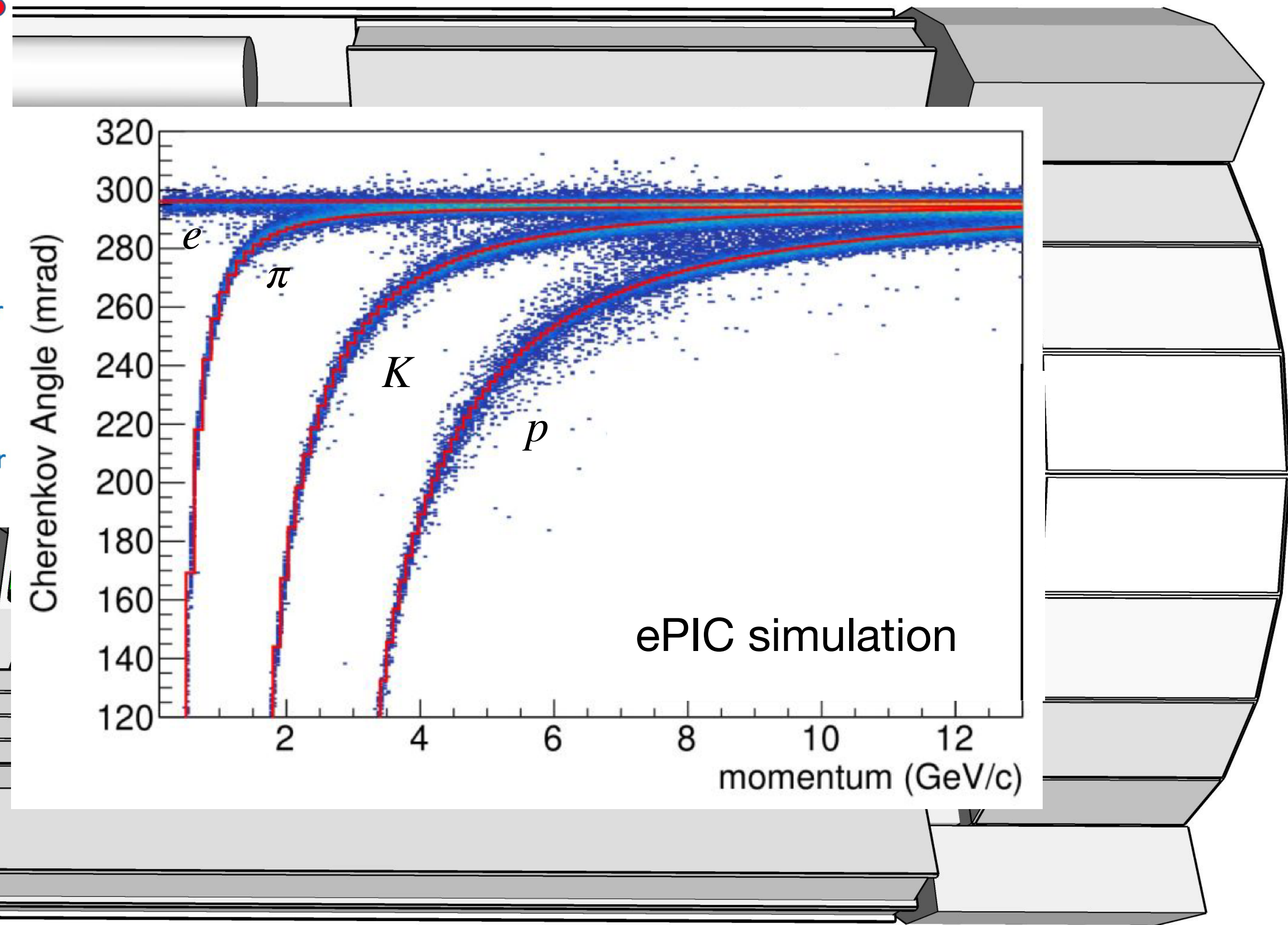


Particle identification

HRPPD photosensors, include TOF

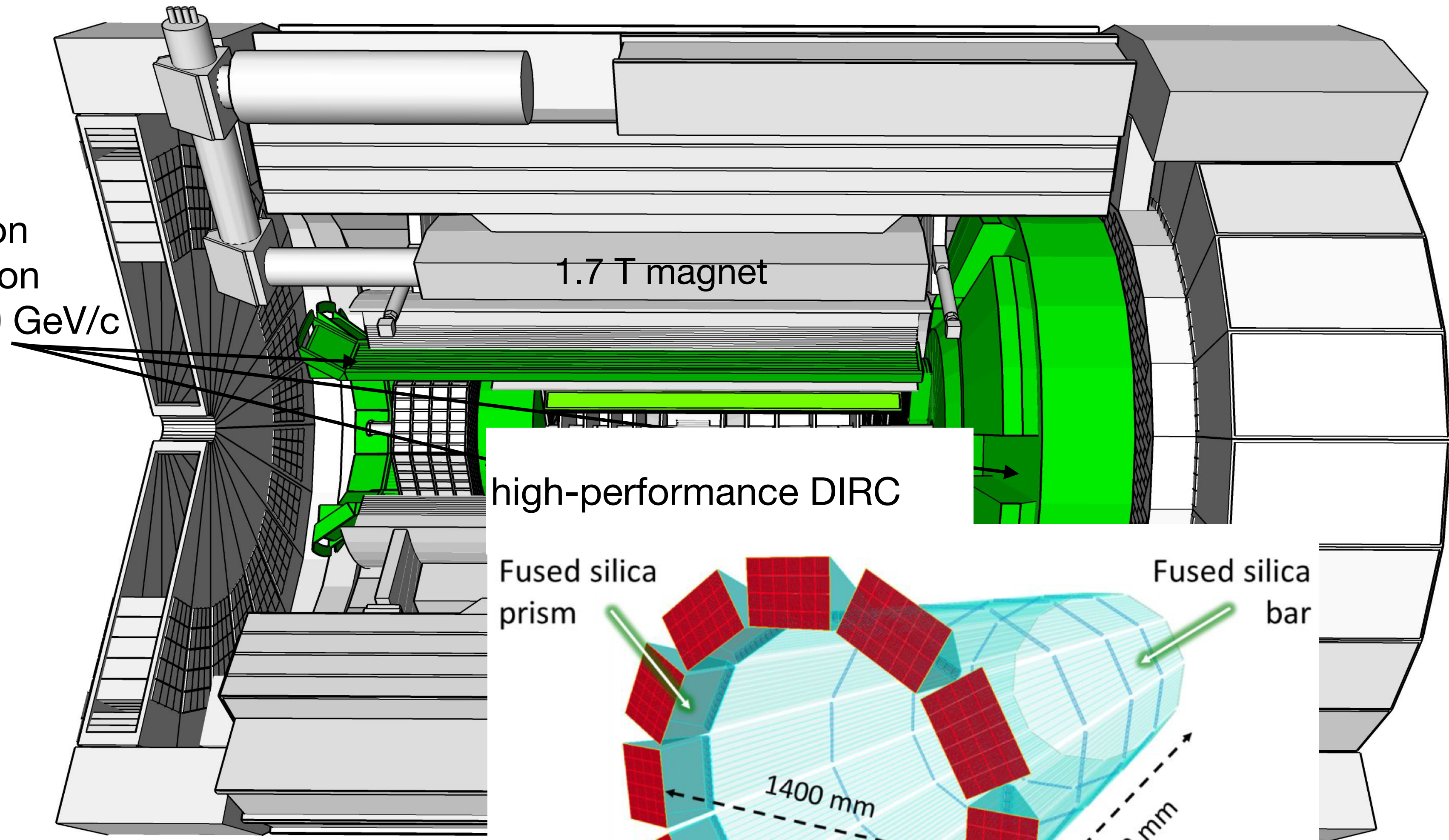


IP



Particle identification

detectors based on Cherenkov radiation for $1 \text{ GeV}/c < p < 50 \text{ GeV}/c$



high-performance DIRC

Fused silica prism

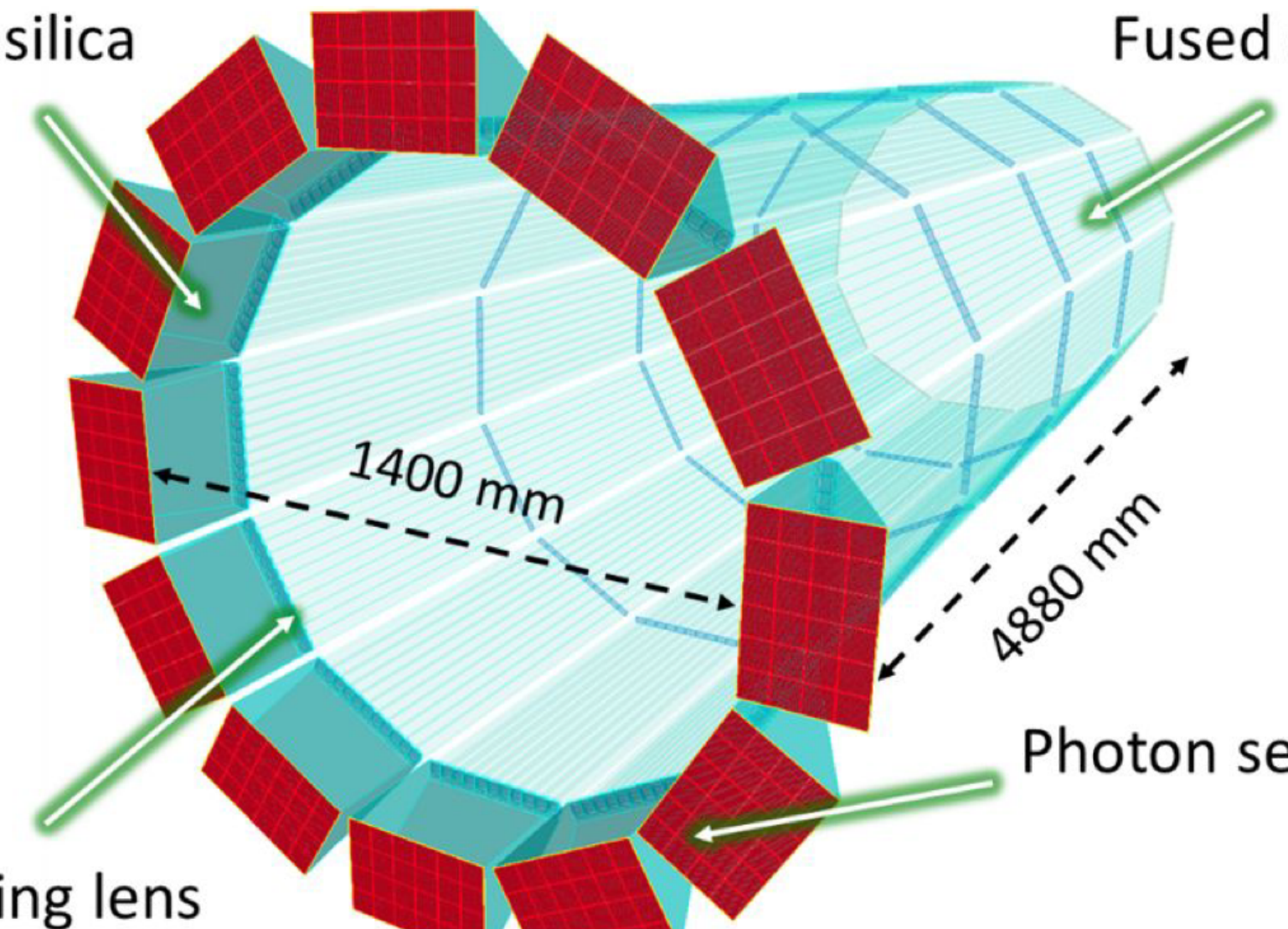
Fused silica bar

1400 mm

4880 mm

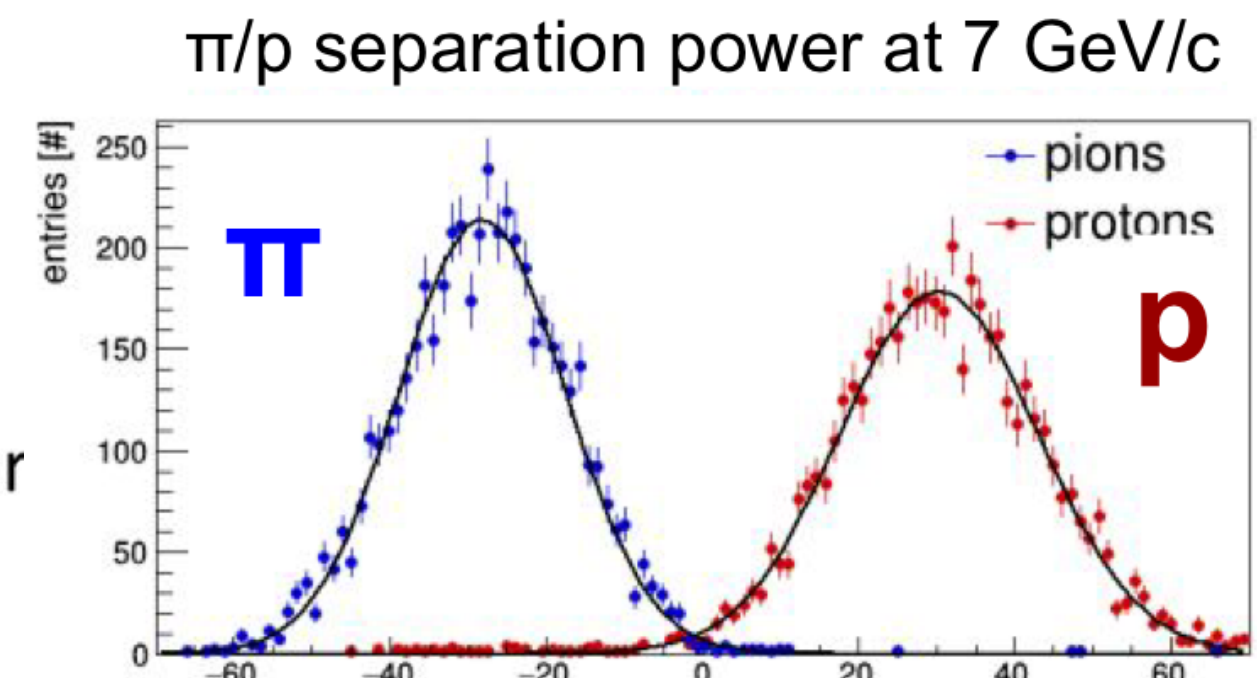
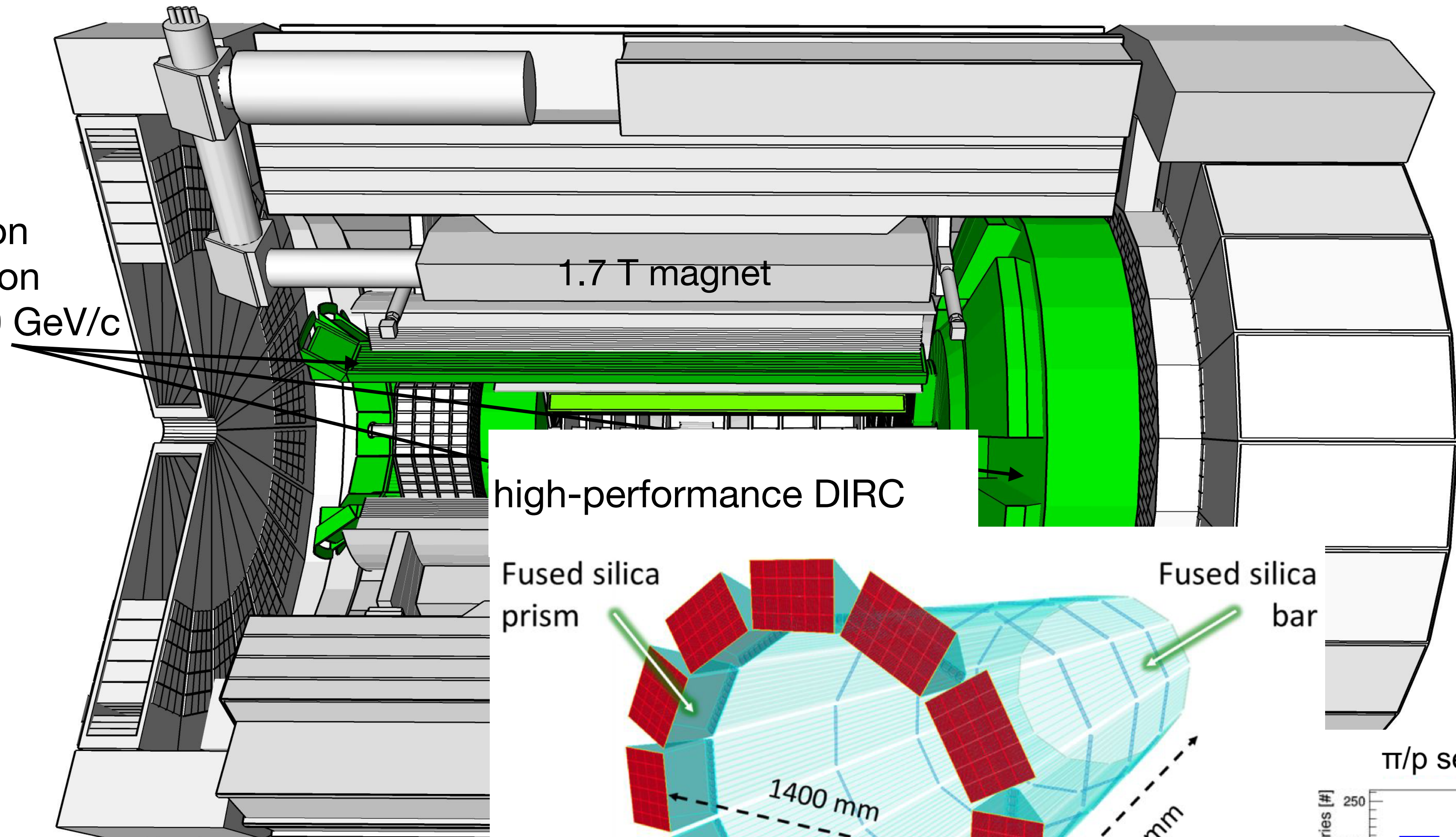
Photon sensor

Focusing lens



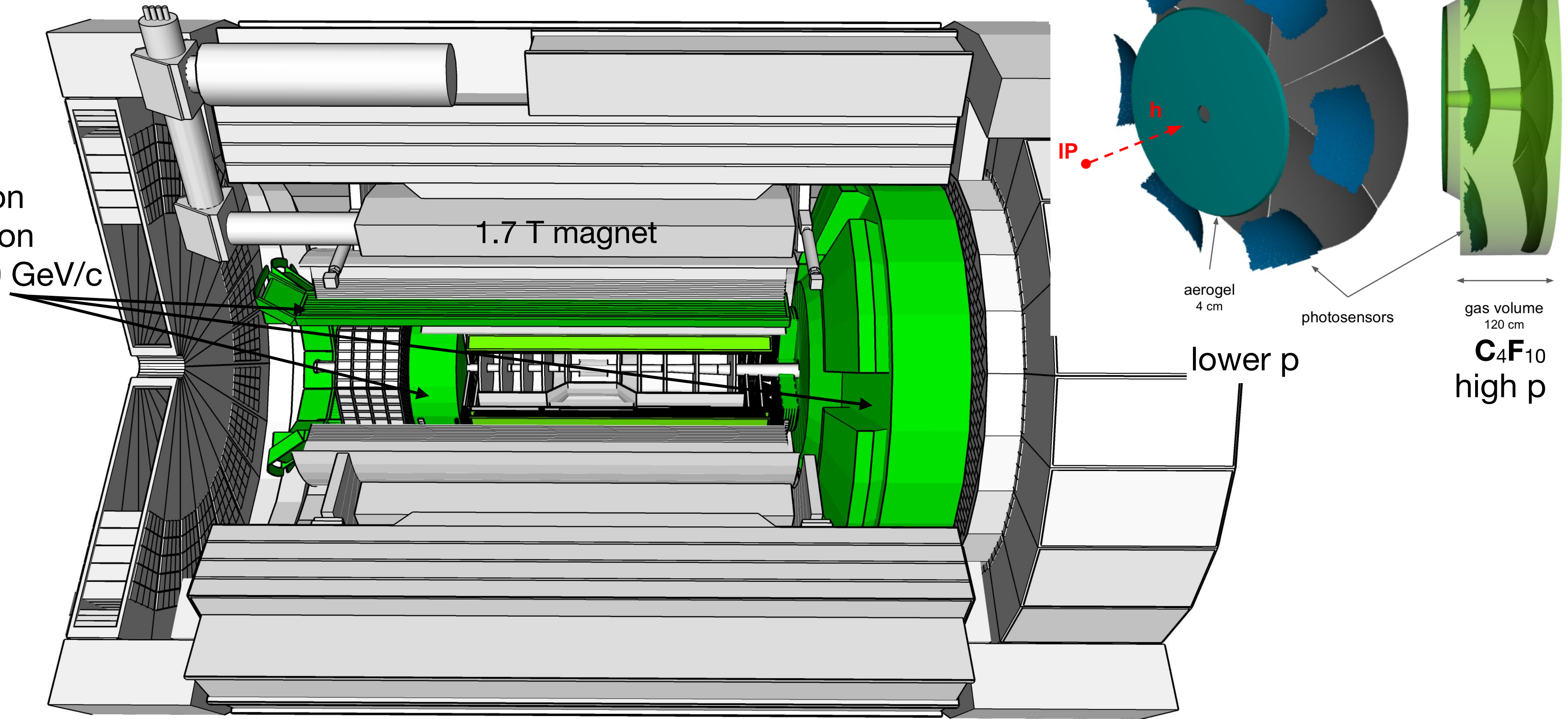
Particle identification

detectors based on Cherenkov radiation for $1 \text{ GeV}/c < p < 50 \text{ GeV}/c$



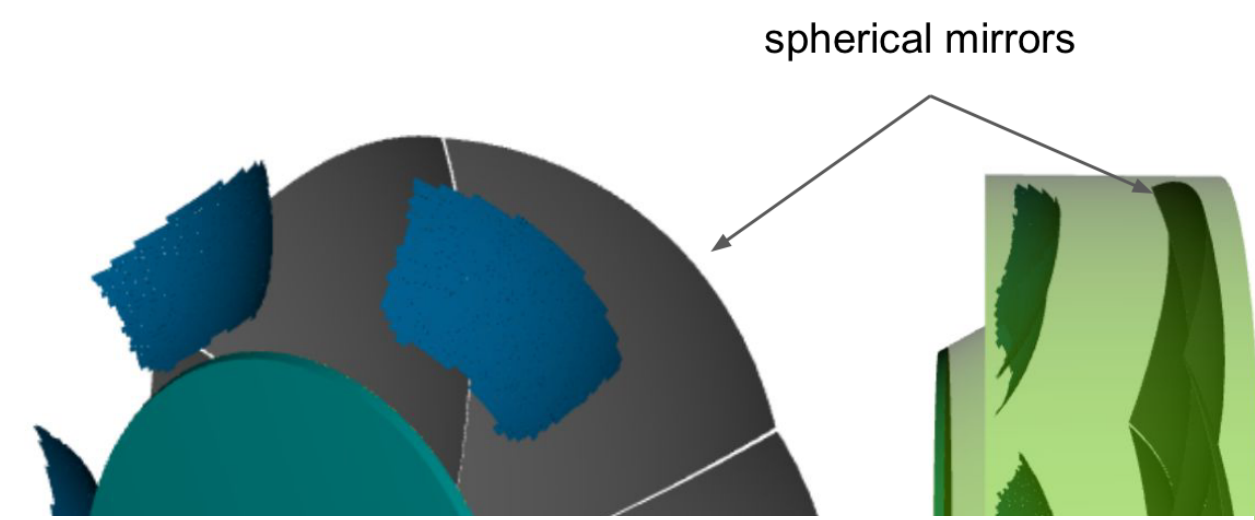
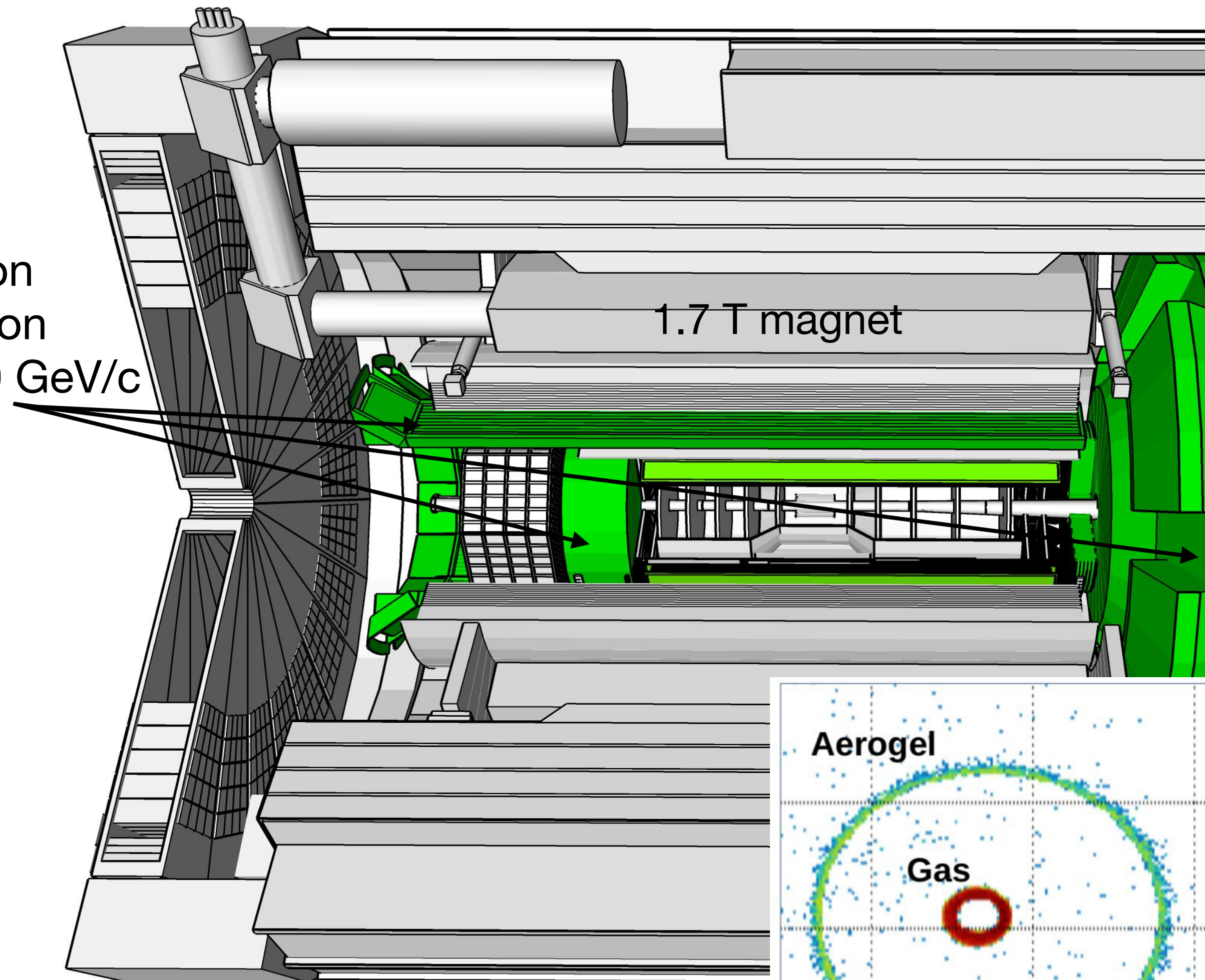
Particle identification

detectors based on Cherenkov radiation for $1 \text{ GeV}/c < p < 50 \text{ GeV}/c$

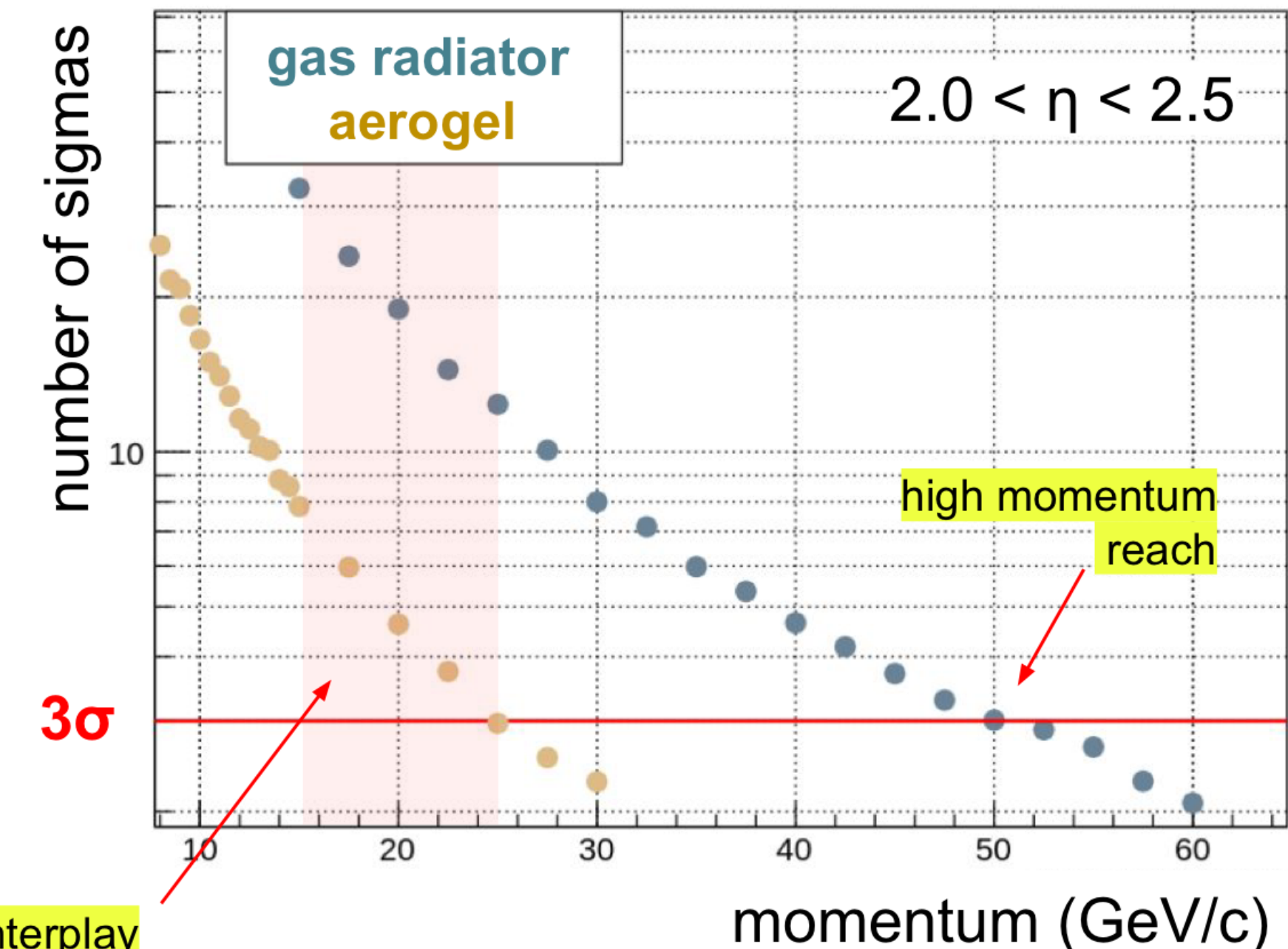


Particle identification

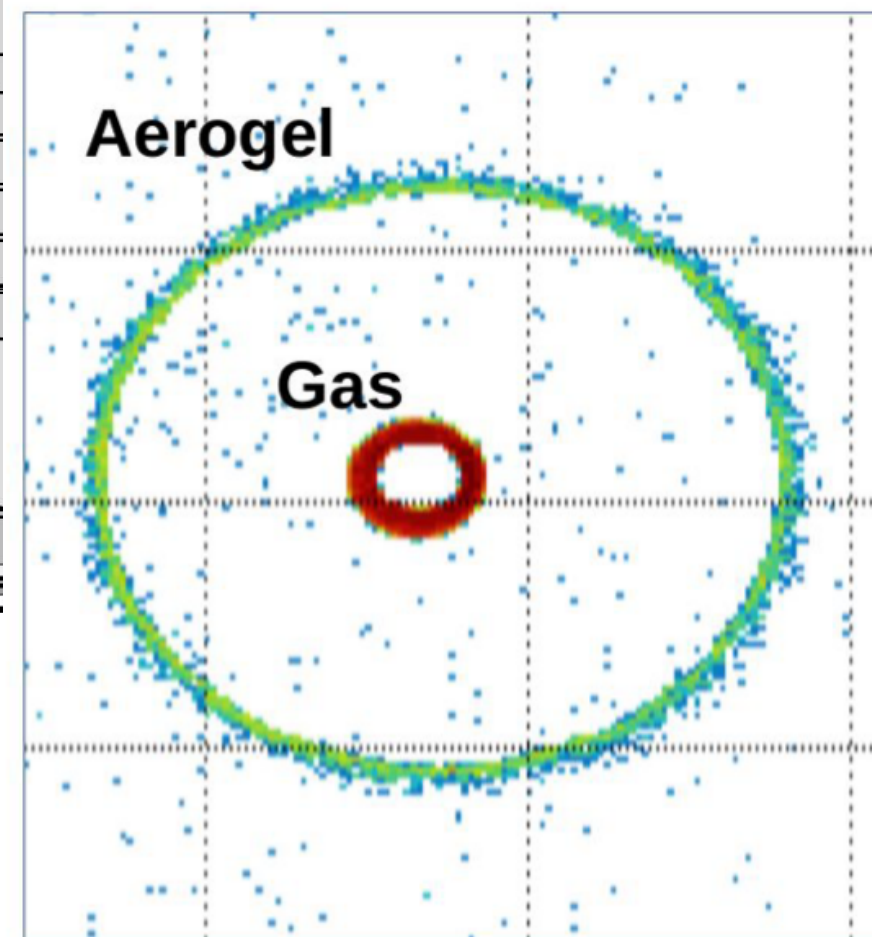
detectors based on Cherenkov radiation for $1 \text{ GeV}/c < p < 50 \text{ GeV}/c$



π/K separation power



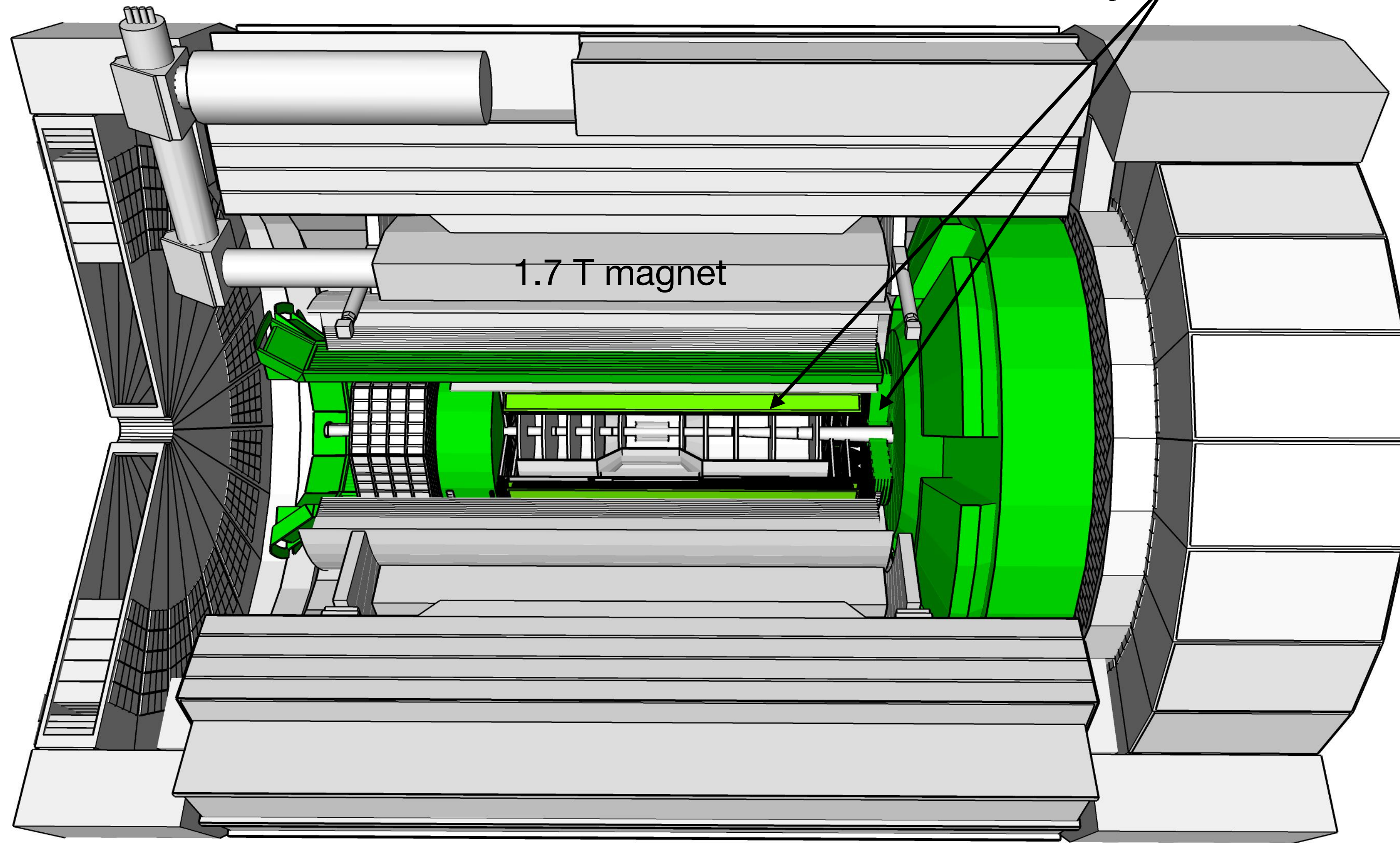
within ePIC simulation framework



Particle identification

AC-LGAD based TOF, for $p < 0.5 - 3 \text{ GeV}/c$

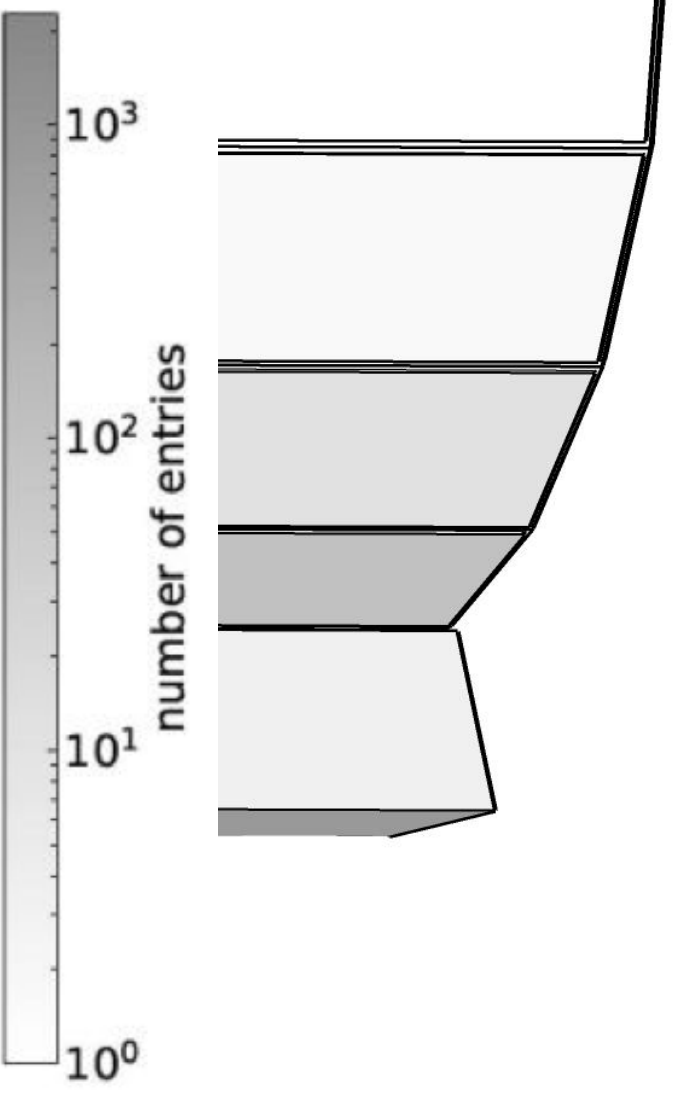
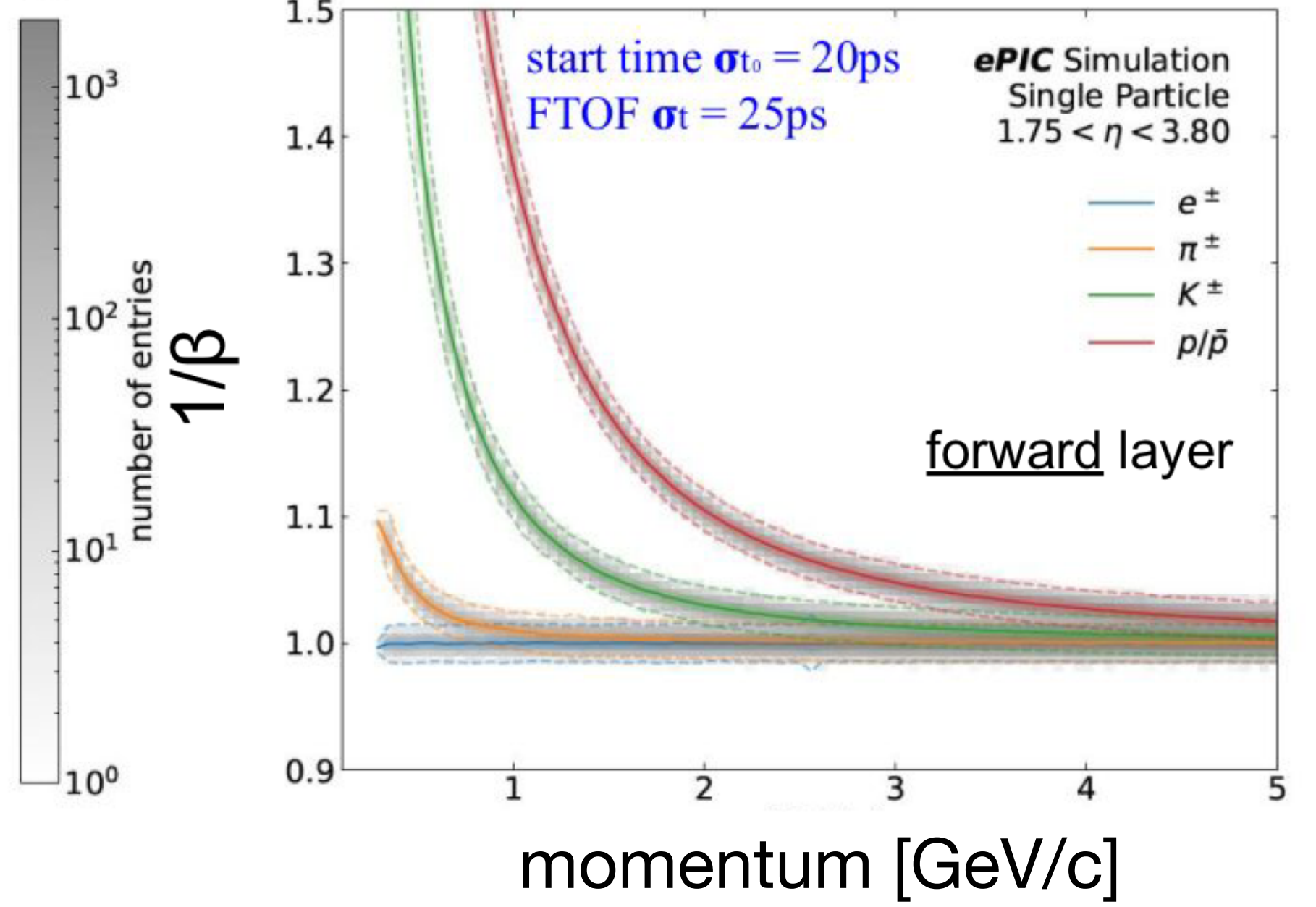
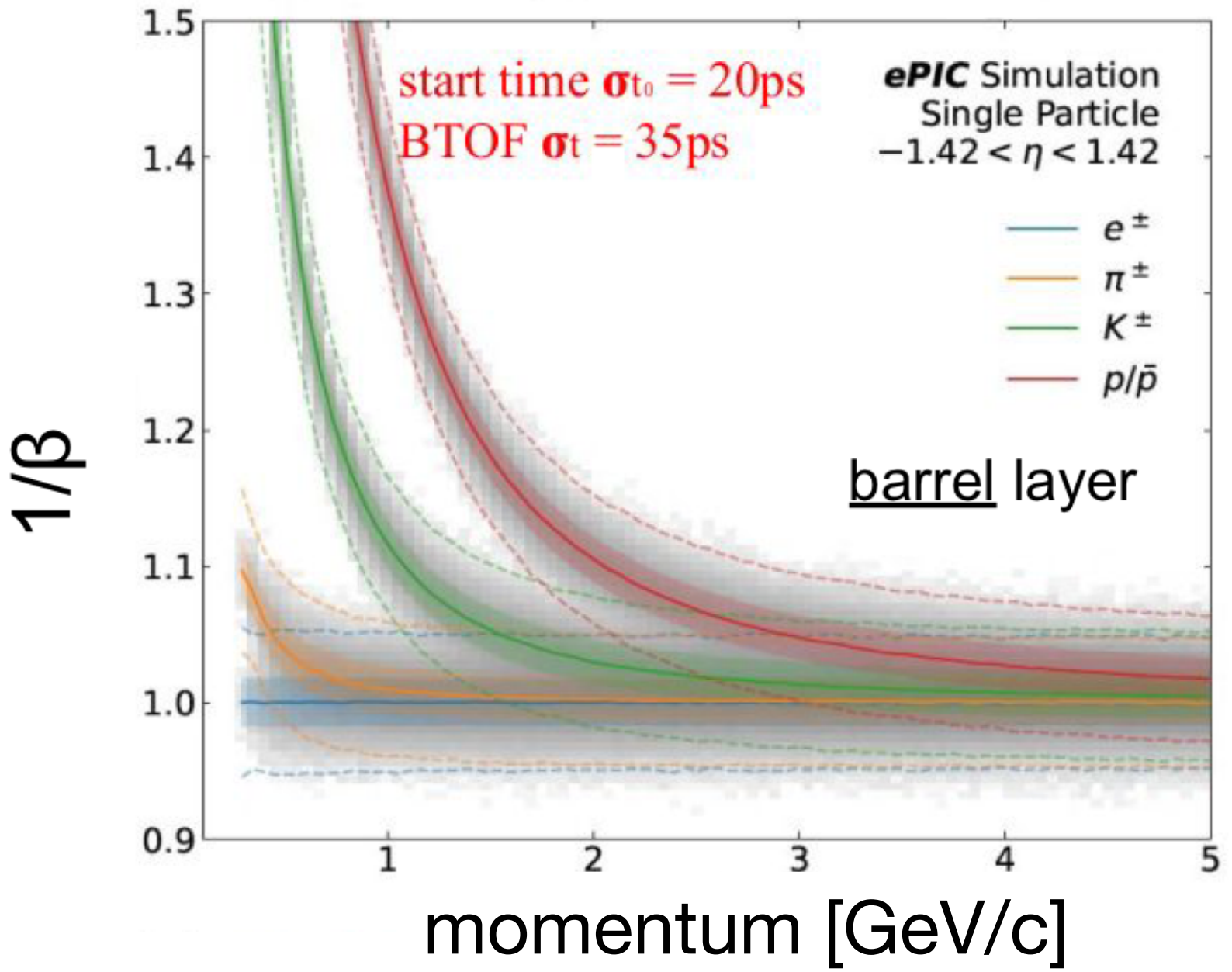
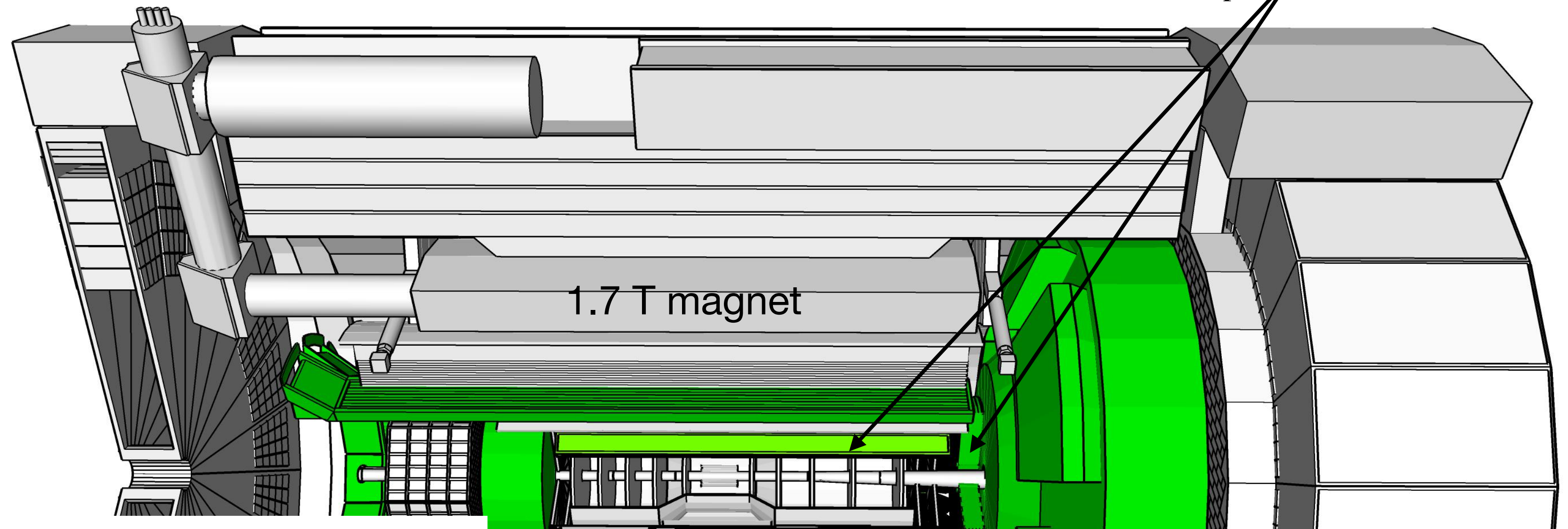
$$v = \frac{L}{t_{stop} - t_{start}}$$



Particle identification

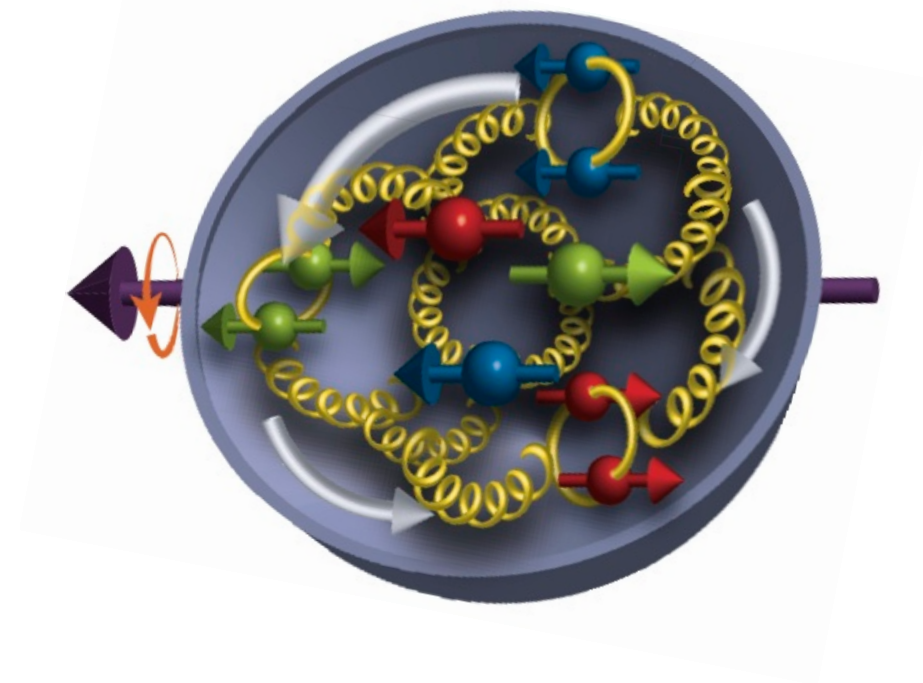
AC-LGAD based TOF, for $p < 0.5 - 3 \text{ GeV}/c$

$$v = \frac{L}{t_{stop} - t_{start}}$$



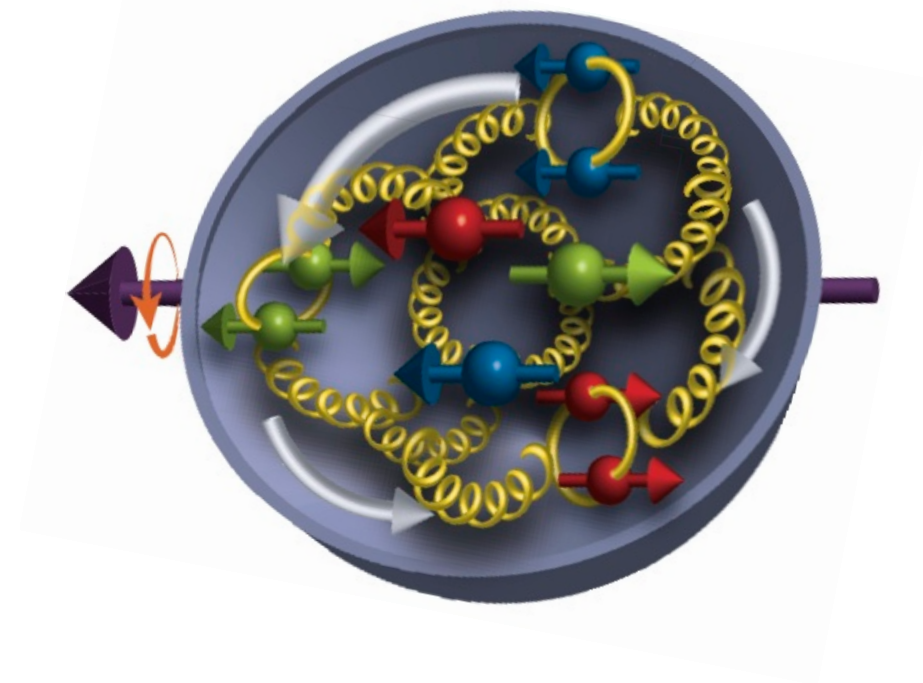
Why an electron-ion collider

nucleon spin

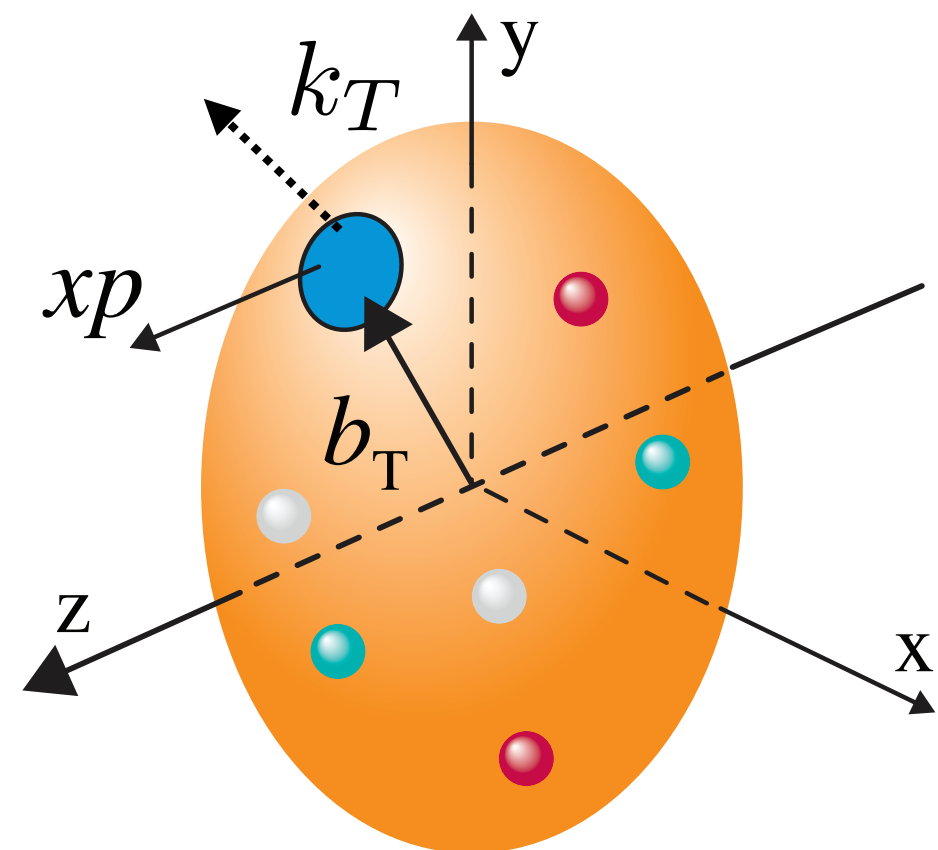


Why an electron-ion collider

nucleon spin

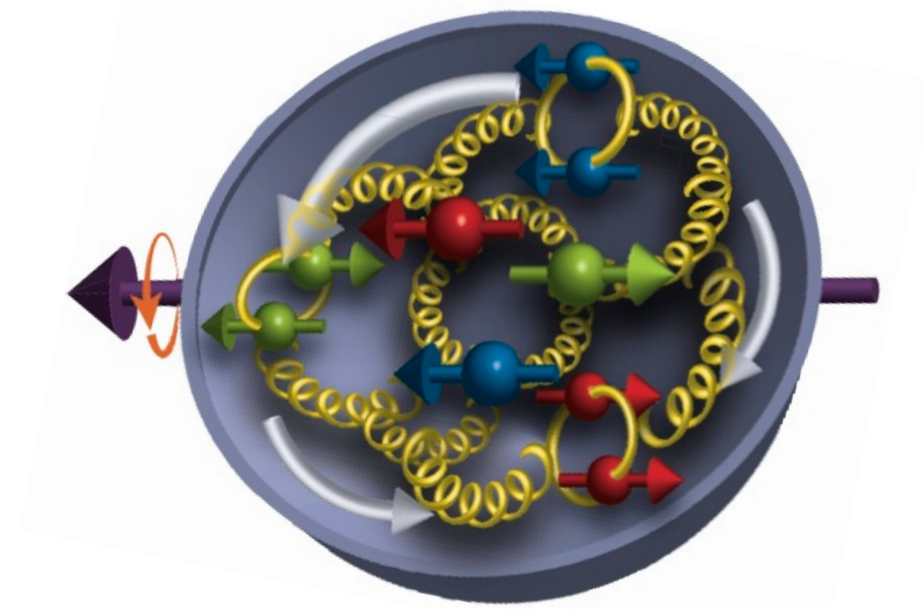


spin-dependent nucleon multi-dimensional structure

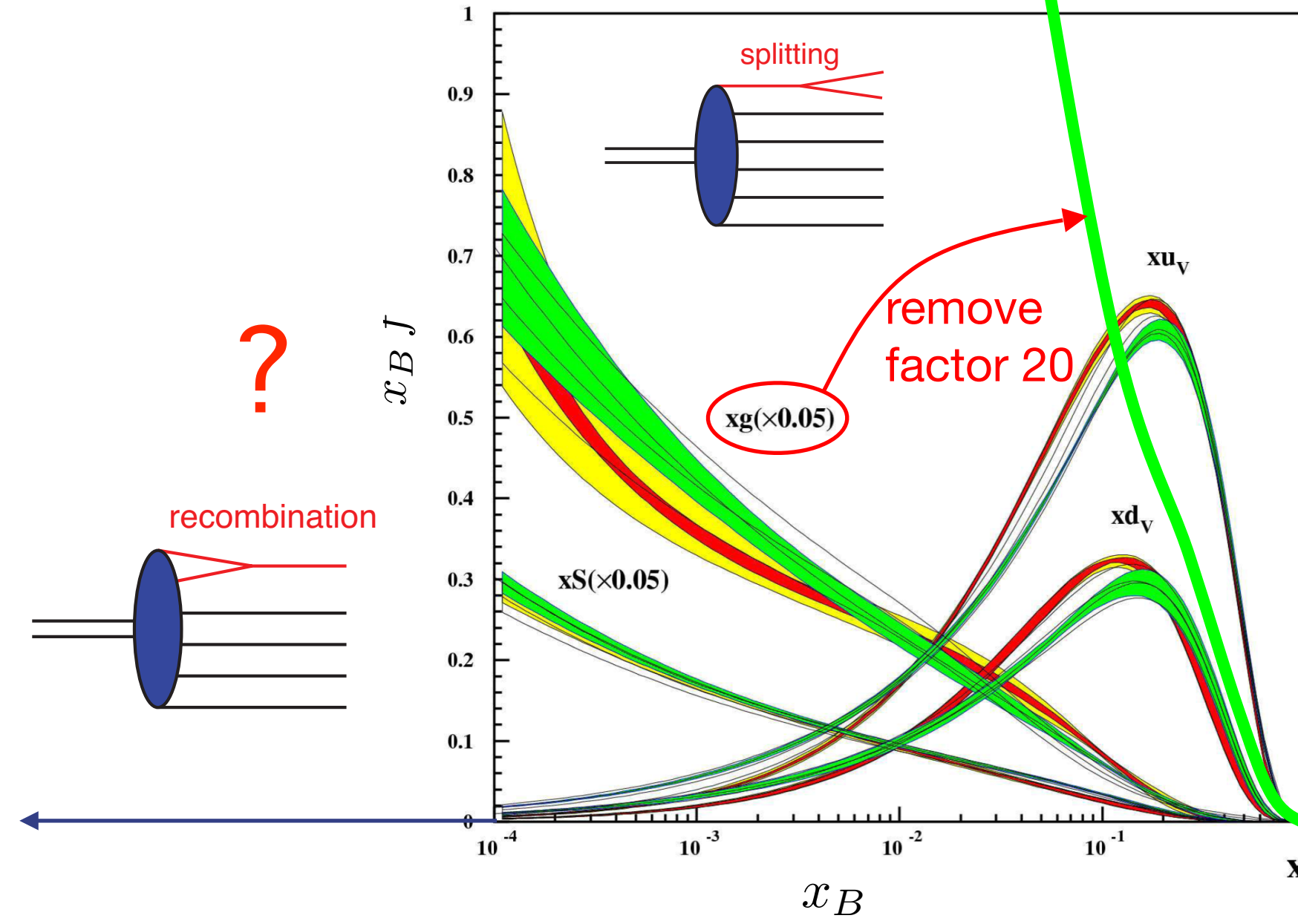


Why an electron-ion collider

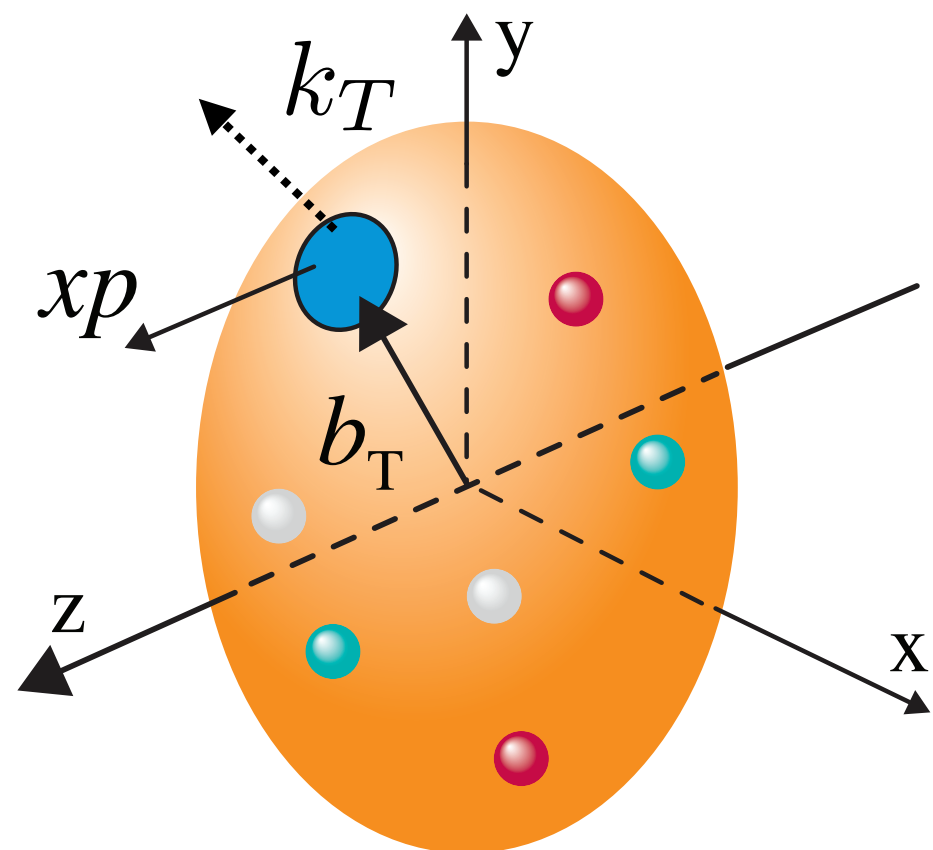
nucleon spin



probing saturation

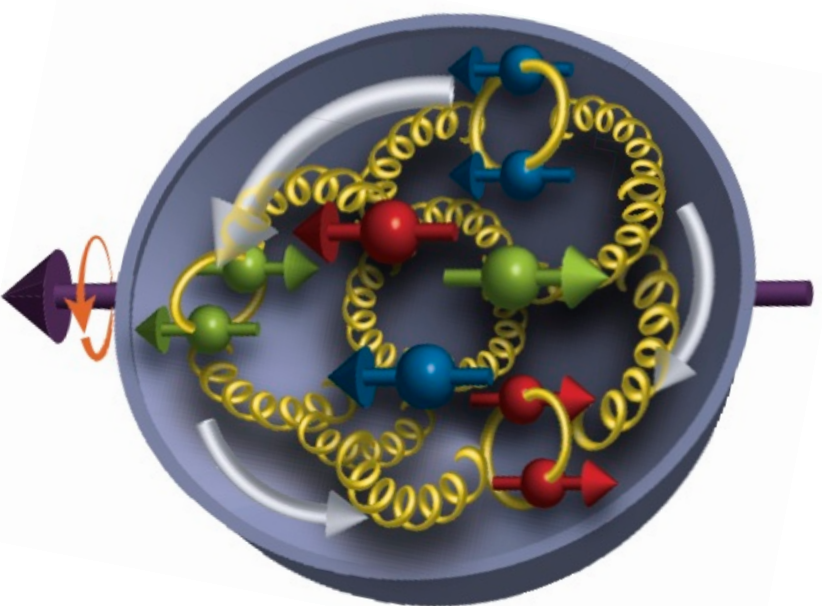


spin-dependent nucleon multi-dimensional structure

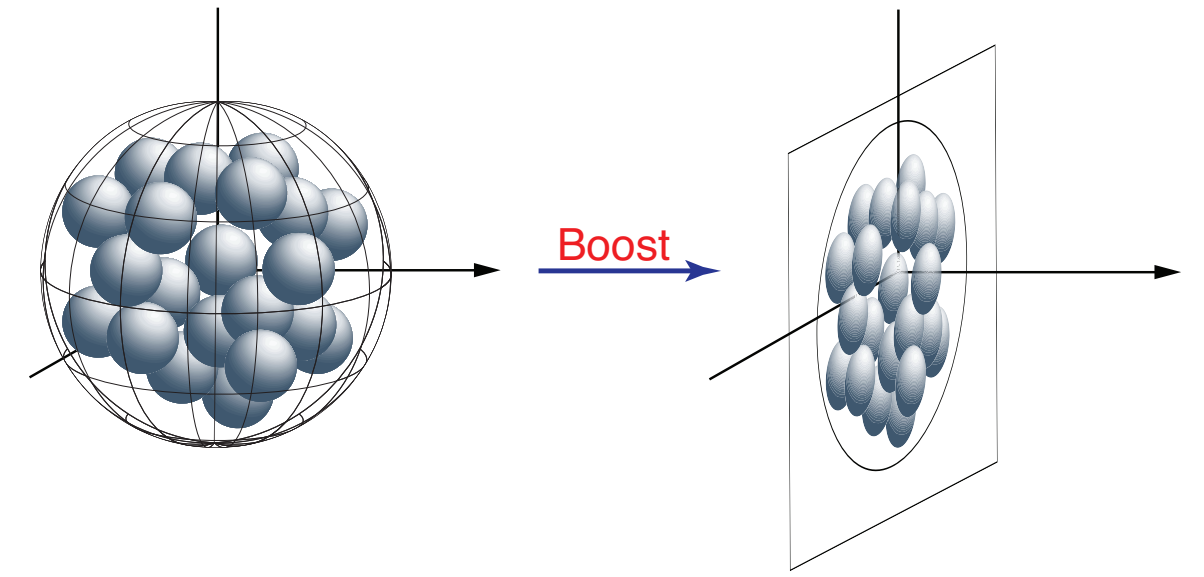
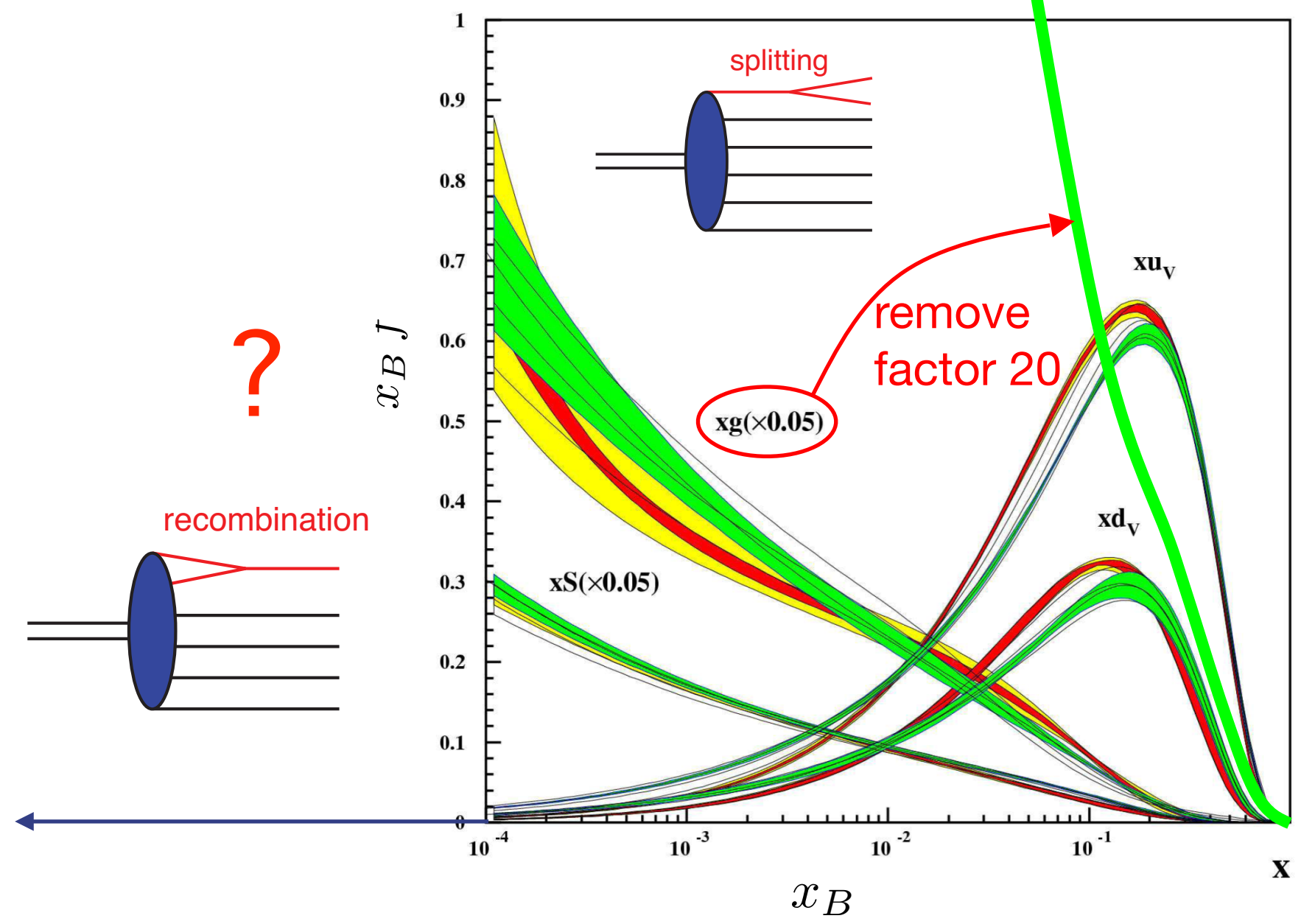


Why an electron-ion collider

nucleon spin

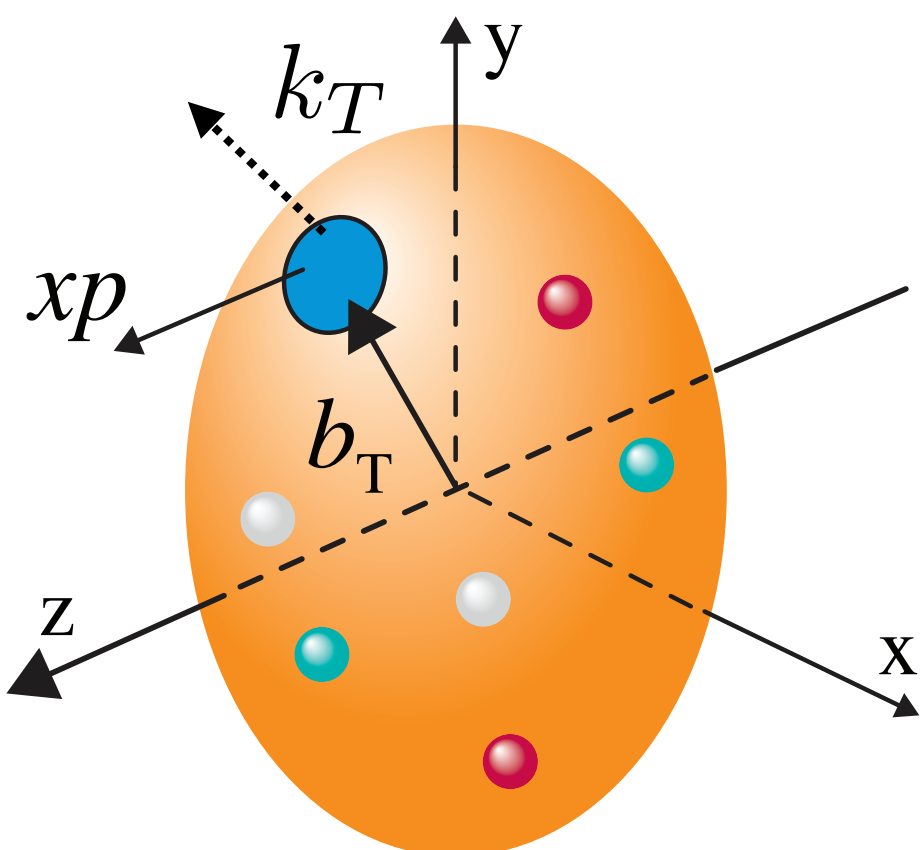


probing saturation



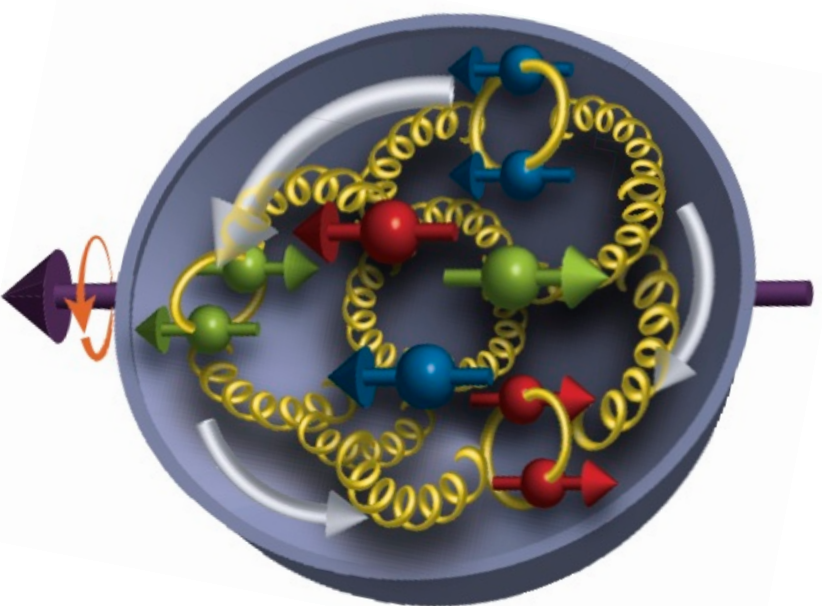
$A^{1/3}$ enhancement of saturation effect for ions

spin-dependent nucleon multi-dimensional structure

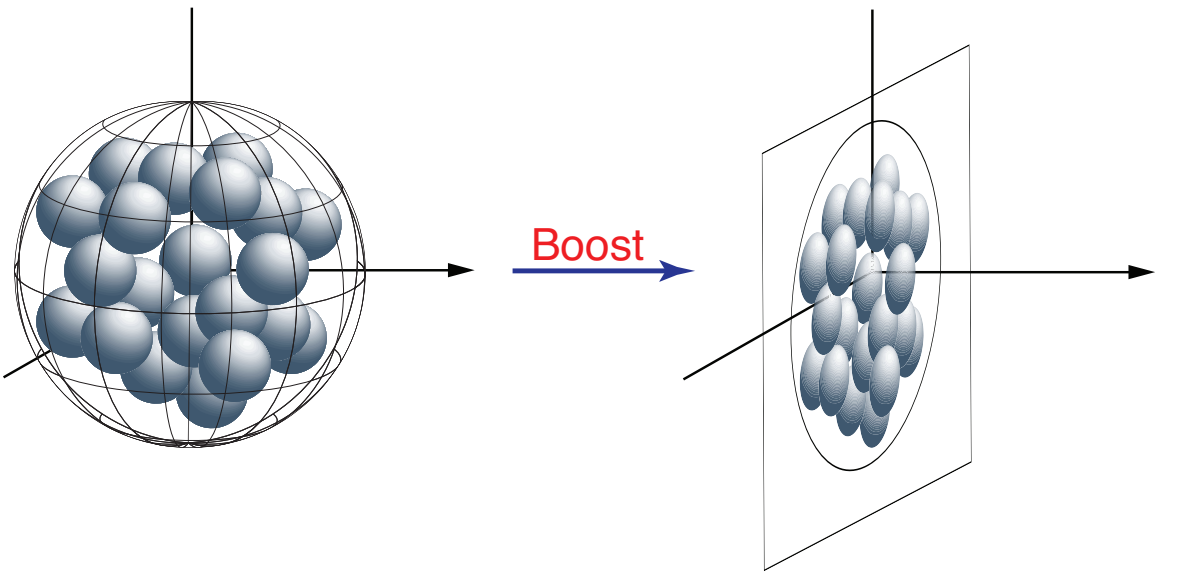
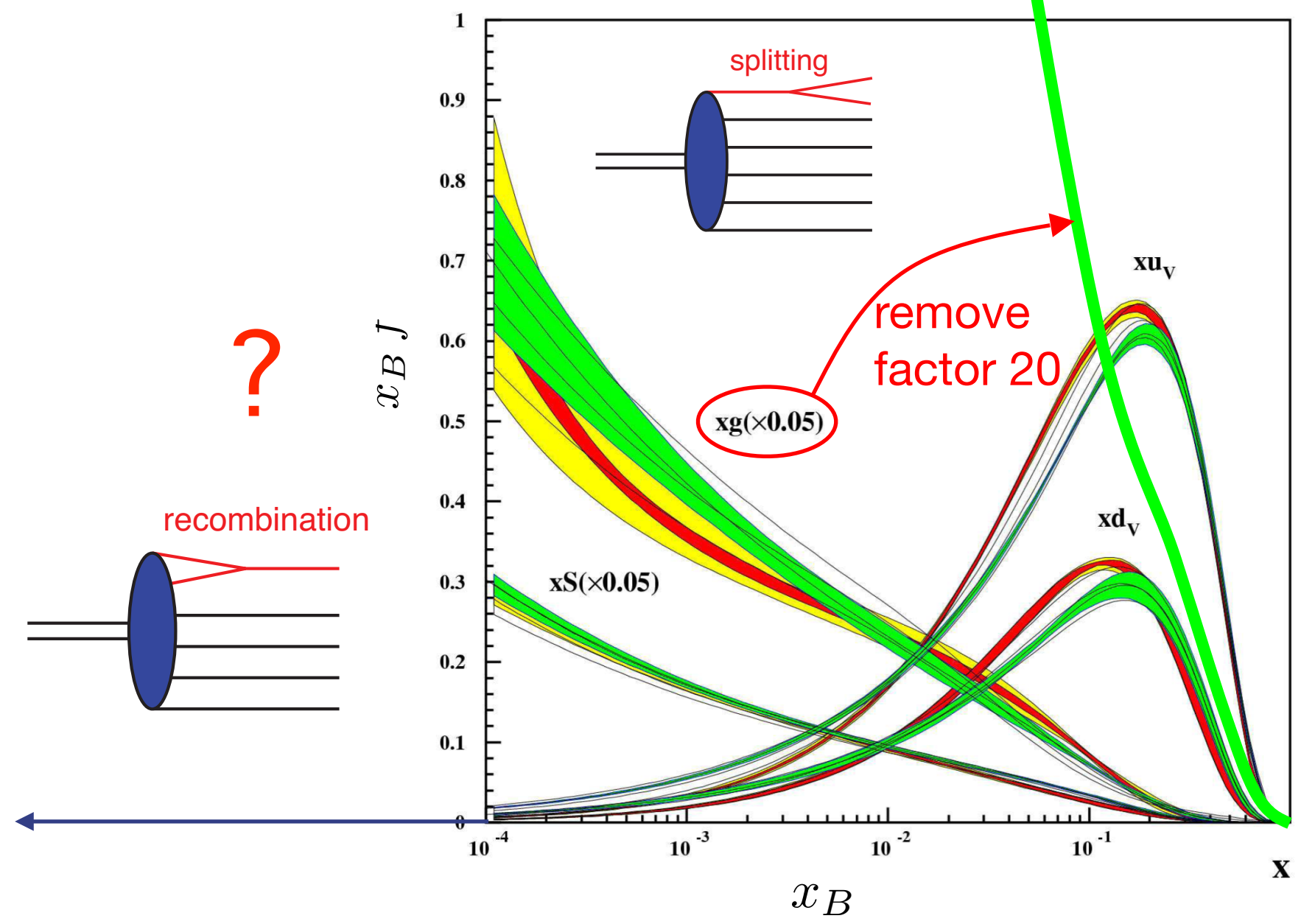


Why an electron-ion collider

nucleon spin

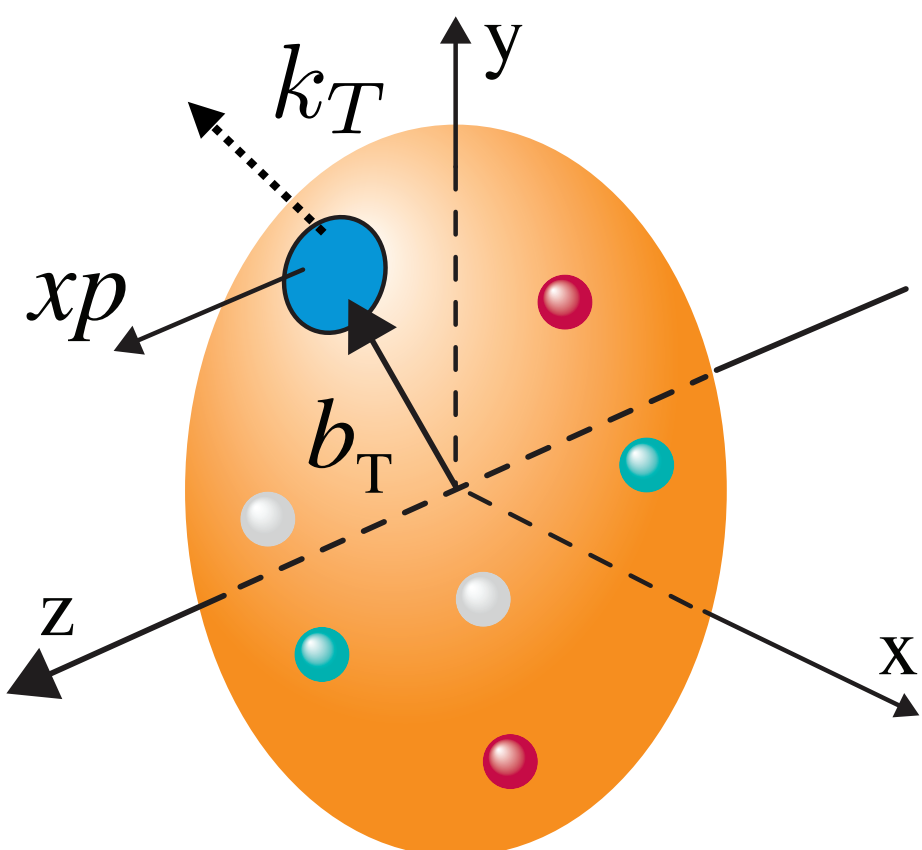


probing saturation



$A^{1/3}$ enhancement of saturation effect for ions

spin-dependent nucleon multi-dimensional structure

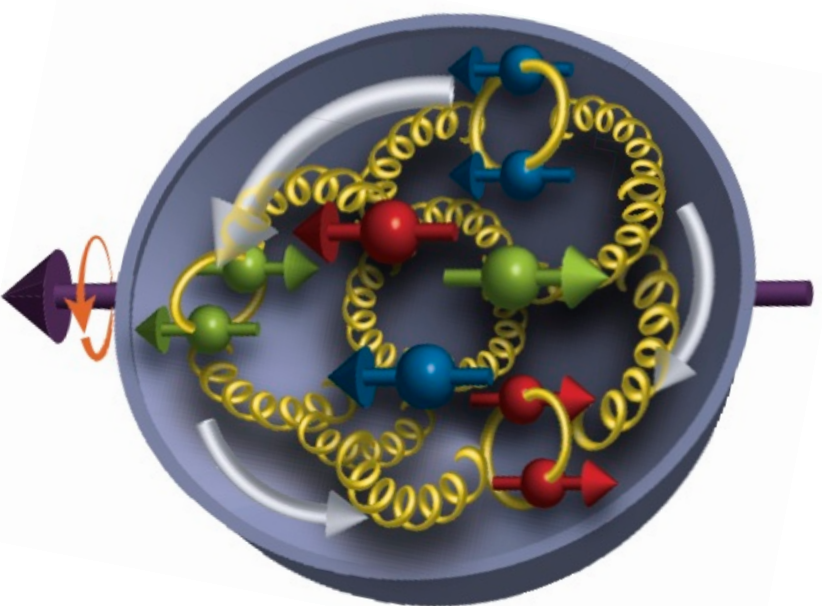


hadronisation

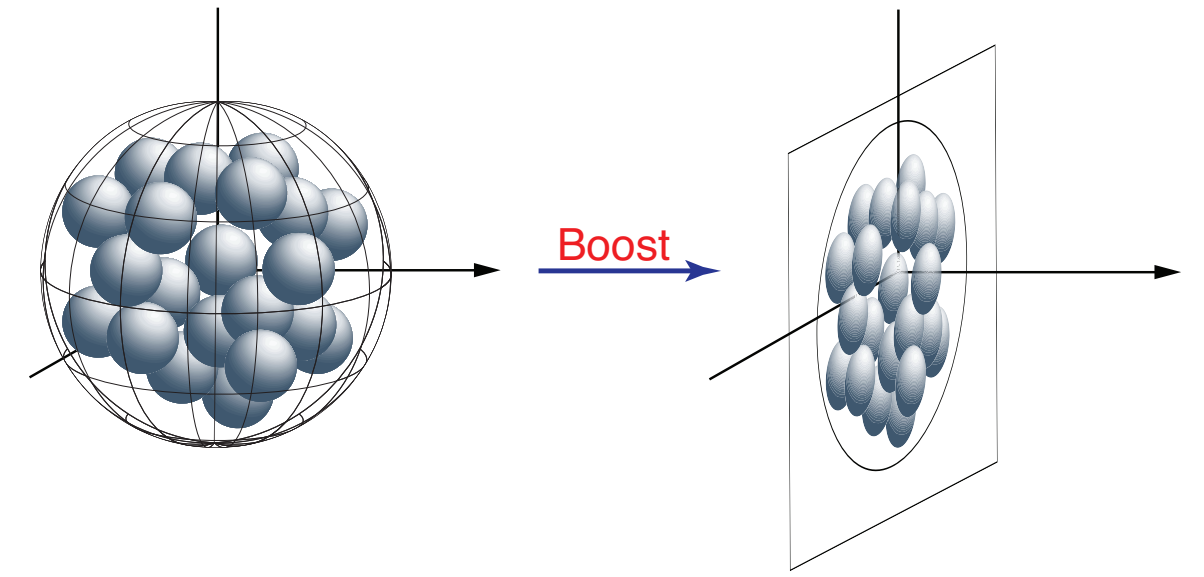
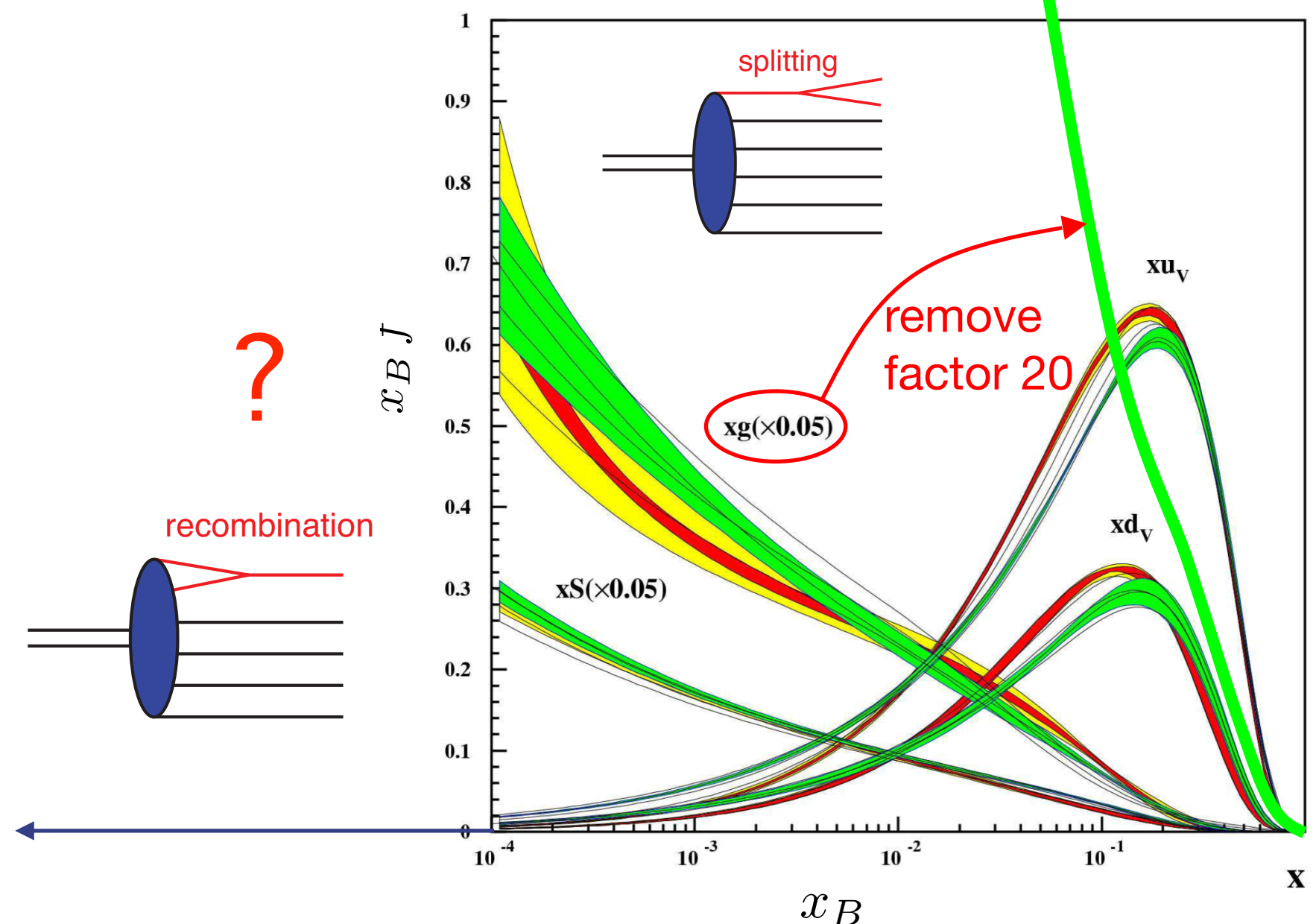


Why an electron-ion collider

nucleon spin

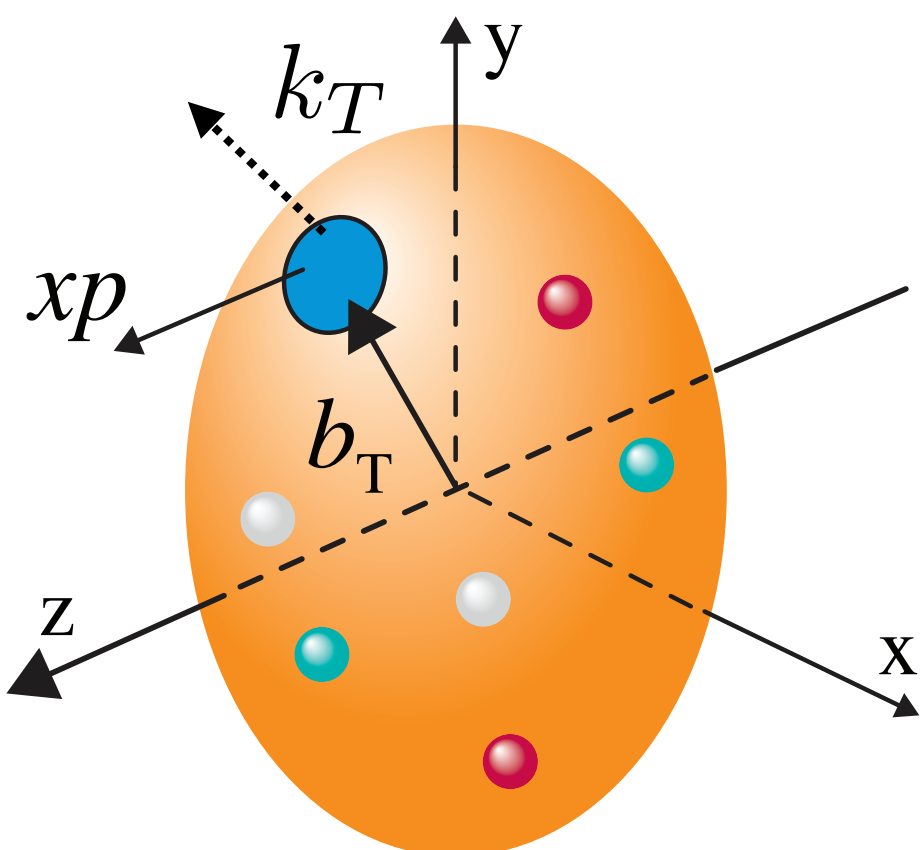


probing saturation

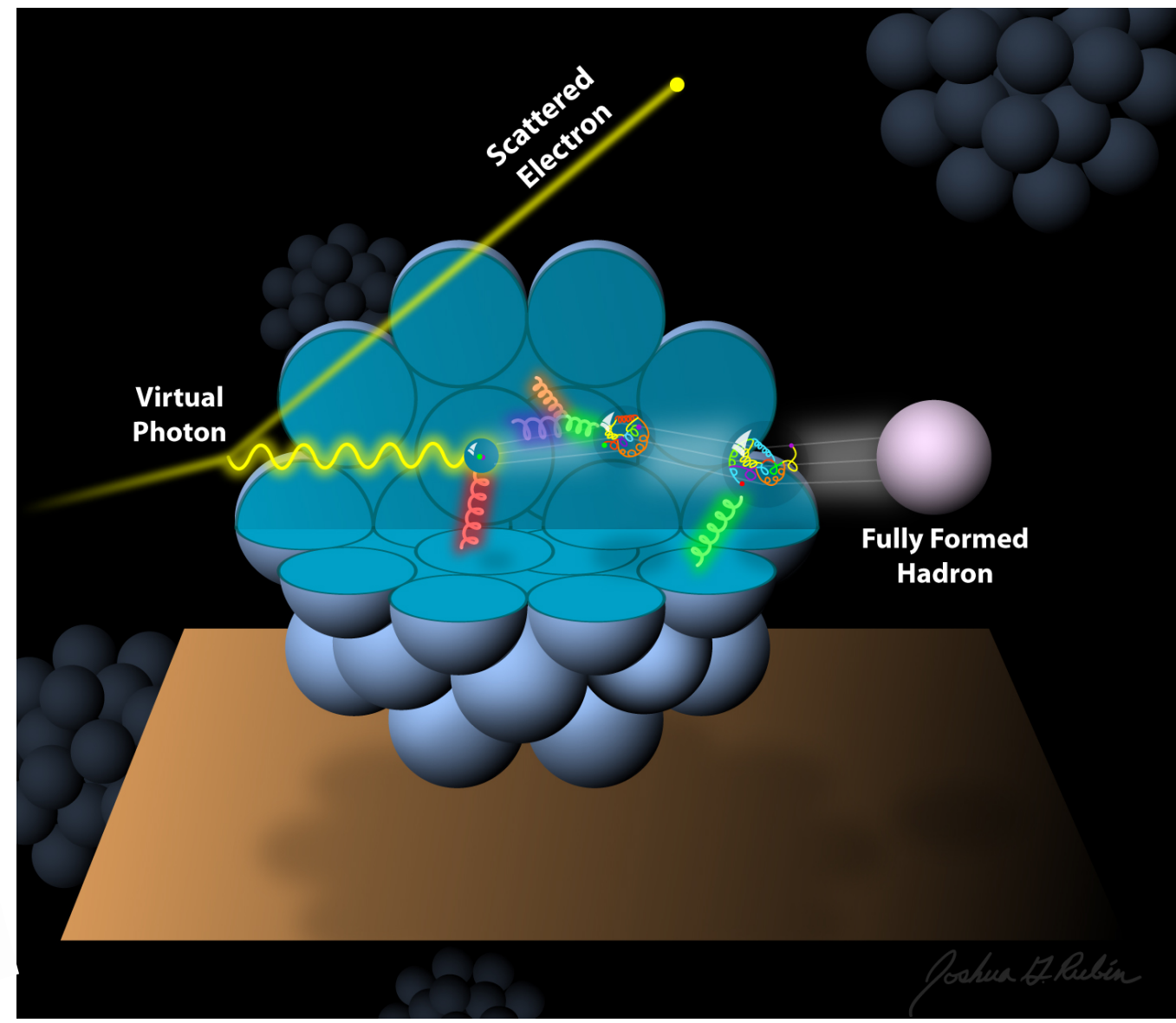


$A^{1/3}$ enhancement of saturation effect for ions

spin-dependent nucleon multi-dimensional structure

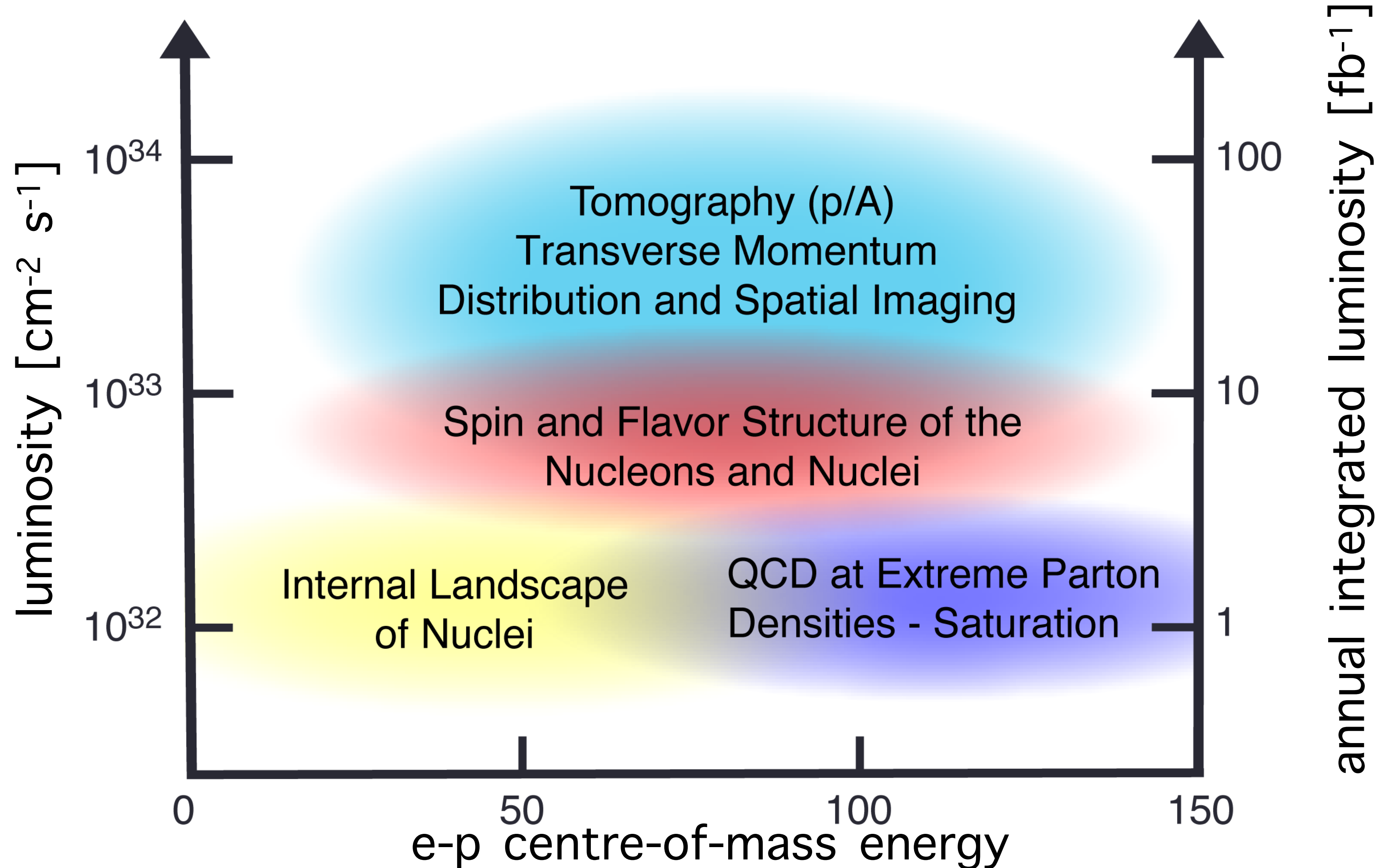


hadronisation

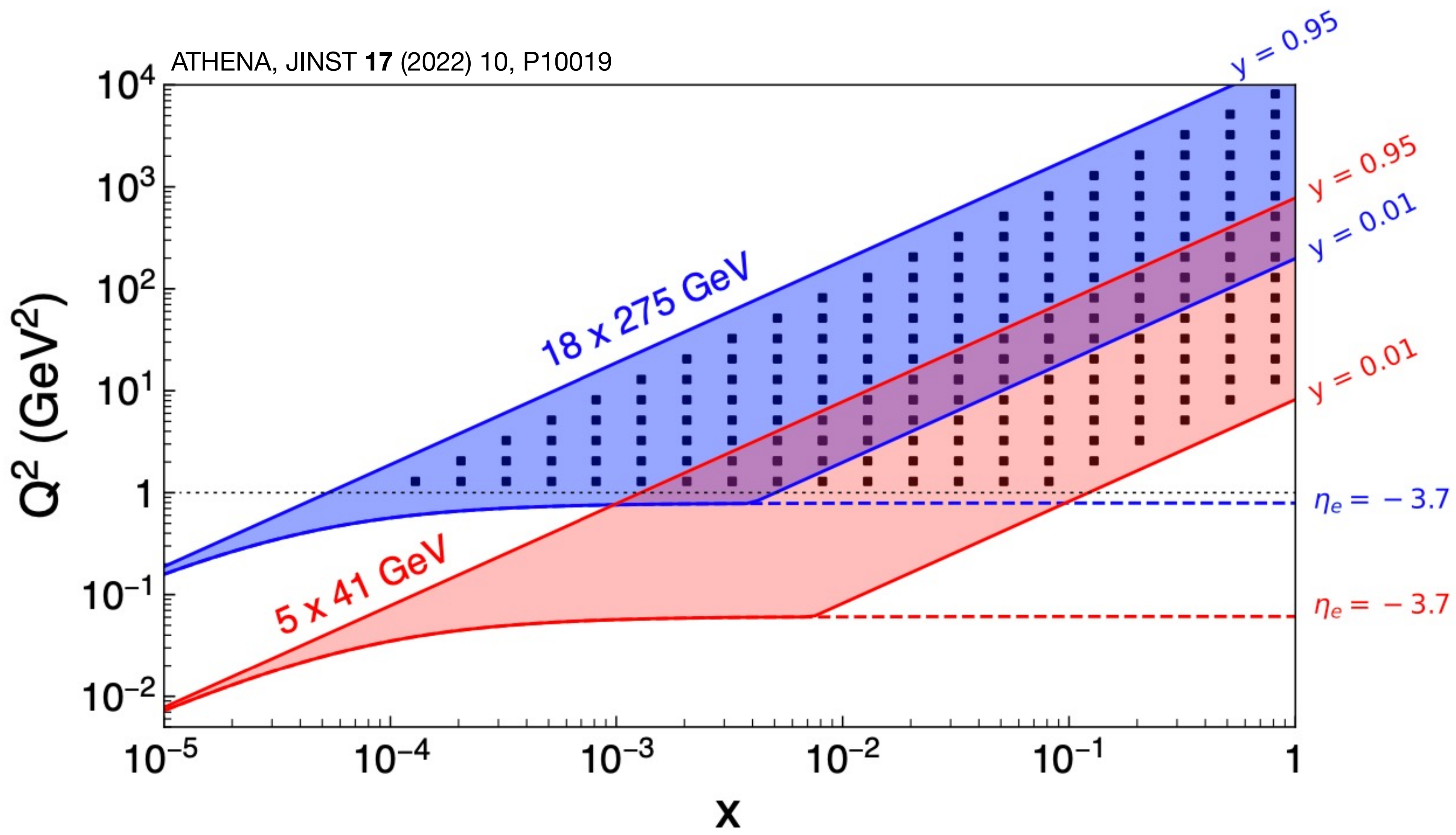


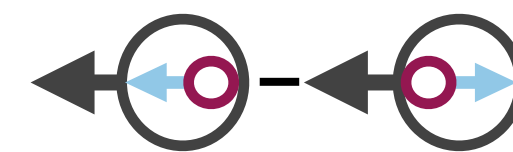
Joshua Z. Rubin

Luminosity and COM E needs for physics topics

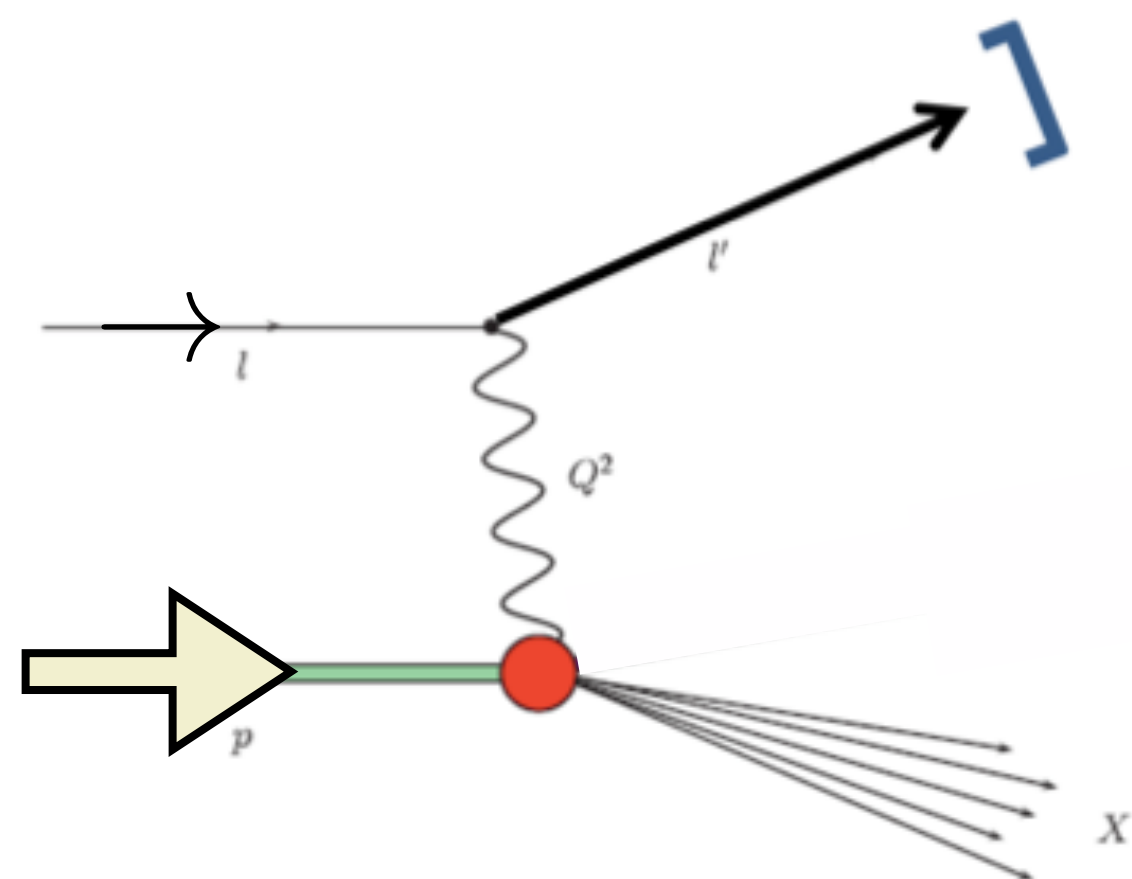


Kinematic coverage at the EIC





Helicity structure of the nucleon: gluons

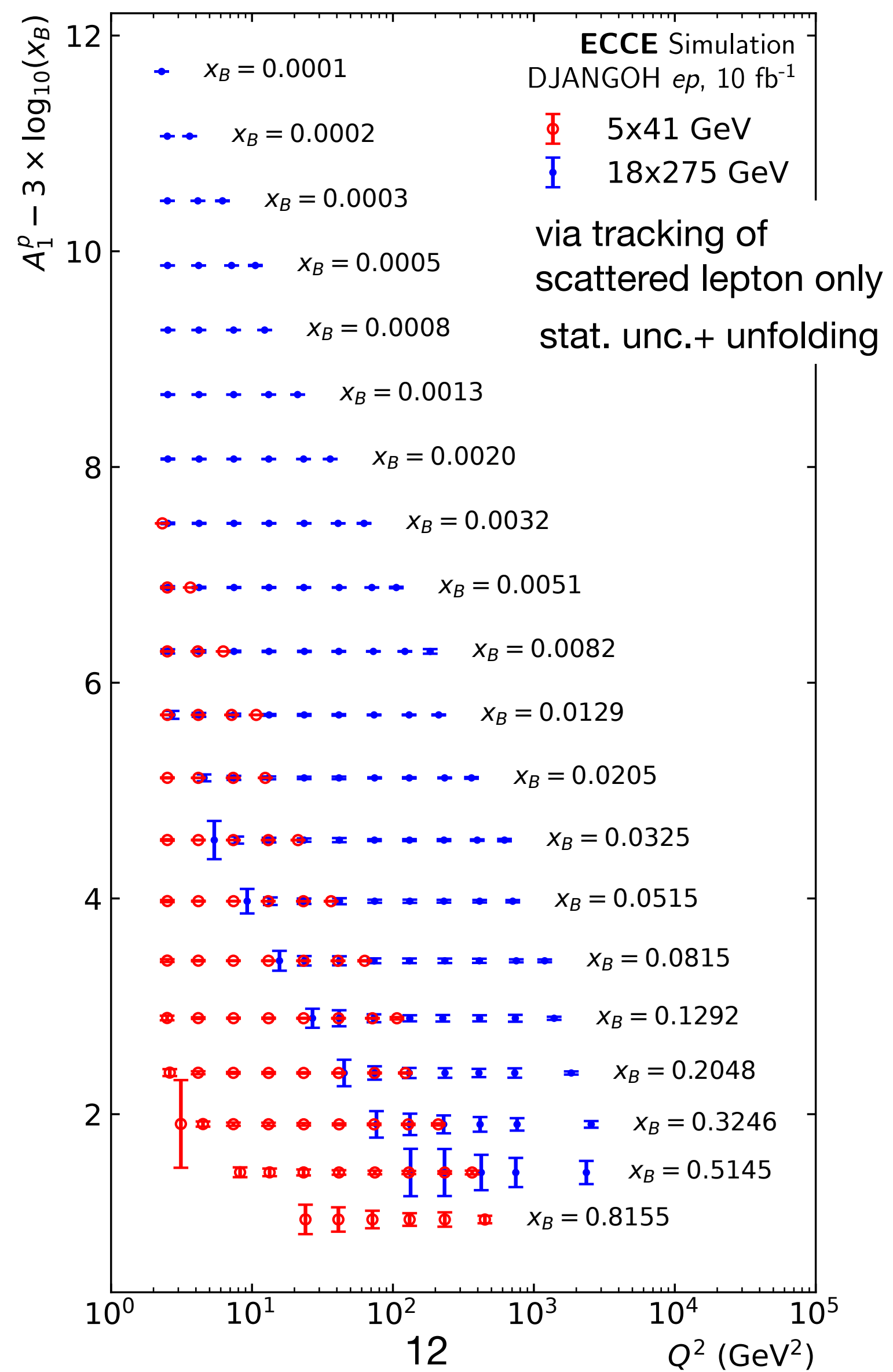


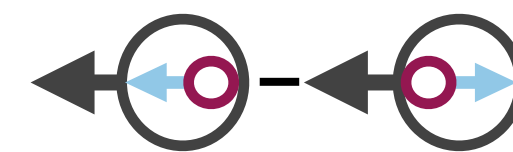
Inclusive measurements
→ access to gluon spin



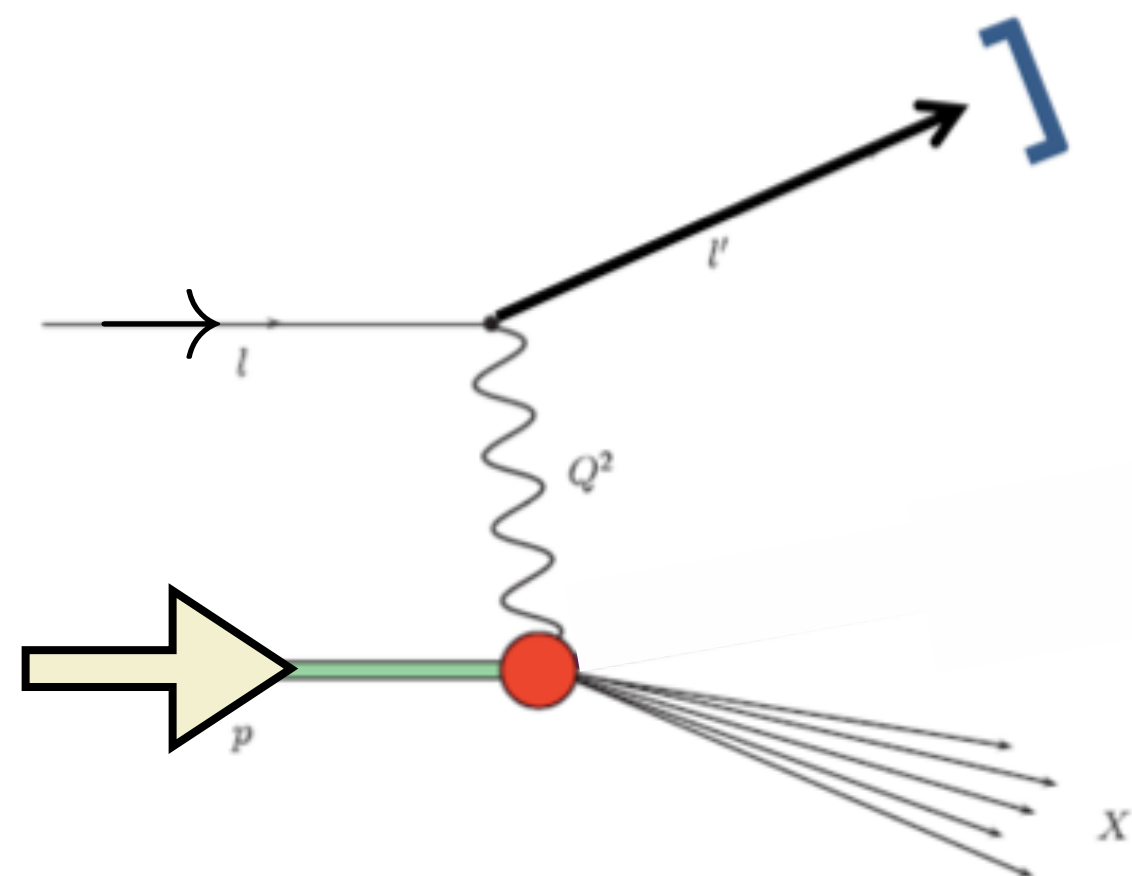
scaling violation from $g_1(x, Q^2)$

ECCE consortium, 10.5281/zenodo.6537587

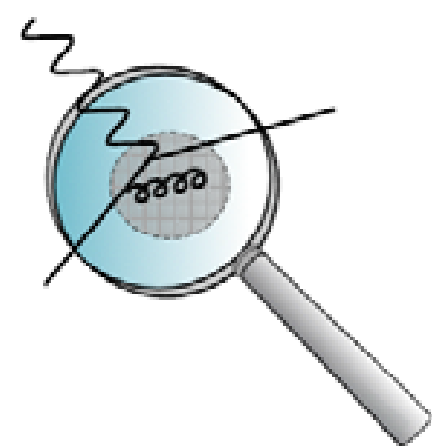




Helicity structure of the nucleon: gluons

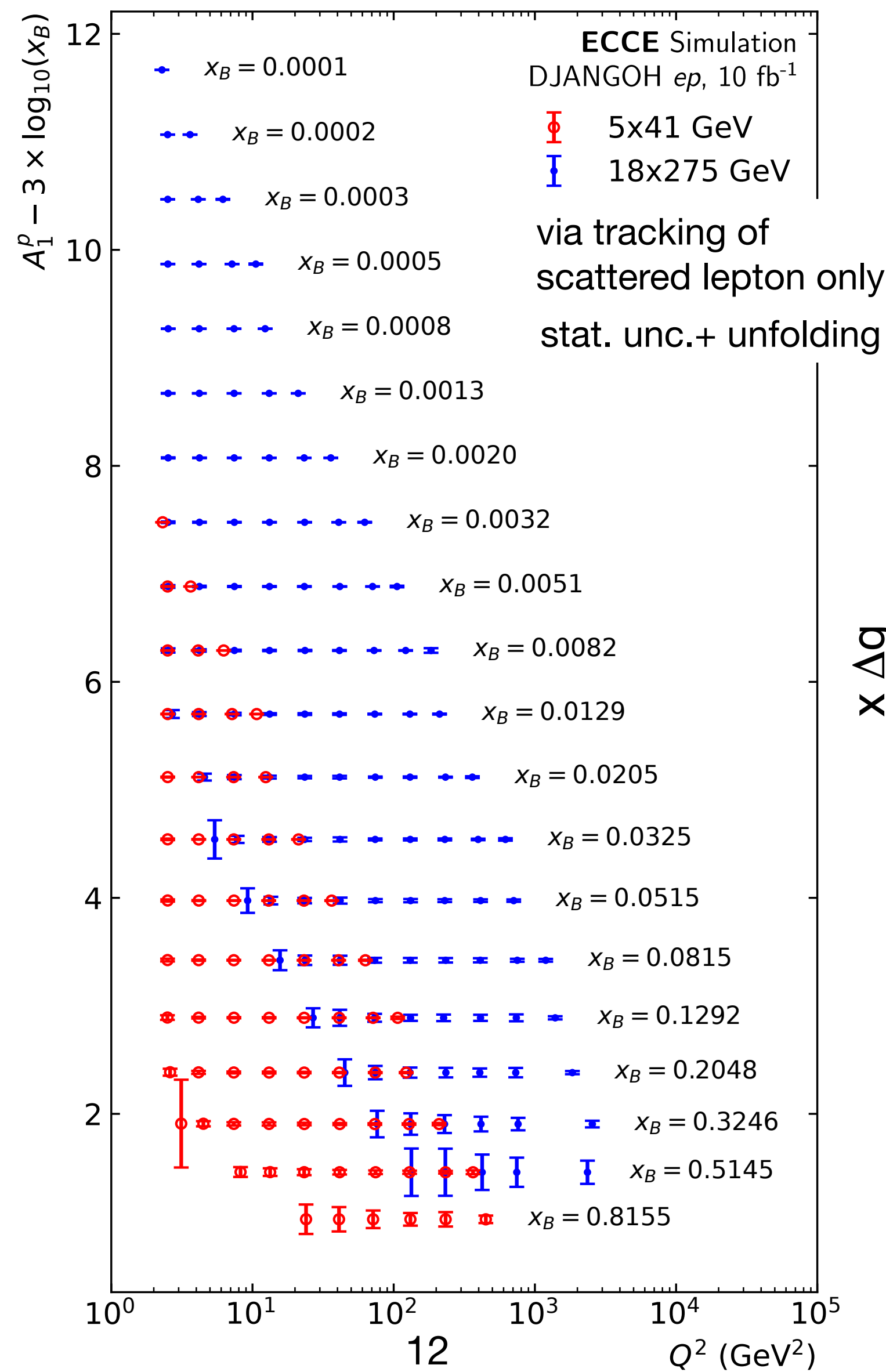


Inclusive measurements
→ access to gluon spin

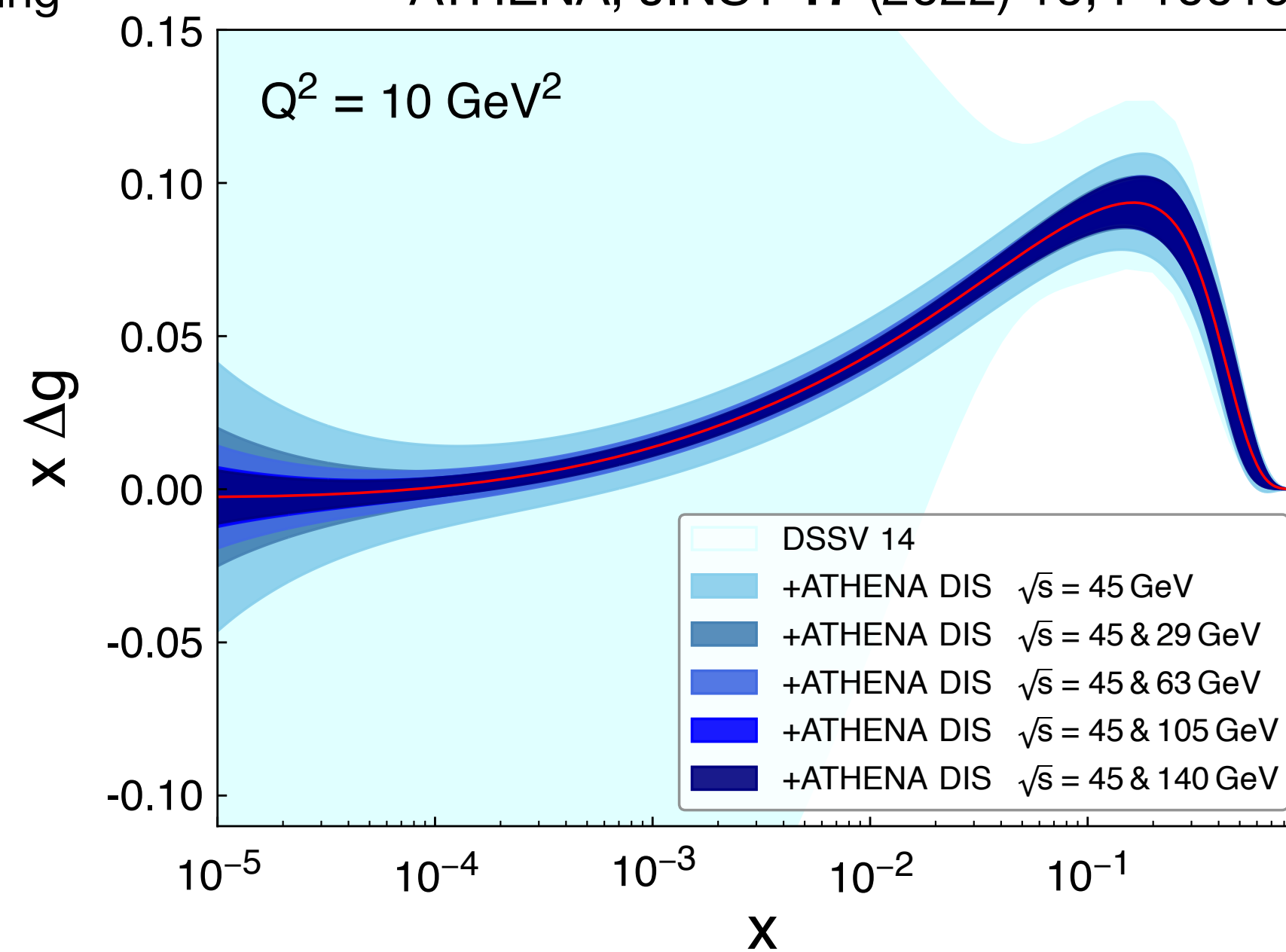


scaling violation from $g_1(x, Q^2)$

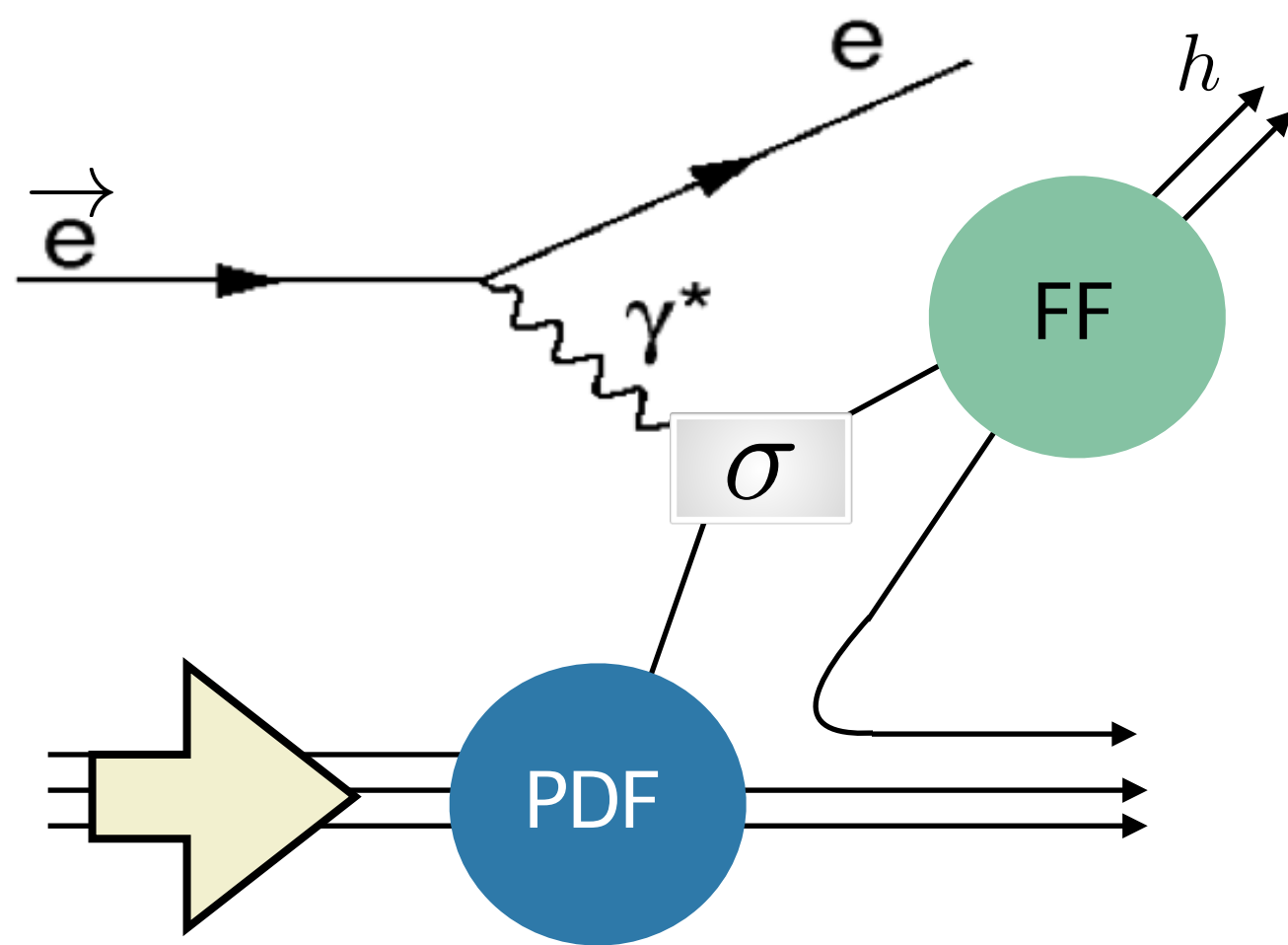
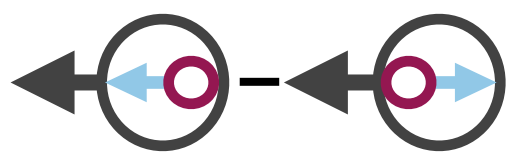
ECCE consortium, 10.5281/zenodo.6537587



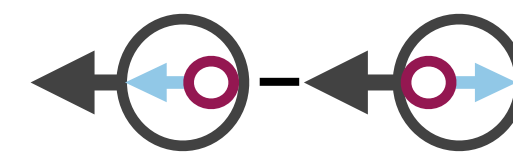
ATHENA, JINST 17 (2022) 10, P10019



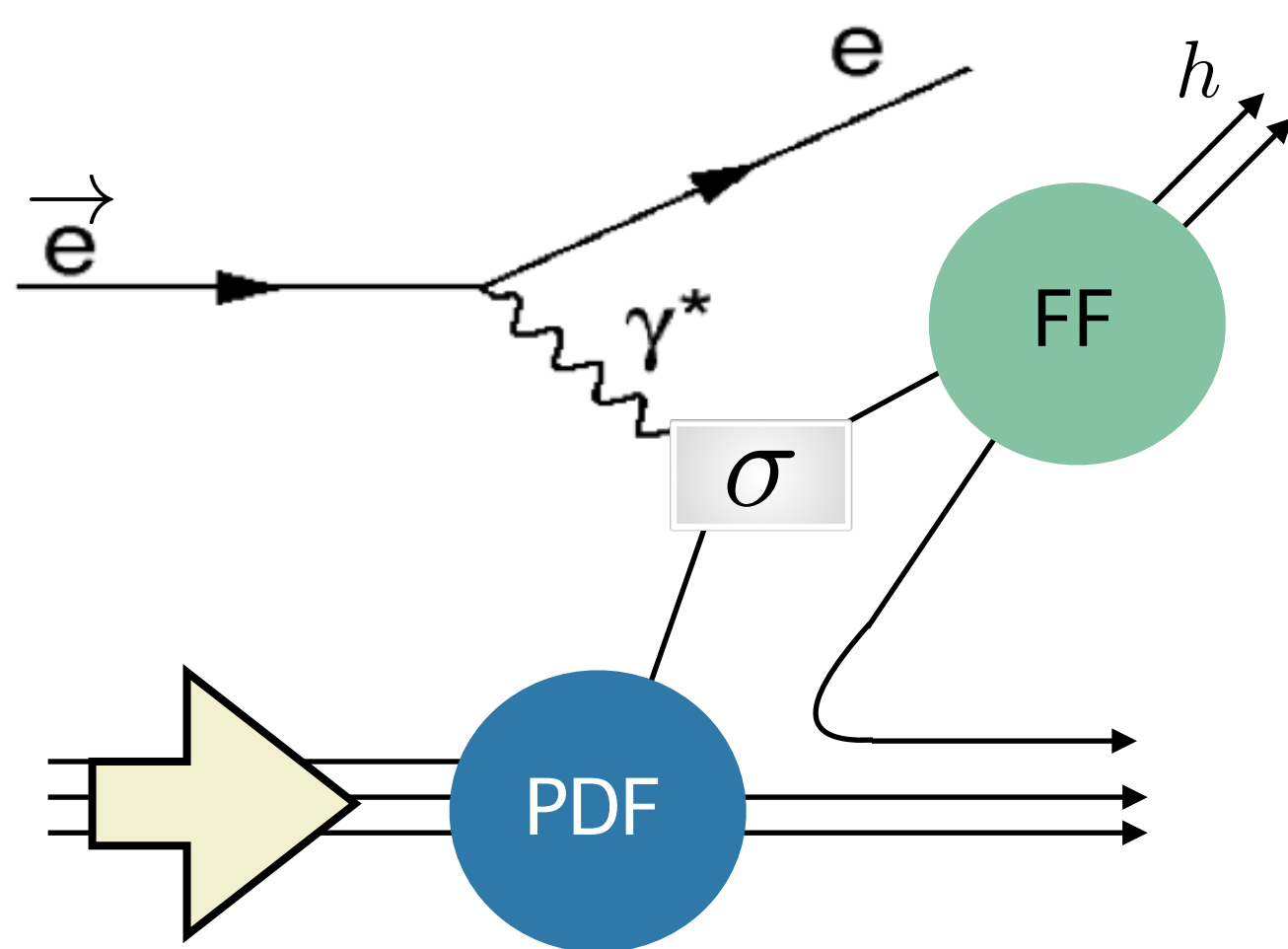
Helicity structure of the proton: sea quarks



Semi-inclusive measurements, via good hadron PID
→ access to sea-quark spin

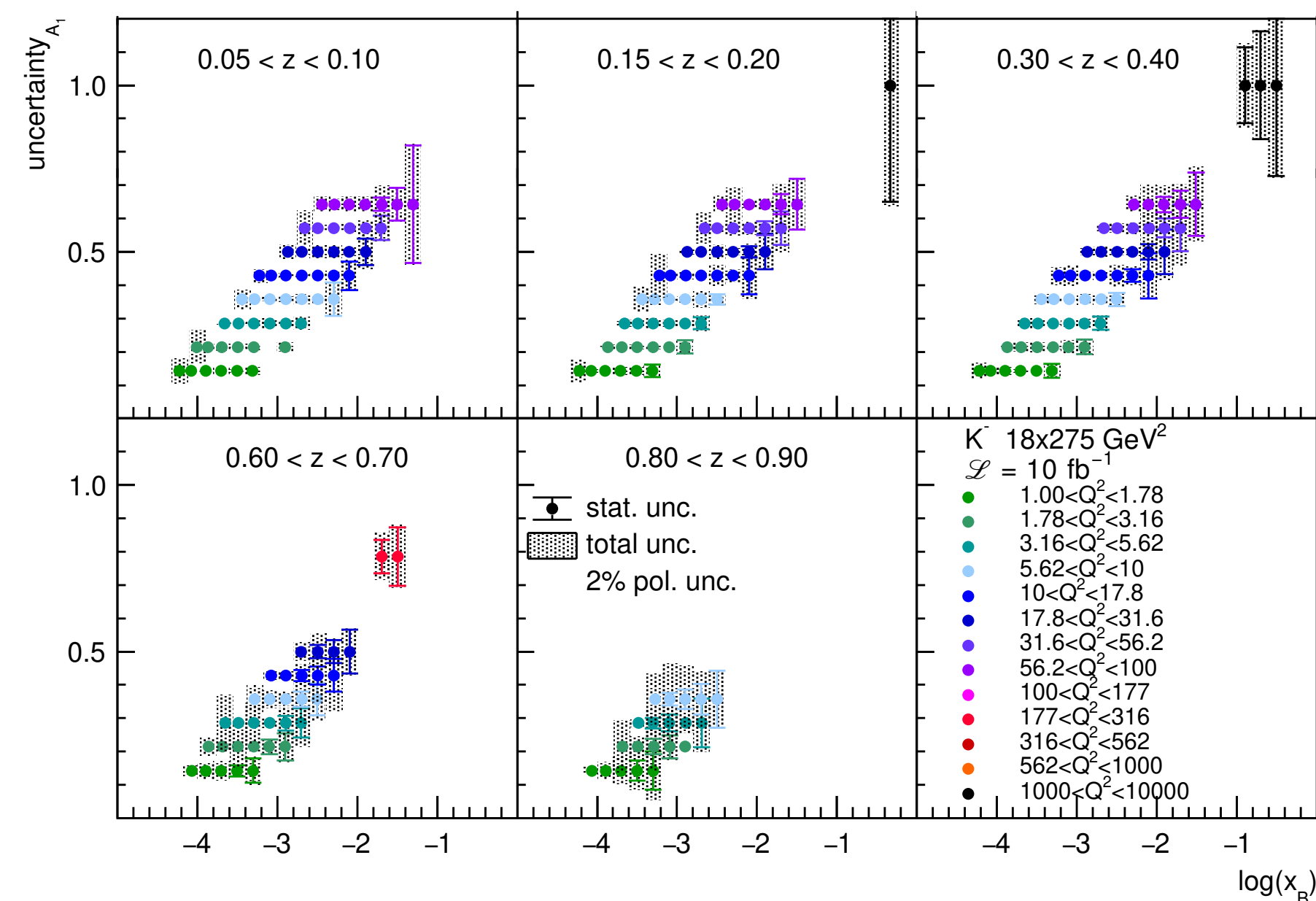
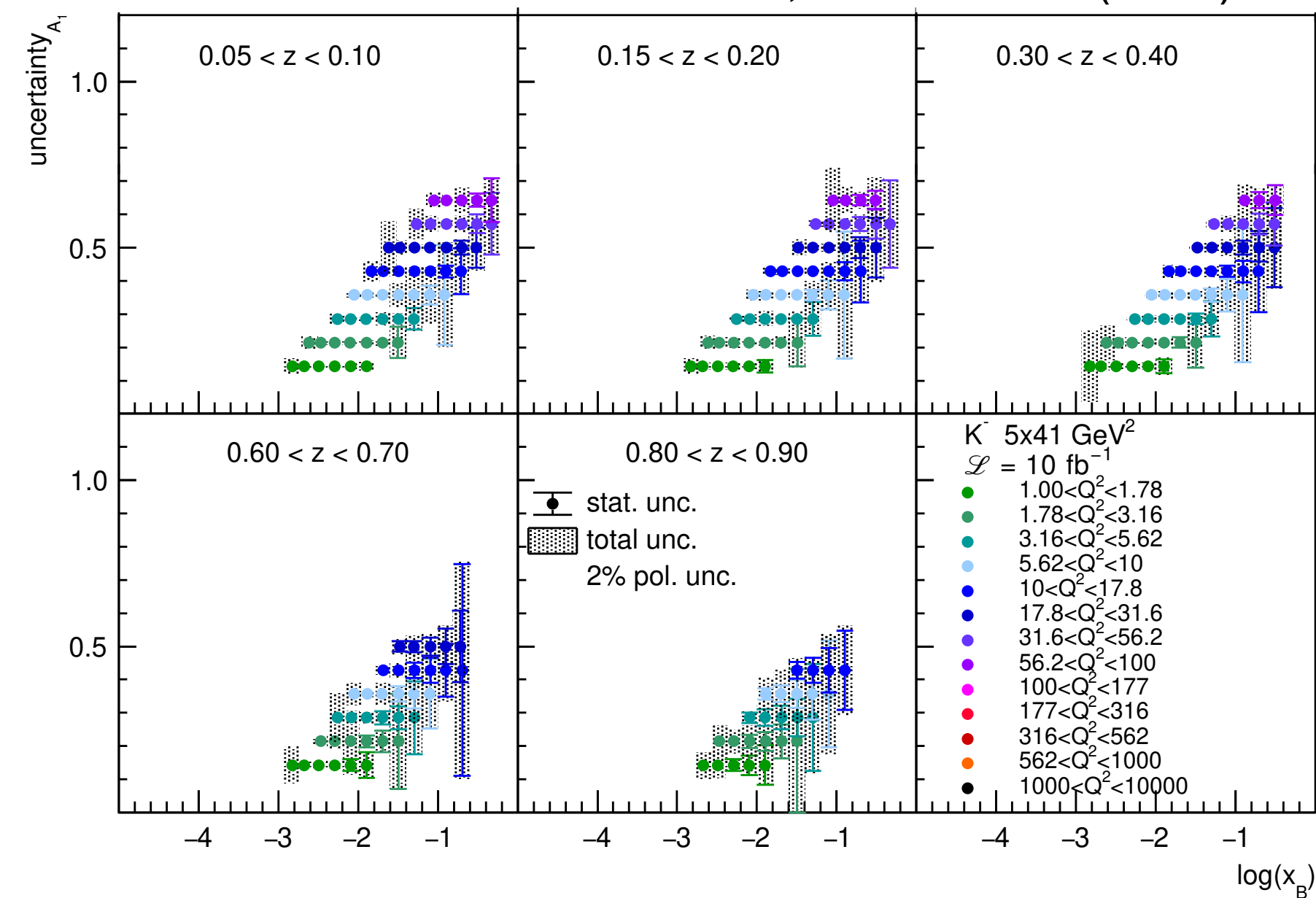


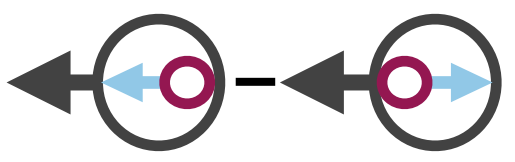
Helicity structure of the proton: sea quarks



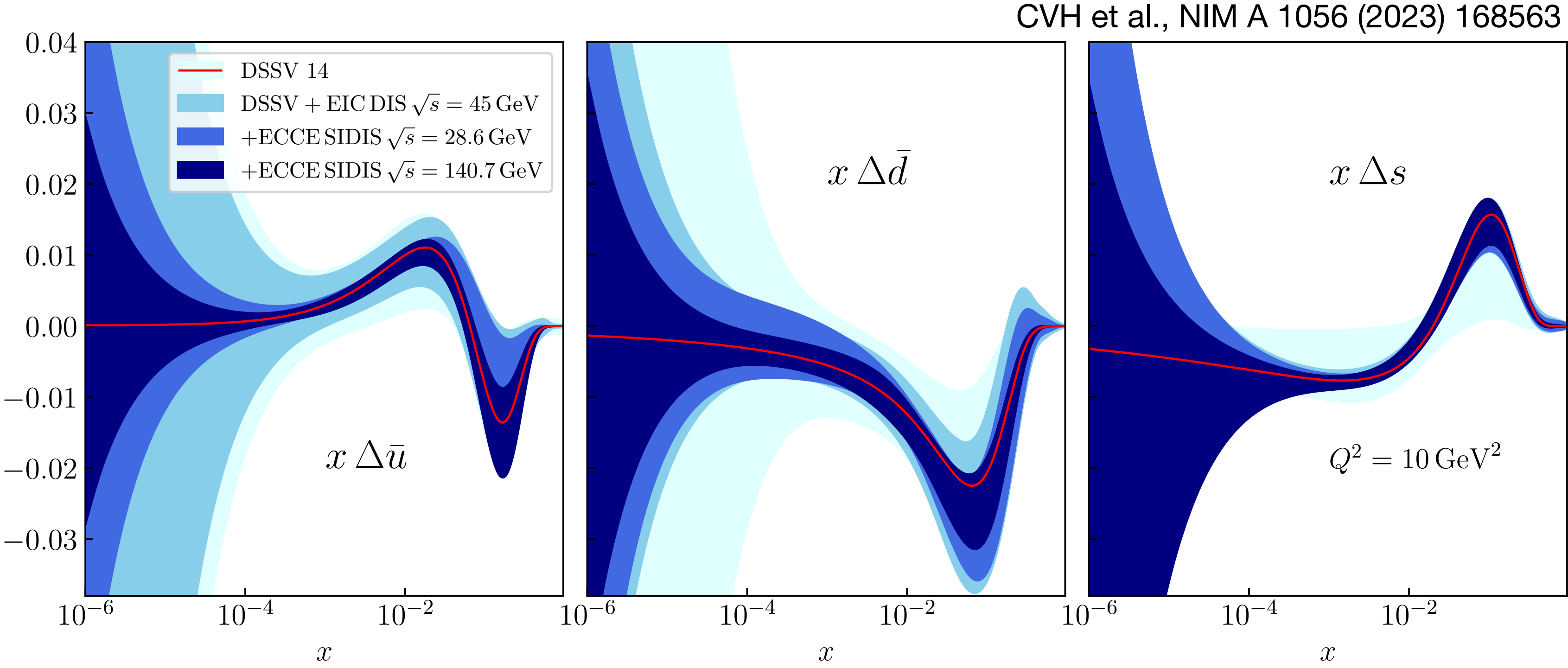
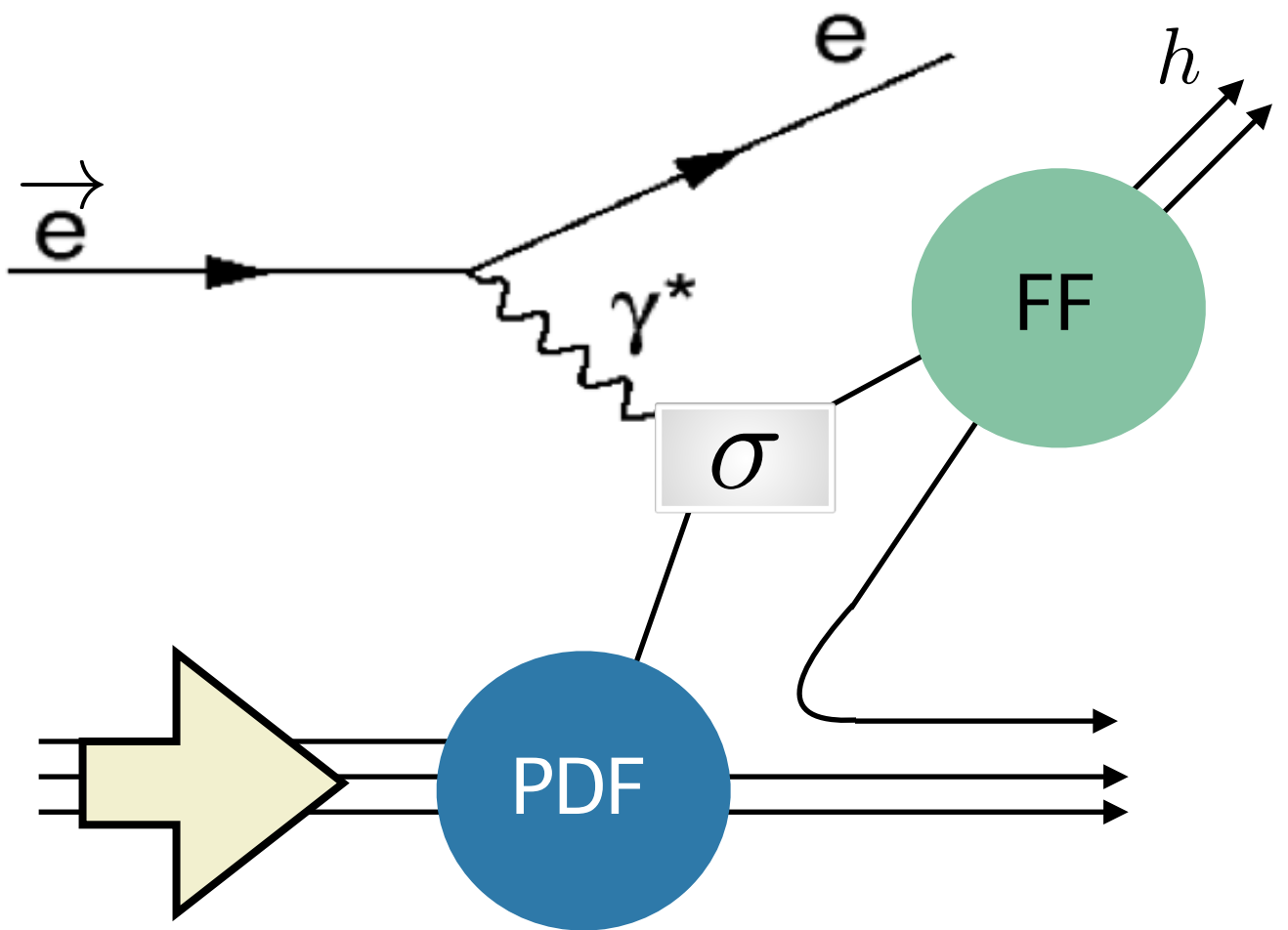
Semi-inclusive measurements, via good hadron PID
 → access to sea-quark spin

CVH et al., NIM A 1056 (2023) 168563



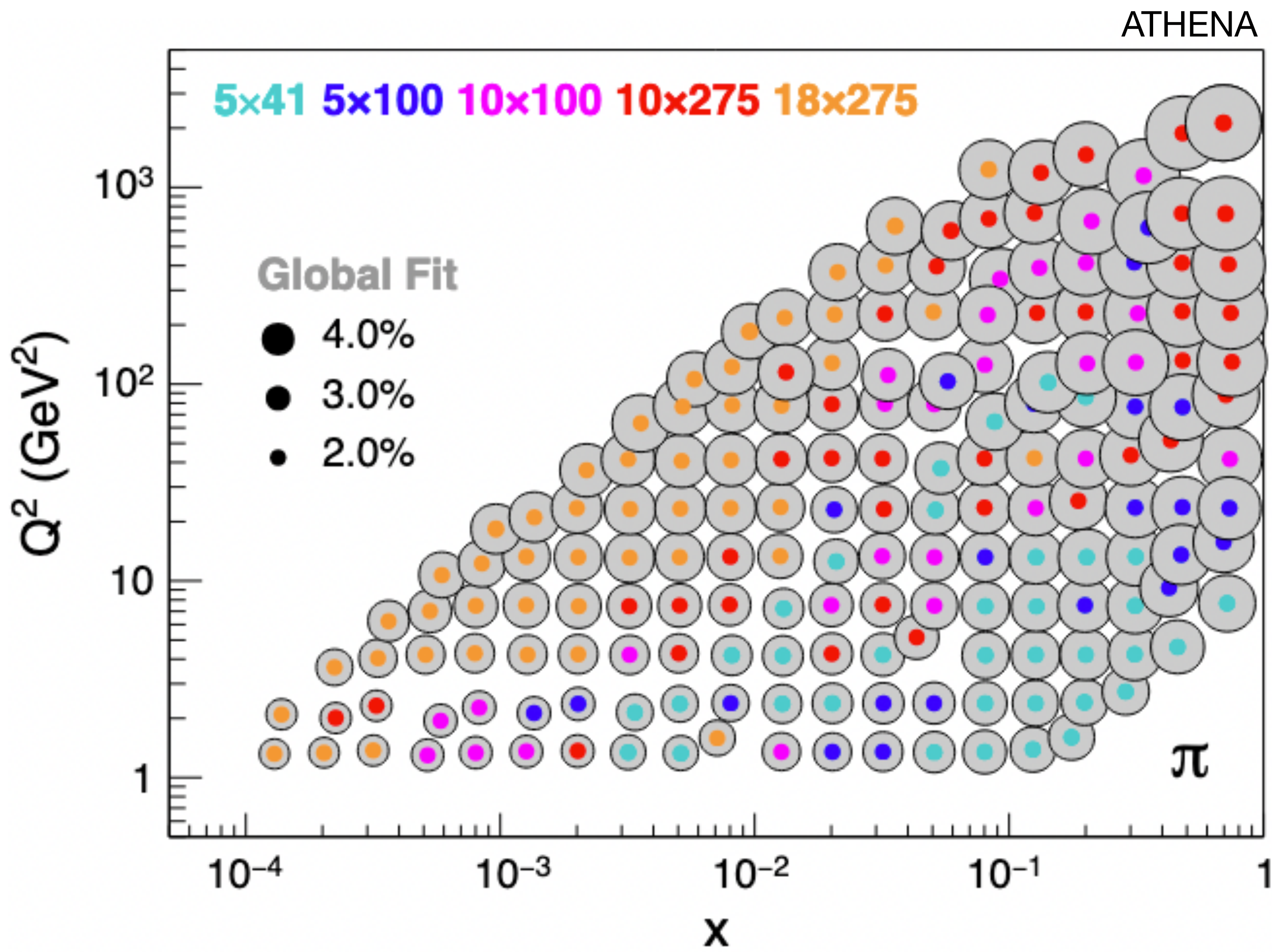


Helicity structure of the proton: sea quarks



Semi-inclusive measurements, via good hadron PID
→ access to sea-quark spin

Spin-independent TMD PDFs at EIC



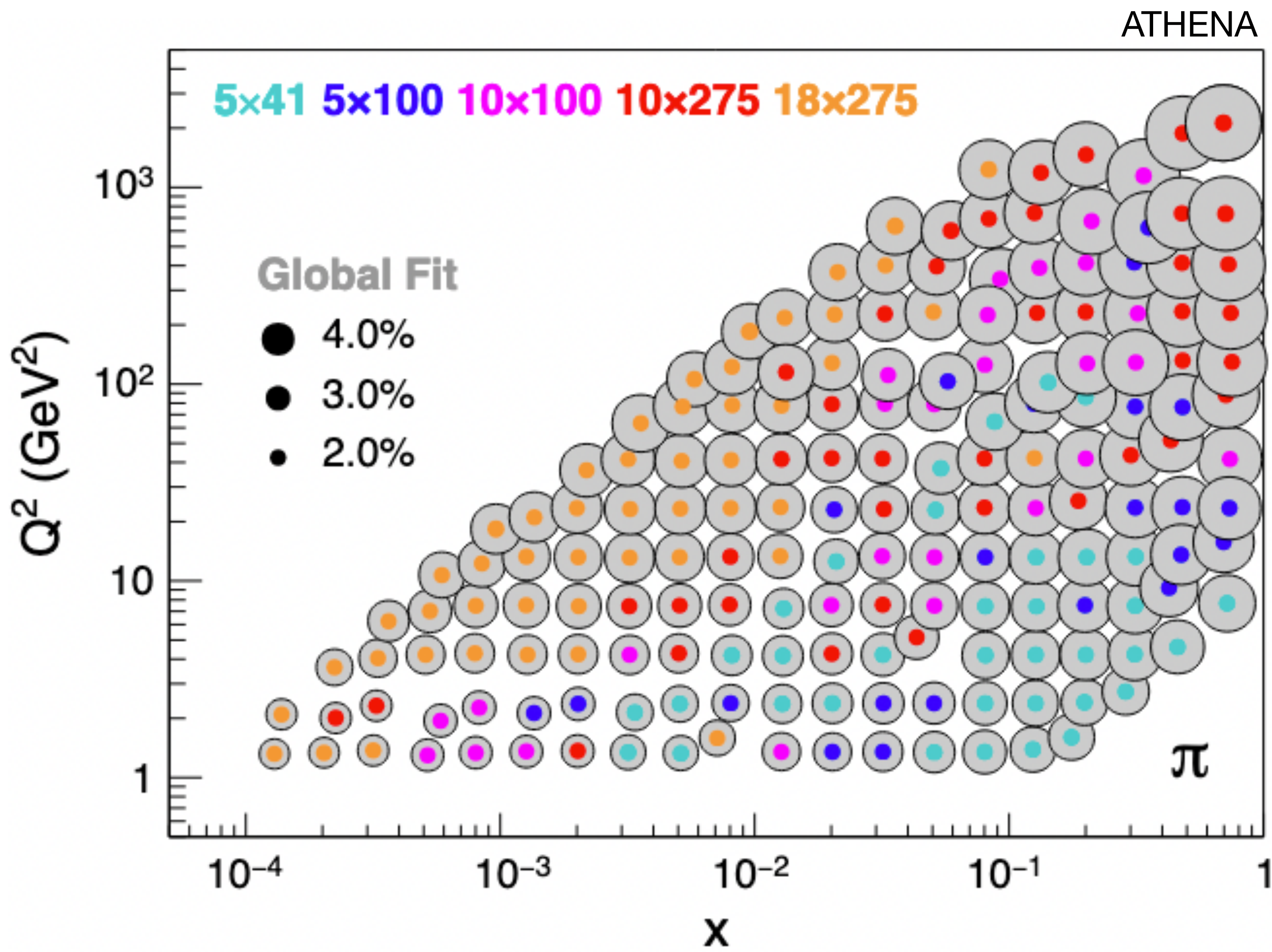
Fit:
 A. Bacchetta et al.,
 JHEP 06 (2017) 081,
 JHEP 06 (2019) 051 (erratum)

EIC uncertainties dominated
 by assumed
 3% point-to-point uncorrelated uncertainty
 3% scale uncertainty

Theory uncertainties dominated by
 TMD evolution.

Spin-independent TMD PDFs at EIC

Large lever-arm in Q^2 over large x range
 → Q^2 evolution of TMD PDF



Fit:
 A. Bacchetta et al.,
 JHEP 06 (2017) 081,
 JHEP 06 (2019) 051 (erratum)

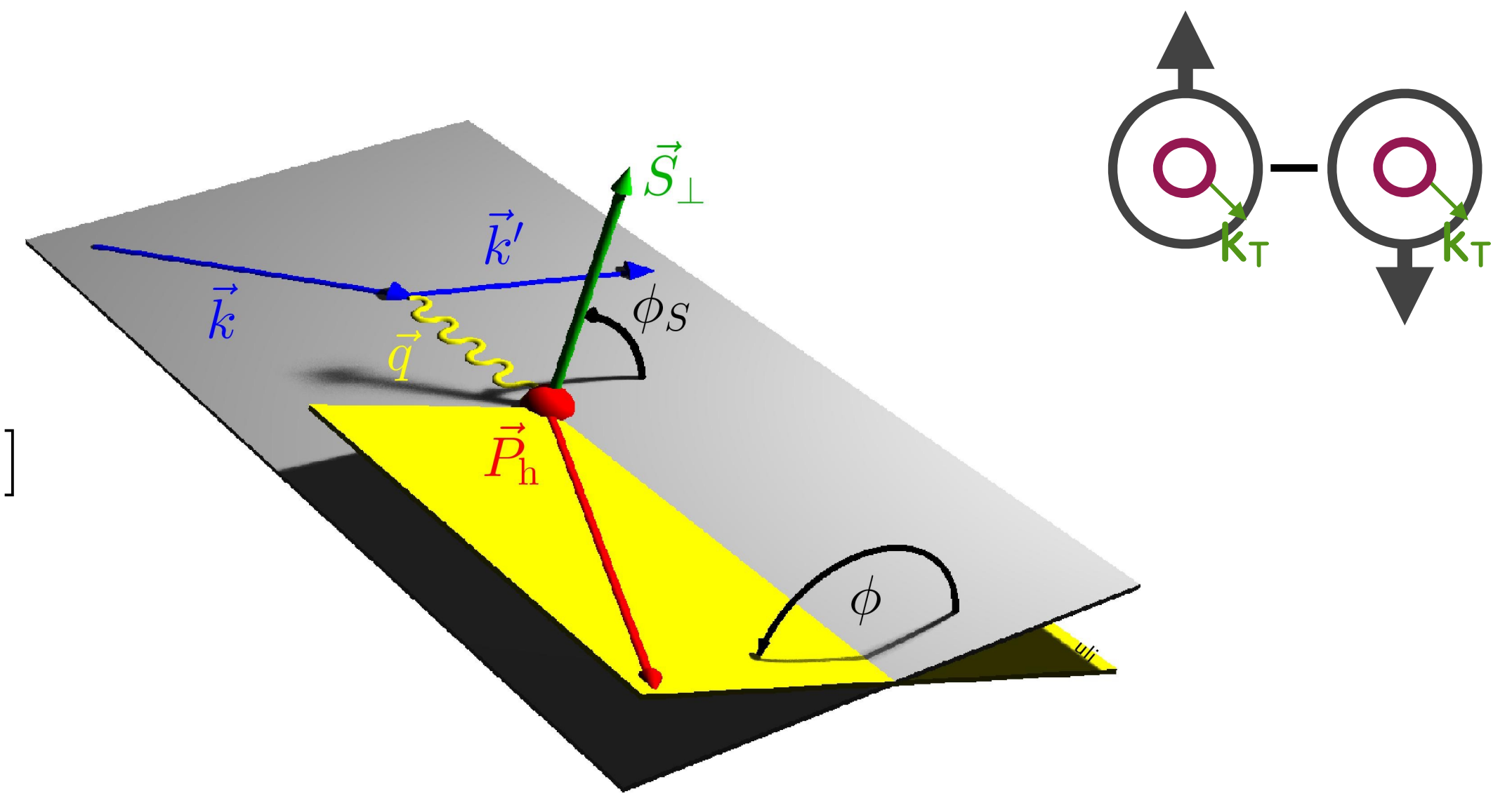
EIC uncertainties dominated
 by assumed
 3% point-to-point uncorrelated uncertainty
 3% scale uncertainty

Theory uncertainties dominated by
 TMD evolution.

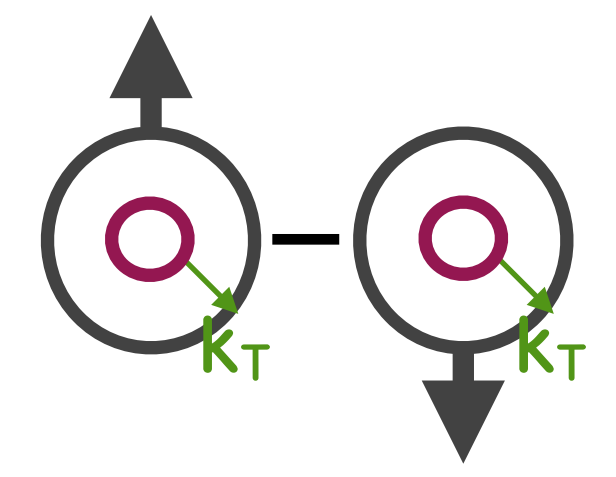
Spin-dependent TMD PDFs: Sivers

Sivers asymmetry

$$\sigma^h(\phi, \phi_S) \propto S_T 2\langle \sin(\phi - \phi_S) \rangle_{UT}^h \sin(\phi - \phi_S) \longrightarrow \mathcal{C}[f_{1T}^\perp \times D_1^{q \rightarrow h}]$$

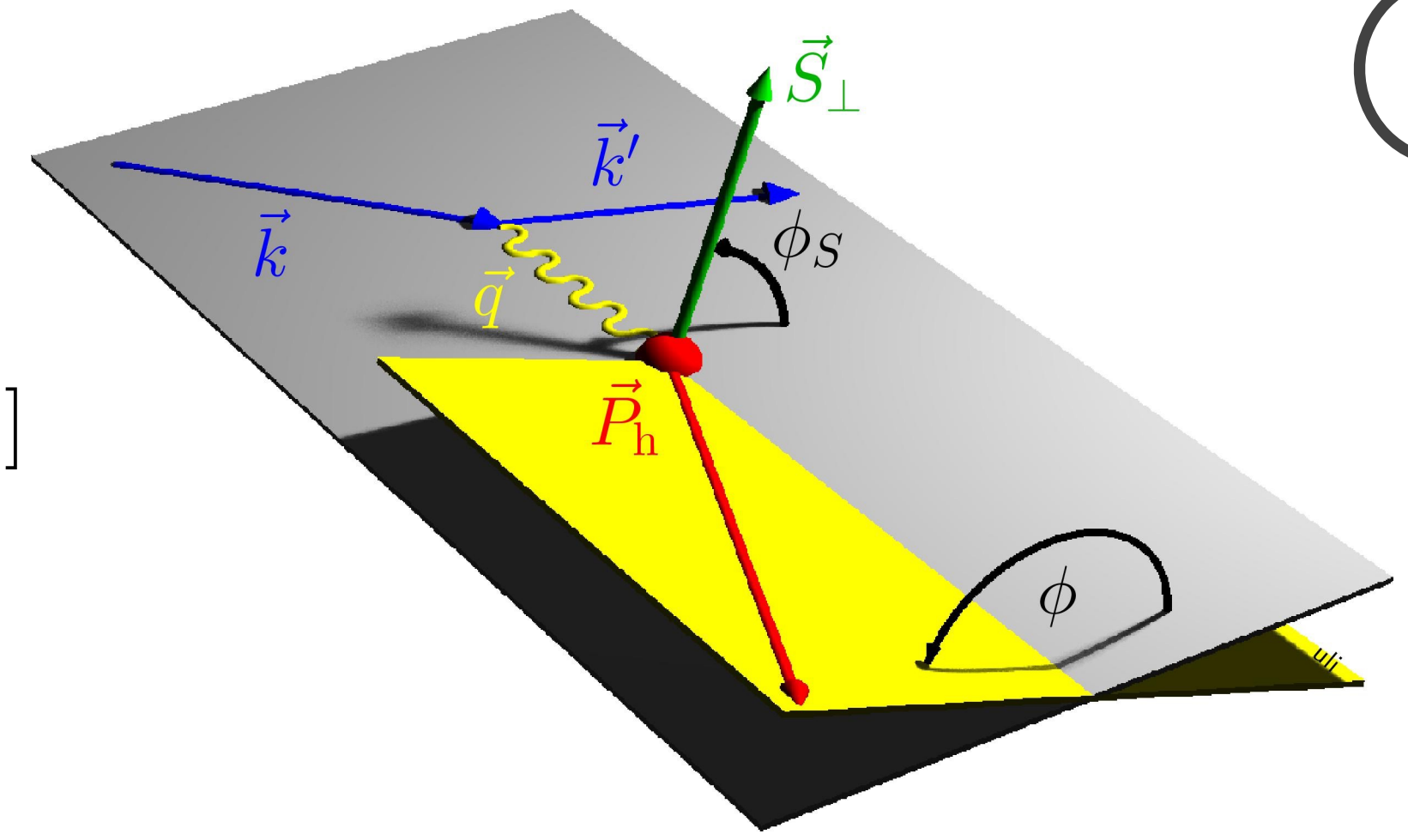


Spin-dependent TMD PDFs: Sivers



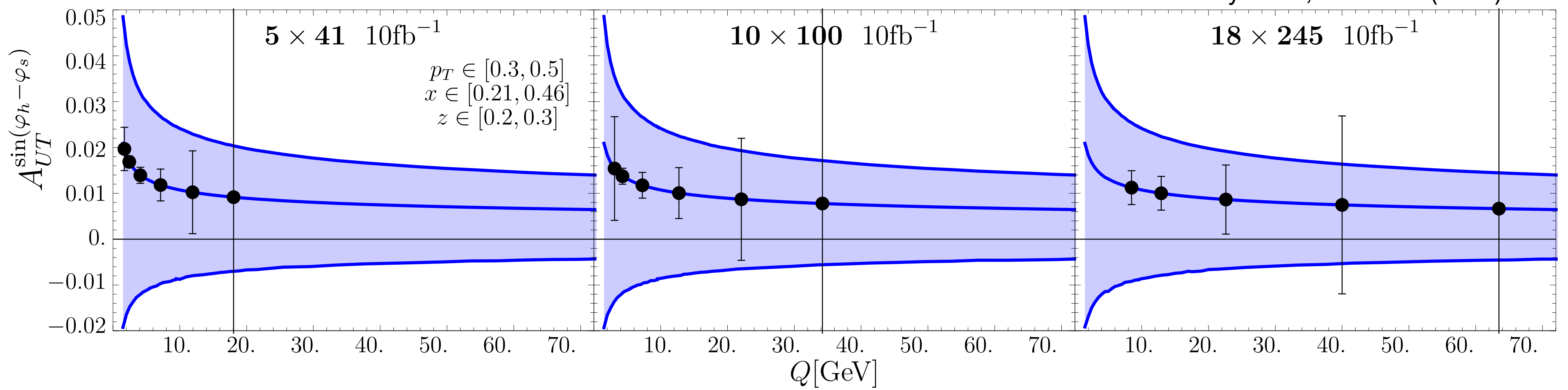
Sivers asymmetry

$$\sigma^h(\phi, \phi_S) \propto S_T 2 \langle \sin(\phi - \phi_S) \rangle_{UT}^h \sin(\phi - \phi_S) \longrightarrow \mathcal{C}[f_{1T}^\perp \times D_1^{q \rightarrow h}]$$



R. Seidl, A. Vladimirov et al., NIM A **1055** (2023) 168458

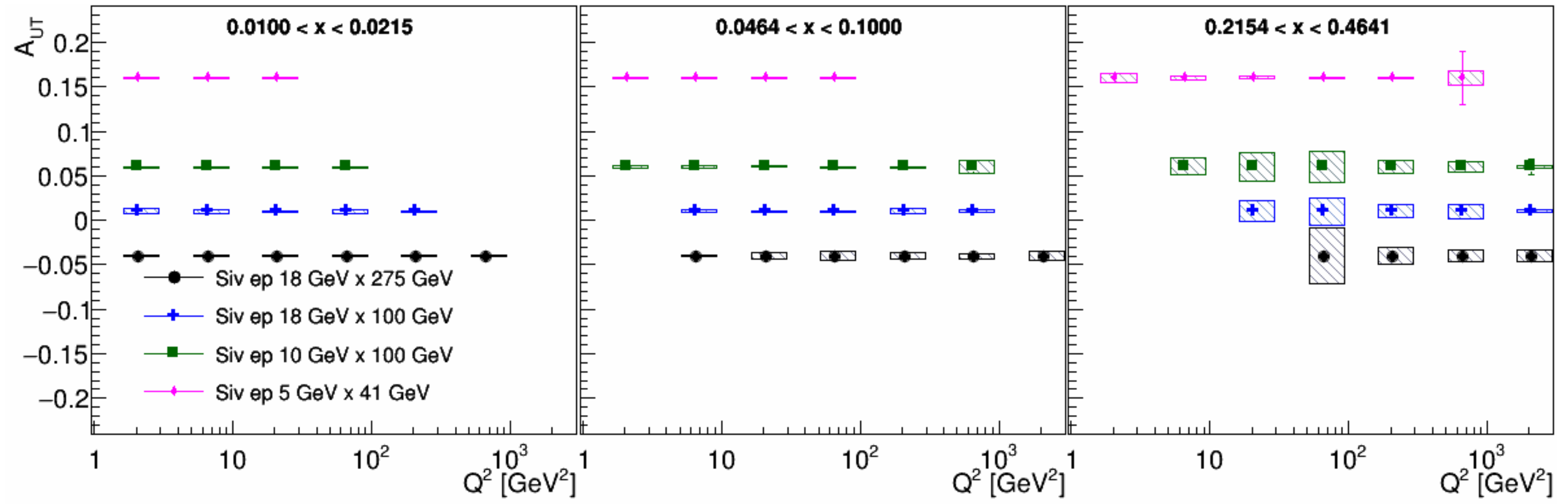
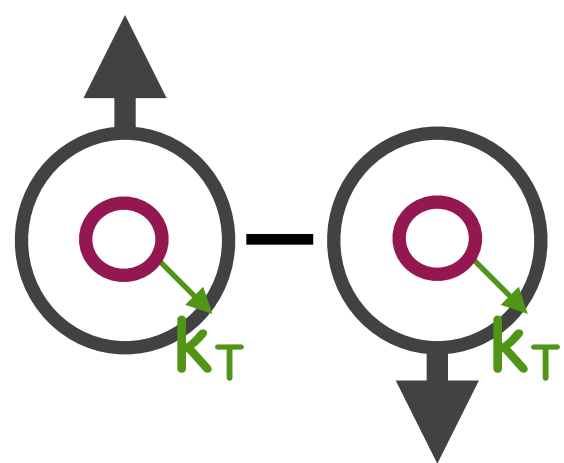
Parametrisation: M. Bury et al., JHEP **05** (2021)151



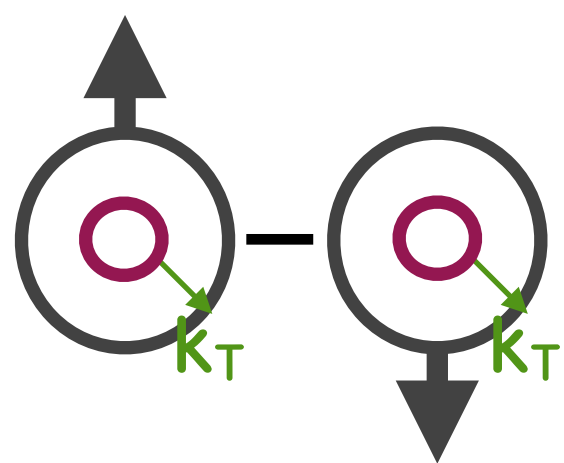
Decrease of asymmetry with increasing $Q^2 \rightarrow$ need high precision ($<1\%$) to measure asymmetry at high Q^2

Impact of EIC on Sivers TMD PDF

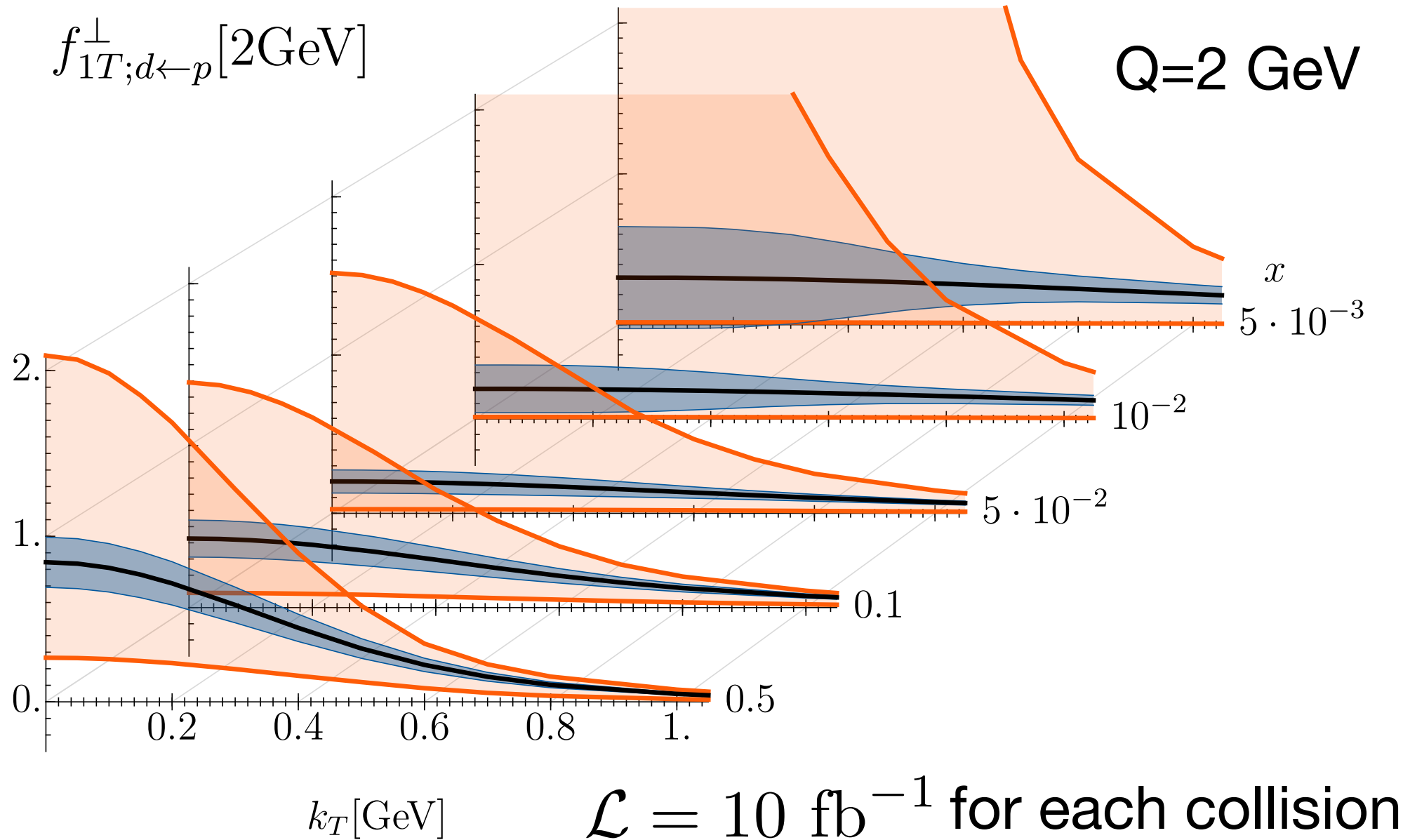
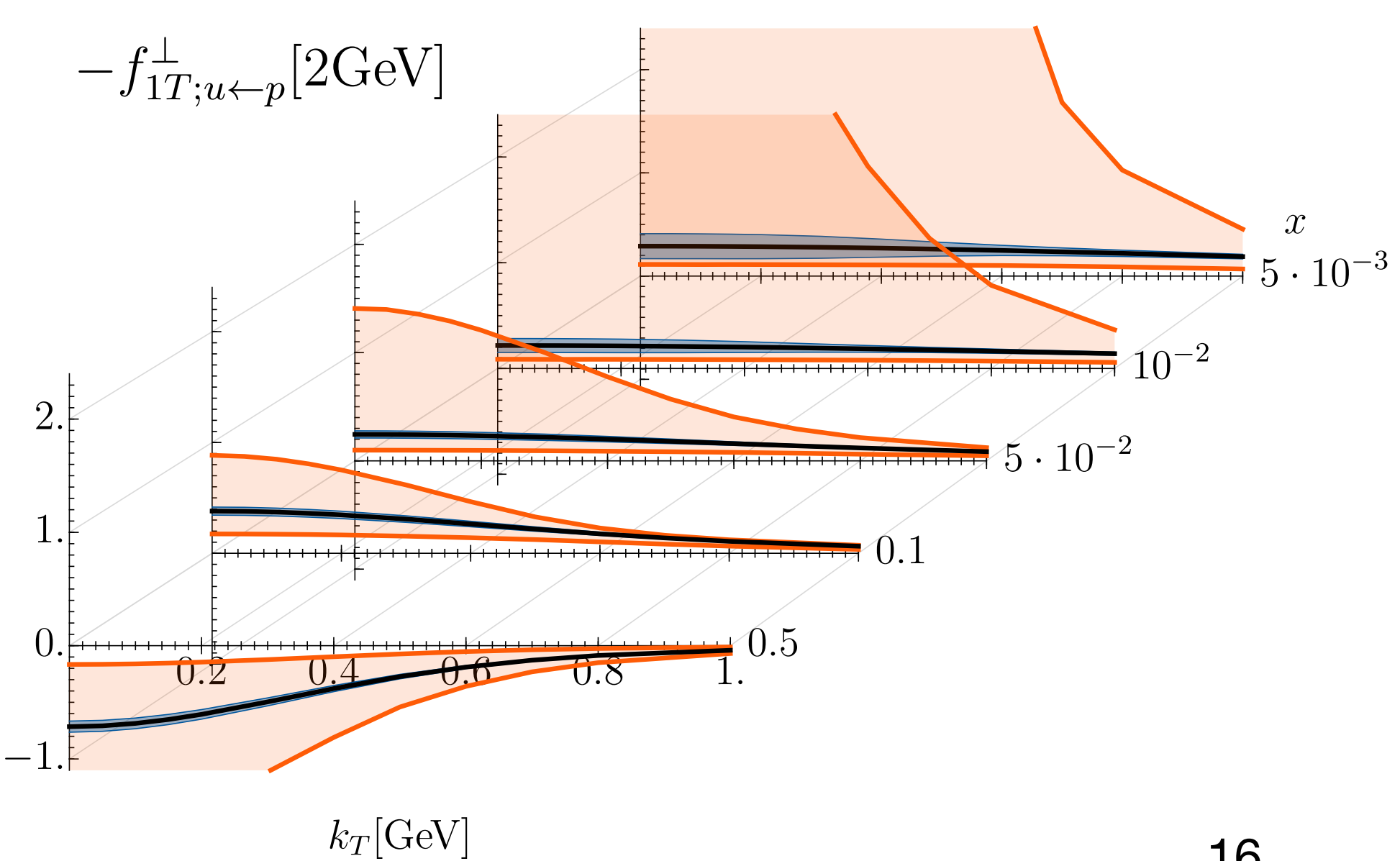
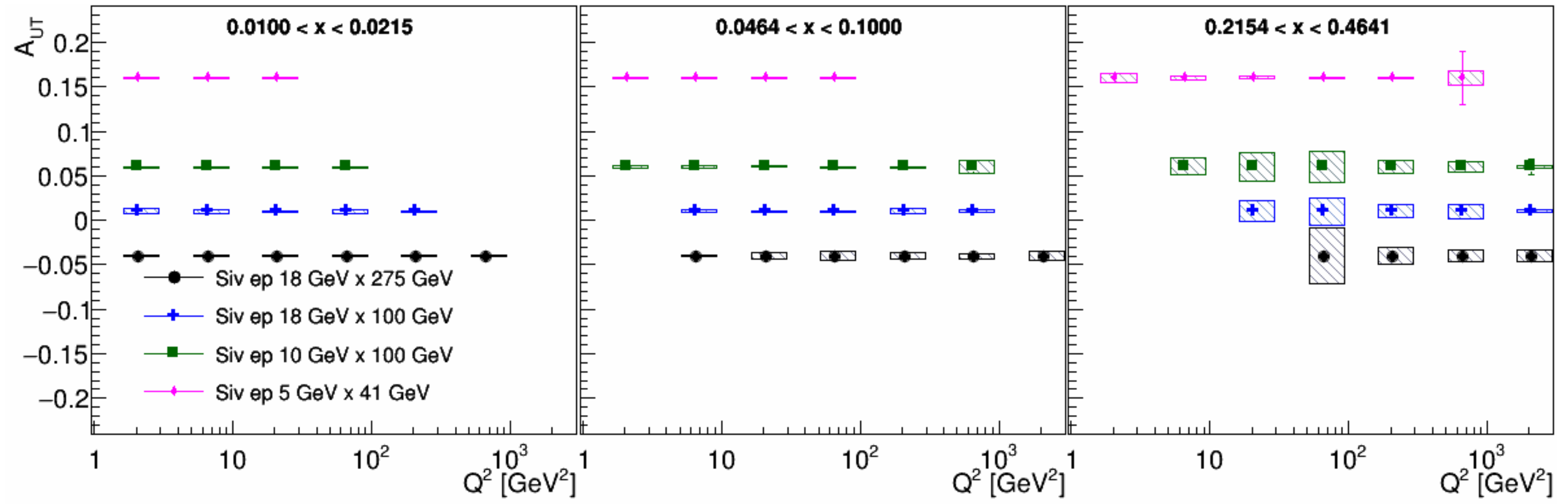
R. Seidl, A. Vladimirov et al., NIM A **1055** (2023) 168458



Impact of EIC on Sivers TMD PDF



R. Seidl, A. Vladimirov et al., NIM A **1055** (2023) 168458

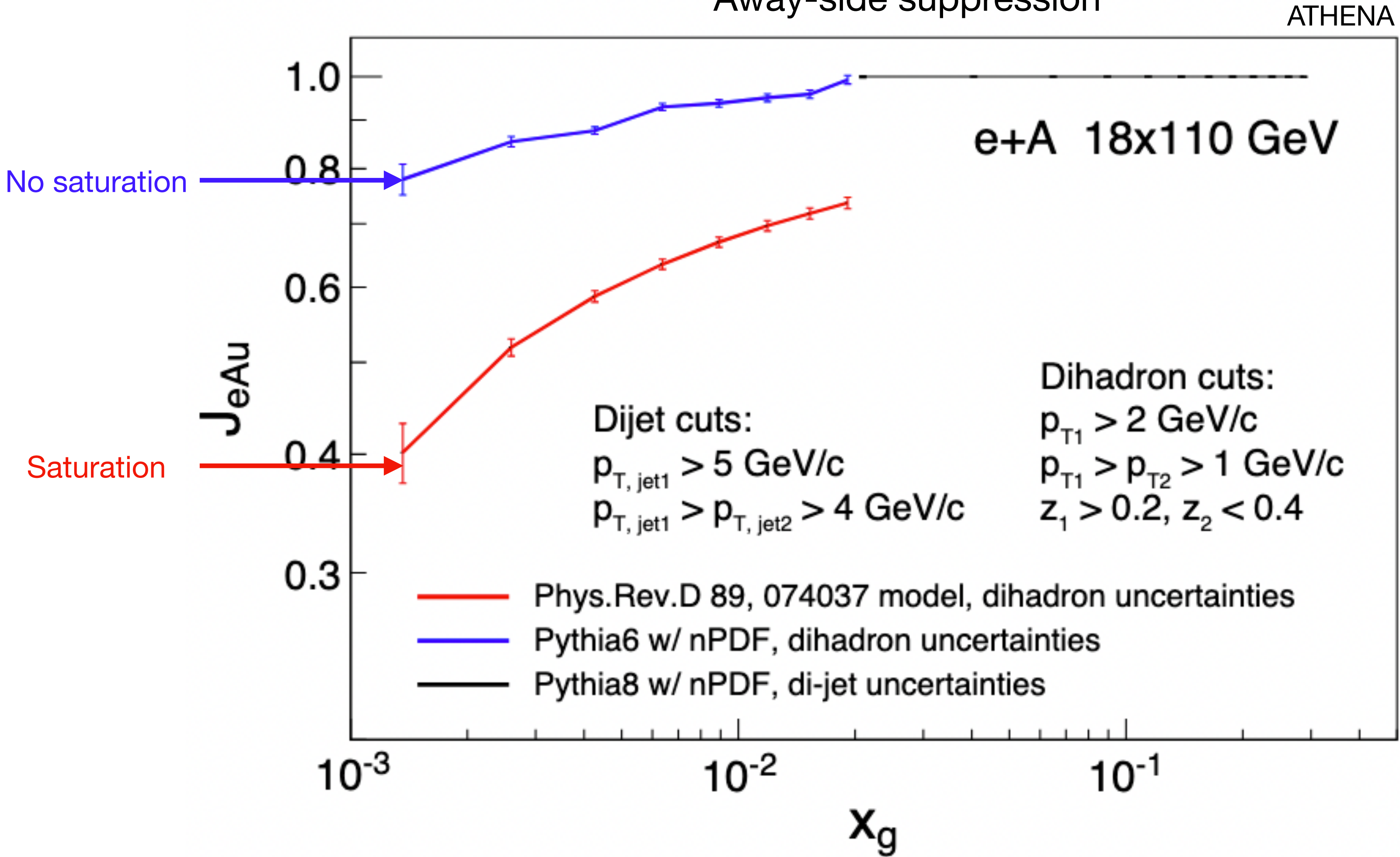
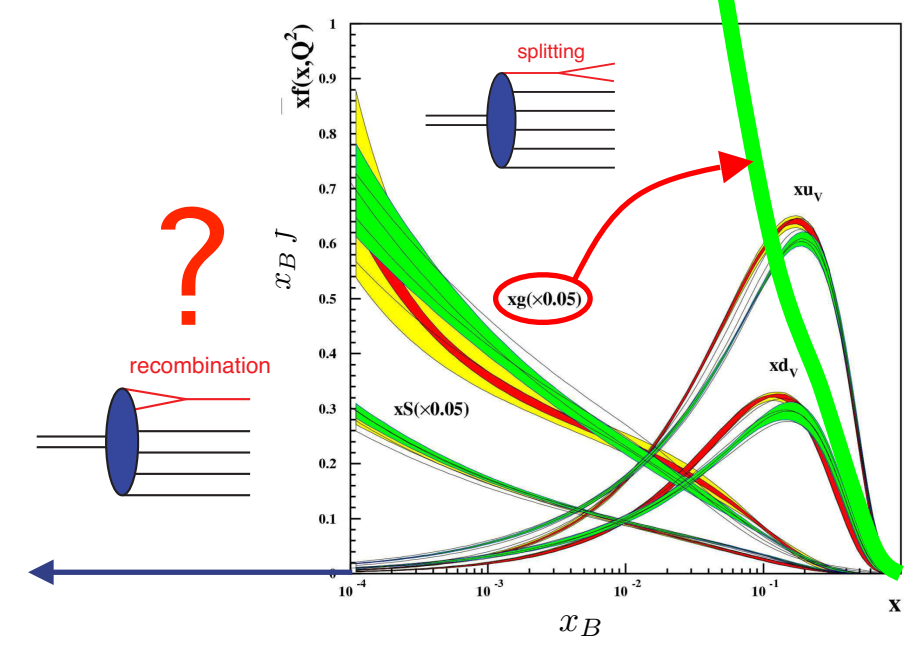


$\mathcal{L} = 10 \text{ fb}^{-1}$ for each collision energy

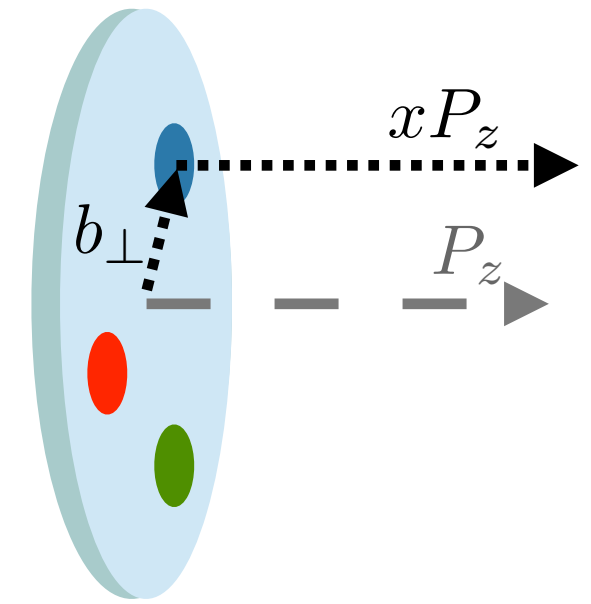
Di-hadron production and jets in eA

- Complementarity region covered by dihadron and jet production

correlated back-to-back hadron pairs in e+Au/e+p scaled by $A^{1/3}$
 Away-side suppression

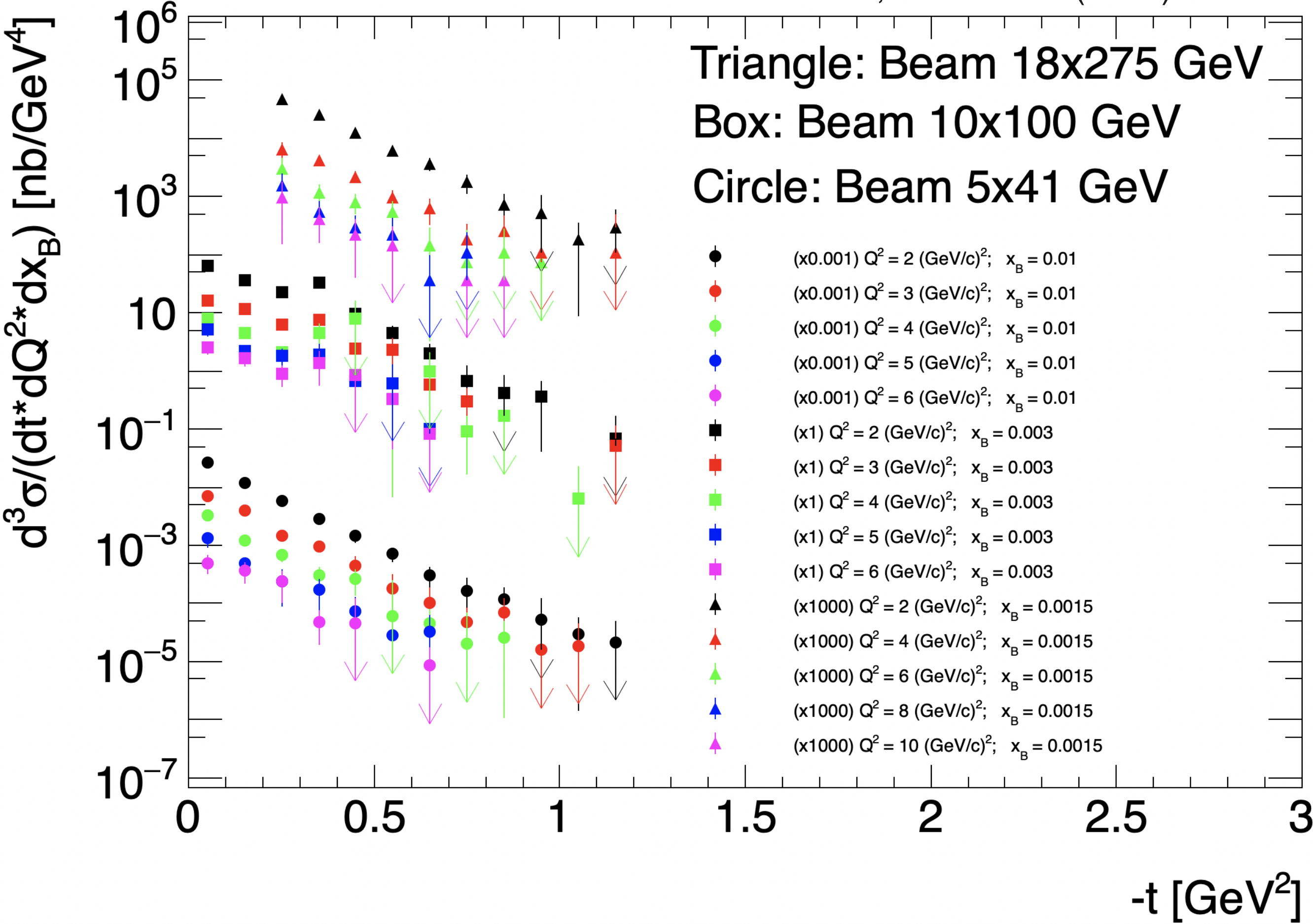


Exclusive measurements on p with the EIC

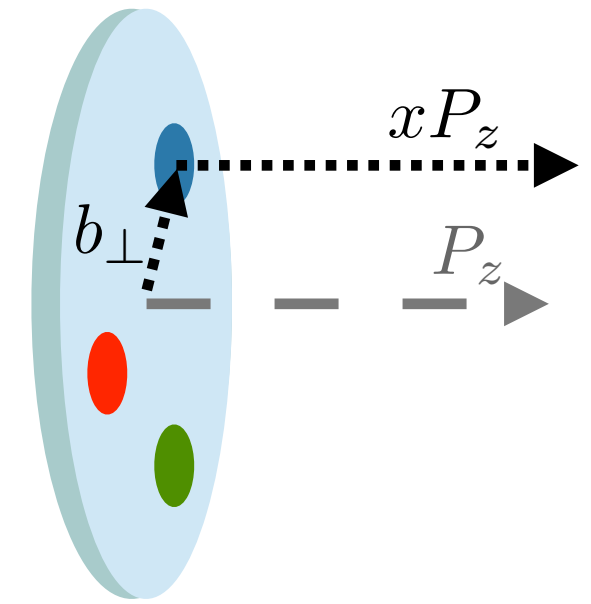


Deeply virtual Compton scattering
 → sensitive to quarks (and gluons)

ECCE, NIMA 1052 (2023) 168238



Exclusive measurements on p with the EIC

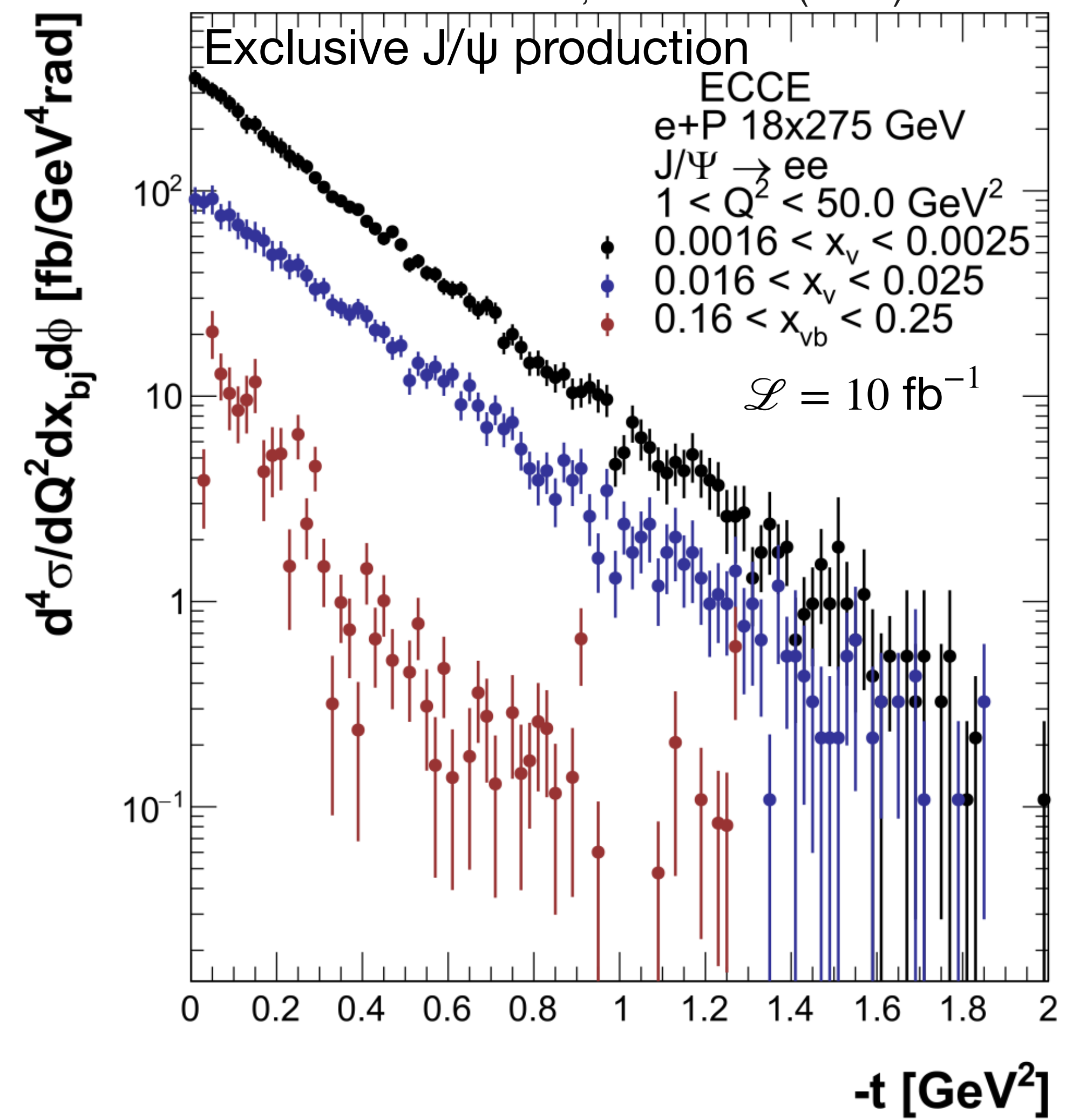
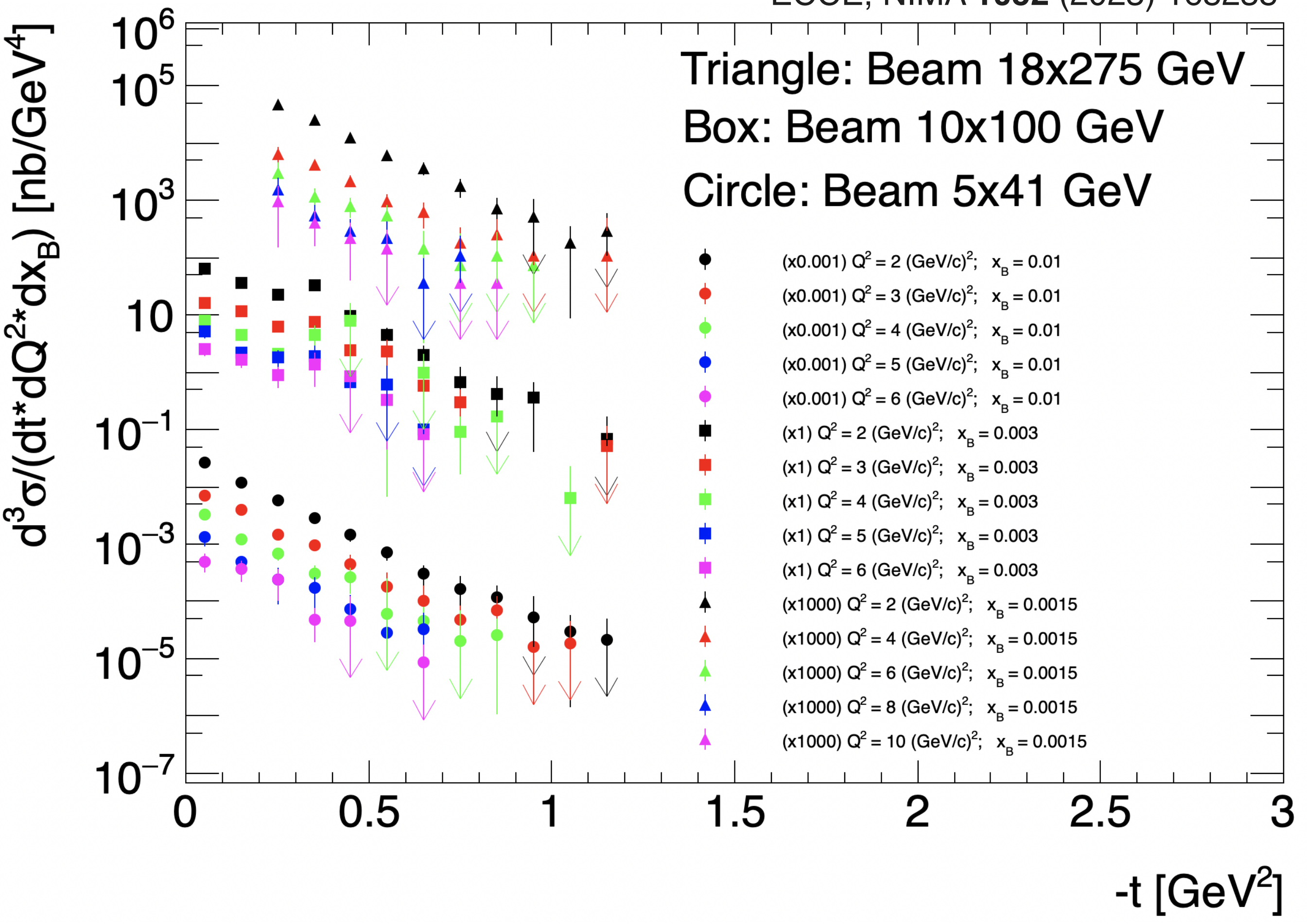


Deeply virtual Compton scattering
 → sensitive to quarks (and gluons)

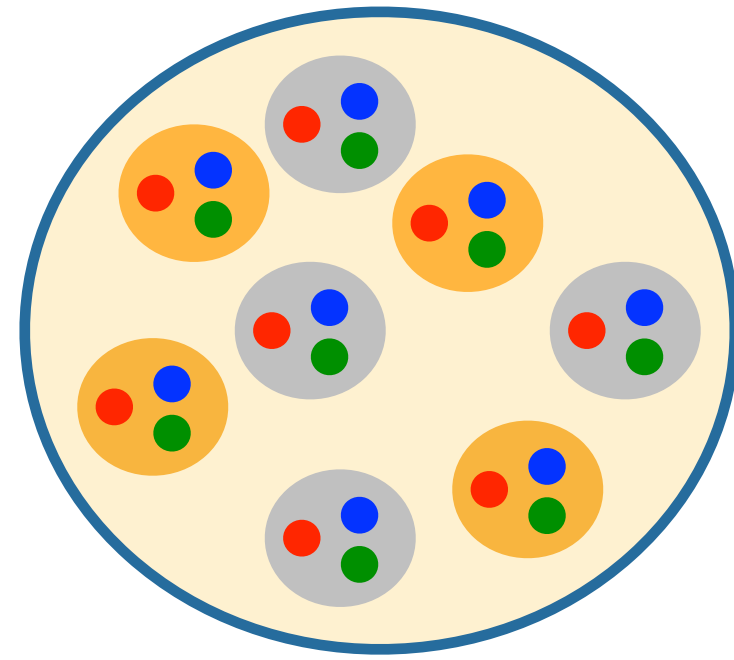
Exclusive J/ψ production
 → excellent to probe gluon GPDs

ECCE, NIMA 1052 (2023) 168238

ECCE, NIMA 1052 (2023) 168238

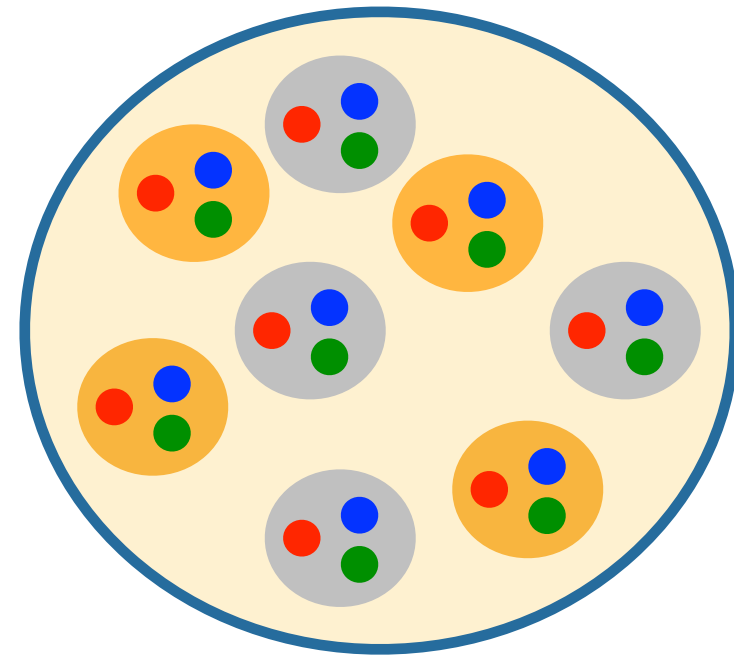


Exclusive measurements on nuclear targets



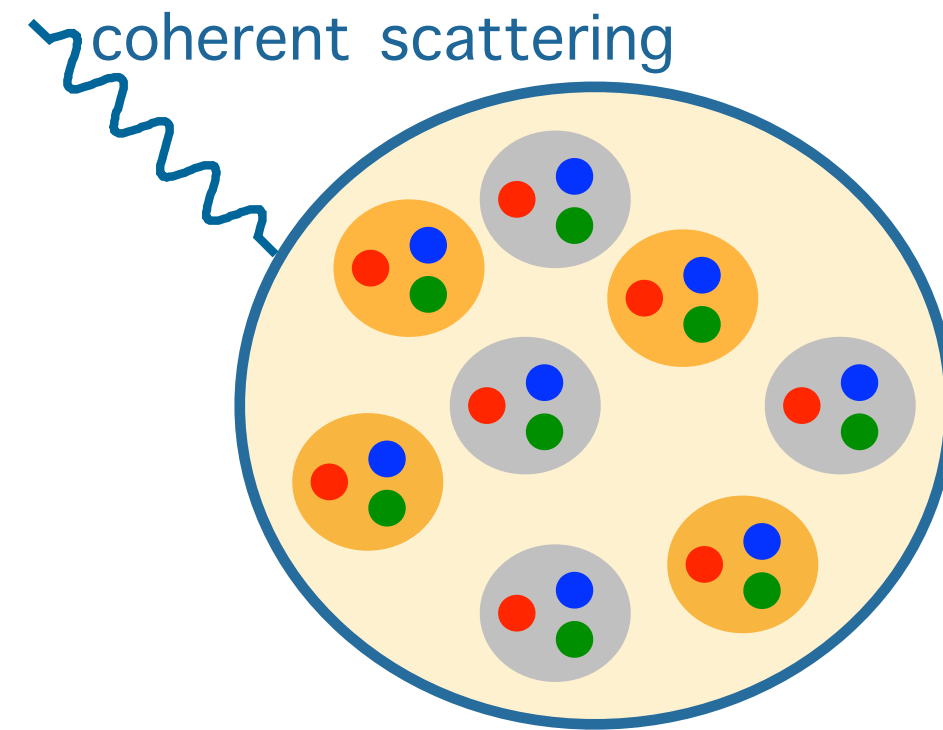
Exclusive measurements on nuclear targets

What object are we probing?



Exclusive measurements on nuclear targets

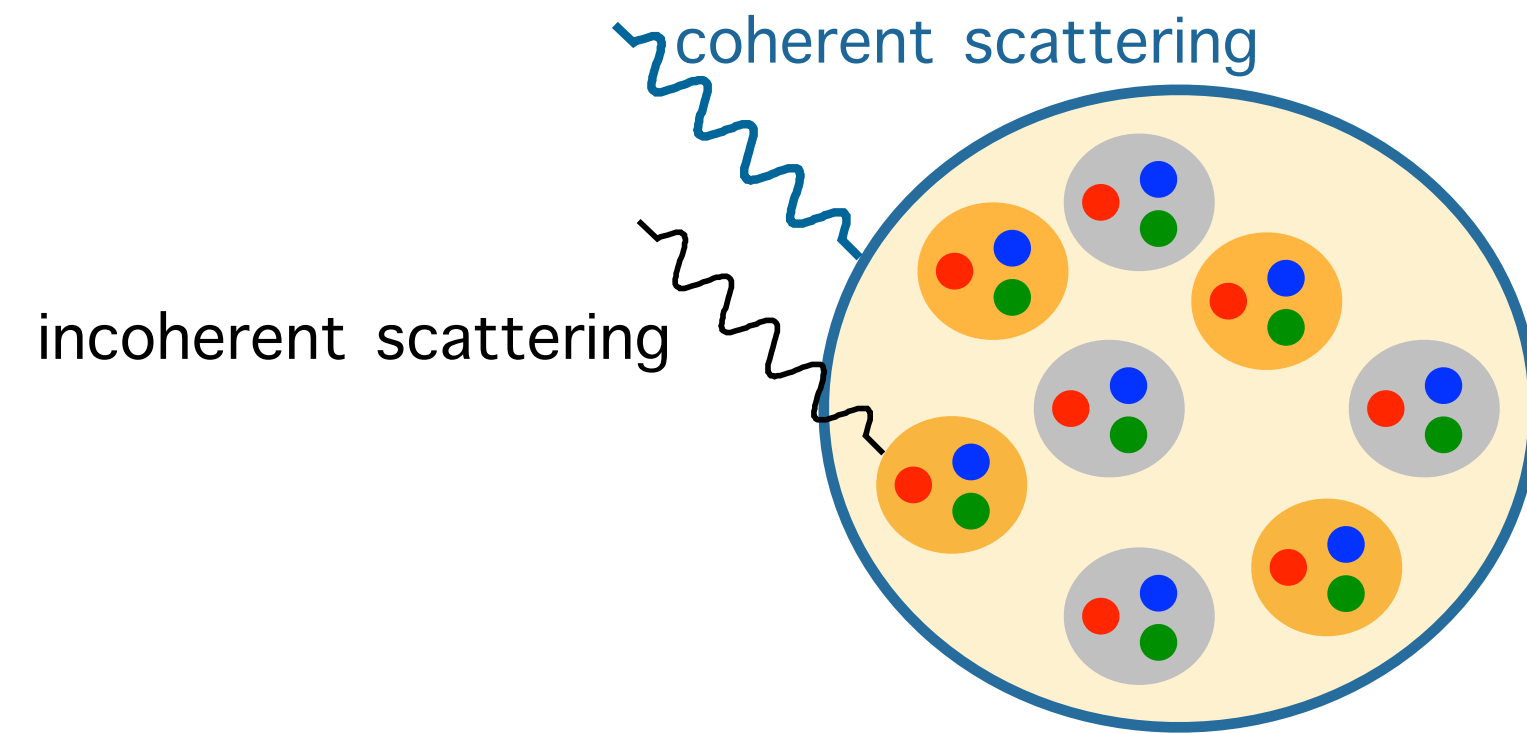
What object are we probing?



Coherent interaction: interaction with target as a whole.
~ target remains in same quantum state.

Exclusive measurements on nuclear targets

What object are we probing?

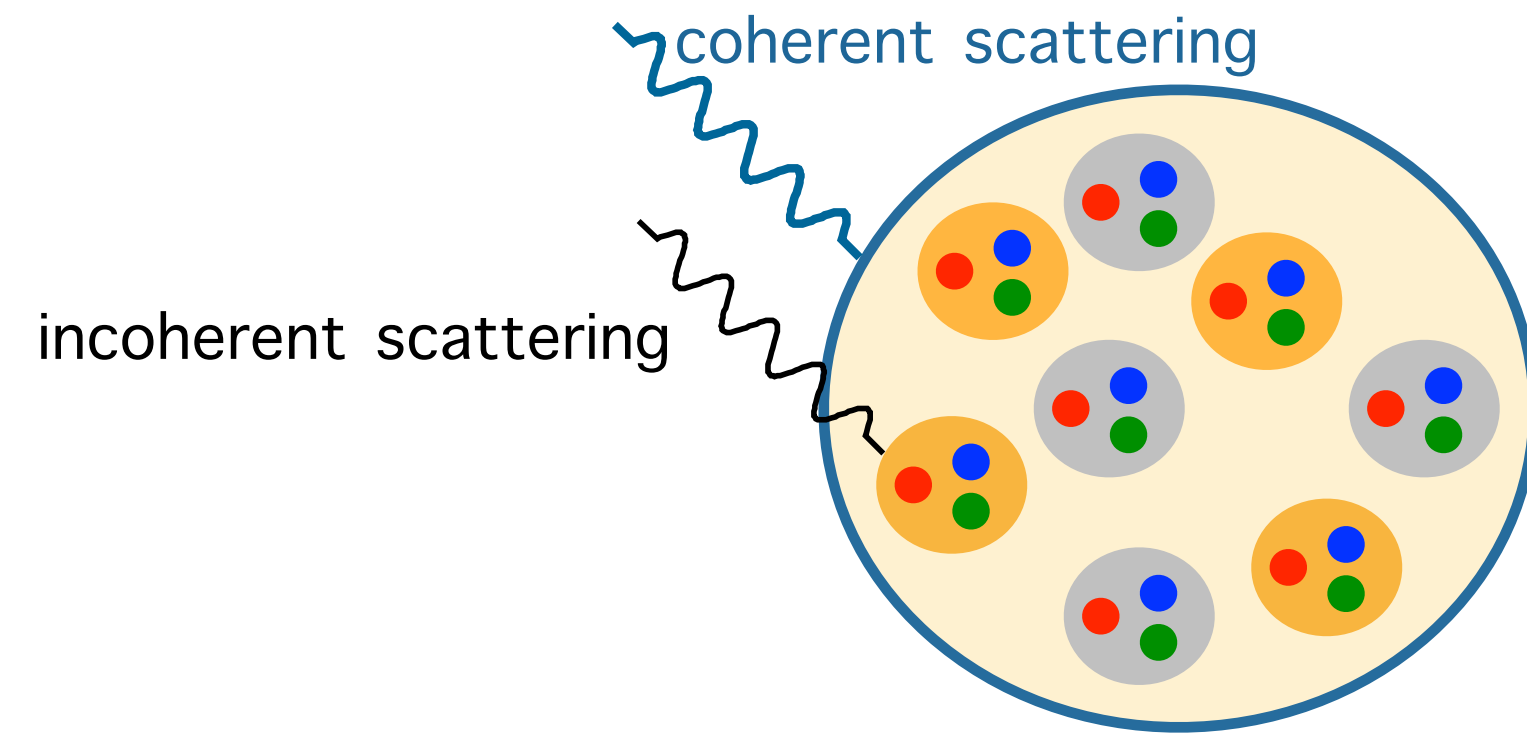


Coherent interaction: interaction with target as a whole.
~ target remains in same quantum state.

Incoherent interaction: interaction with constituents inside target.
~ target does not remain in same quantum state.
Ex.: target dissociation, excitation

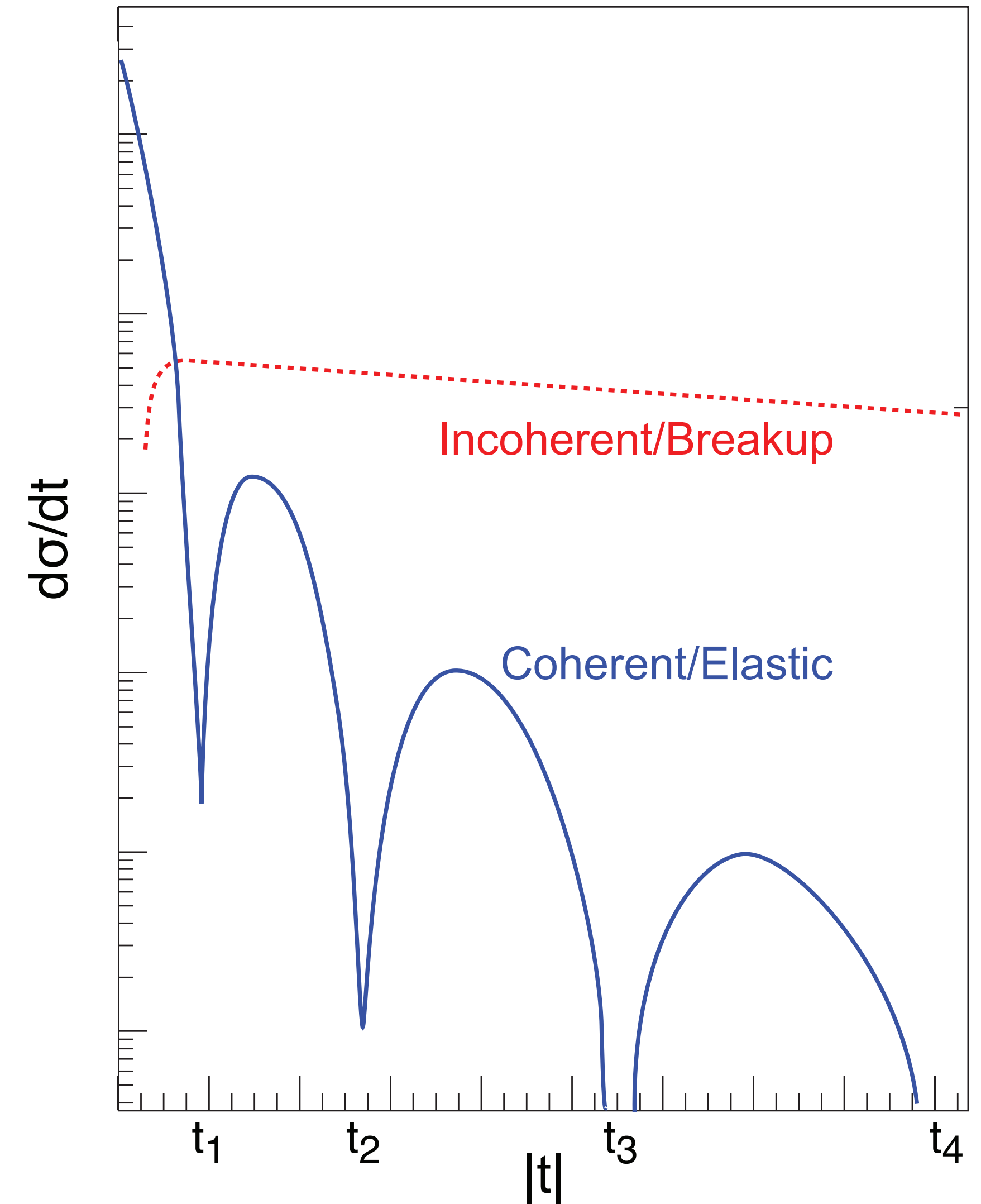
Exclusive measurements on nuclear targets

What object are we probing?



Coherent interaction: interaction with target as a whole.
~ target remains in same quantum state.

Incoherent interaction: interaction with constituents inside target.
~ target does not remain in same quantum state.
Ex.: target dissociation, excitation

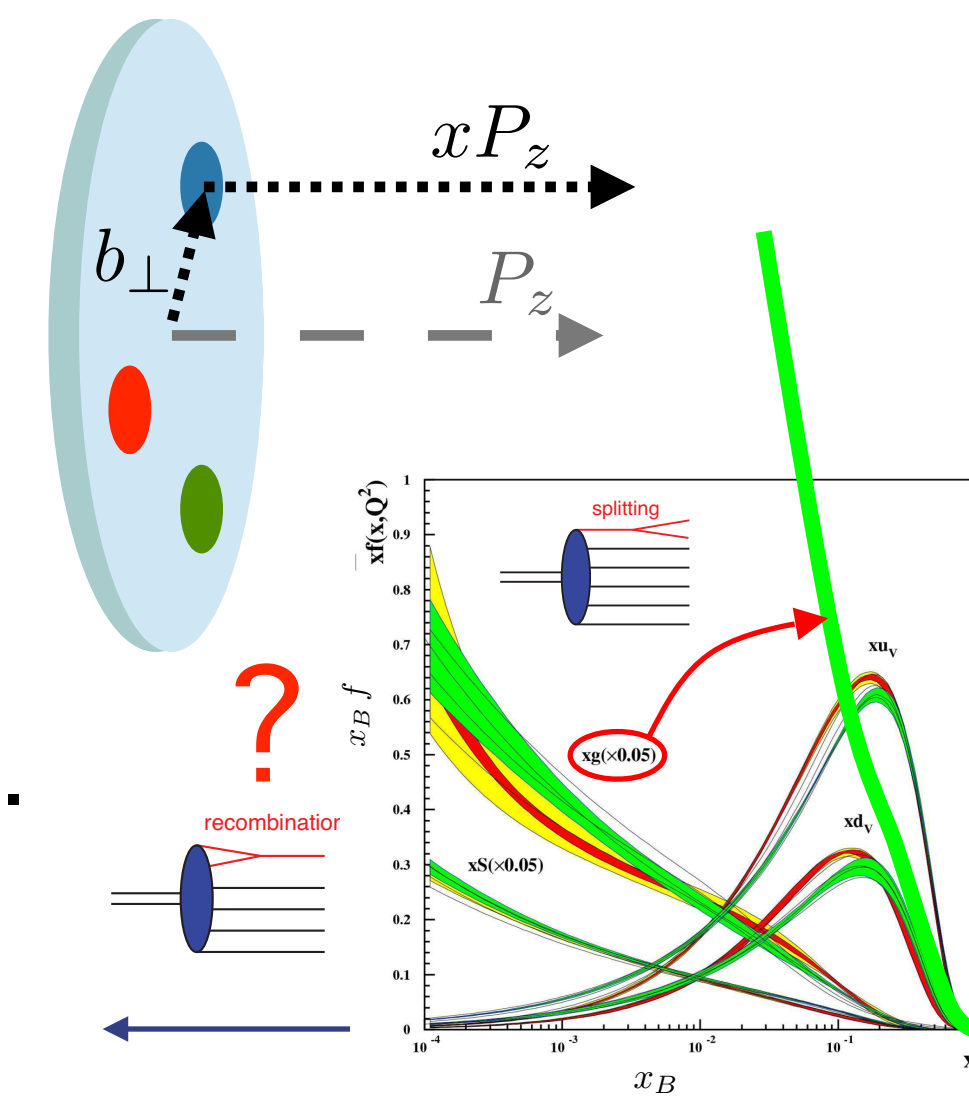


Coherent eA production

- probe gluon saturation
- nuclear imaging in position space:

$$\int_0^{\infty} d\Delta_{\perp} \text{GPD}(x, 0, \Delta_{\perp}) e^{-ib_{\perp}\Delta_{\perp}}$$

Experimentally limited by maximum transverse momentum.
 Need measured p_T range as extended as possible.
 ~third diffractive minimum.



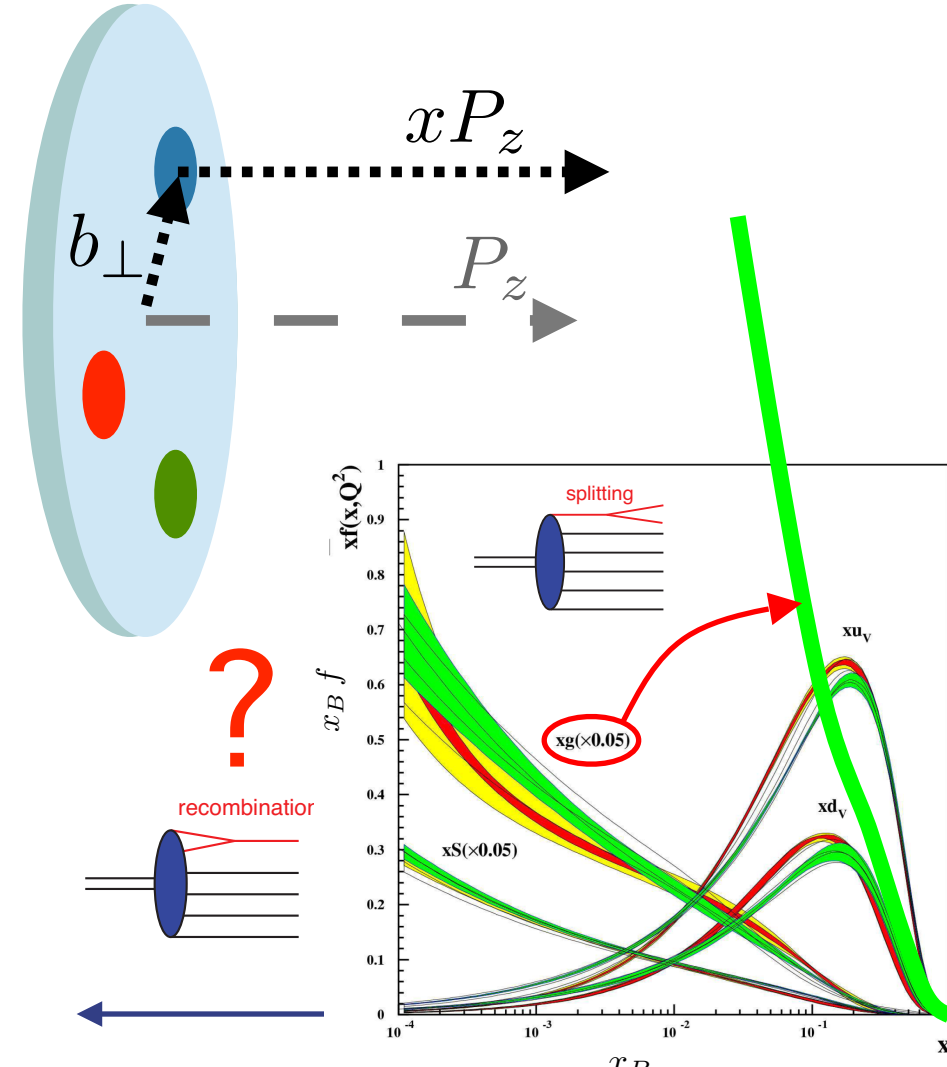
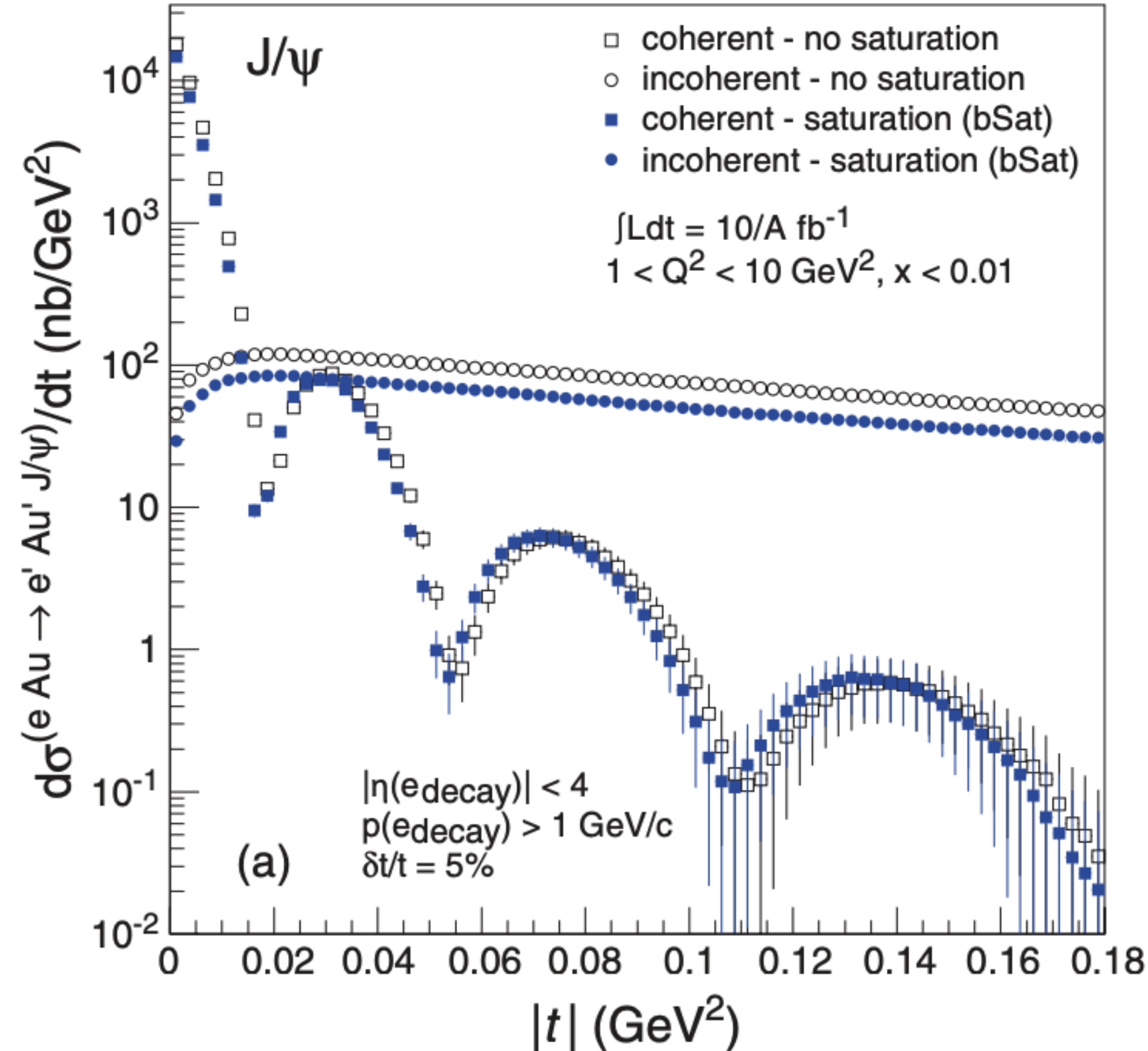
Coherent eA production

- probe gluon saturation
- nuclear imaging in position space:

$$\int_0^\infty d\Delta_\perp \text{GPD}(x, 0, \Delta_\perp) e^{-ib_\perp \Delta_\perp}$$

Experimentally limited by maximum transverse momentum.
 Need measured p_T range as extended as possible.
 ~third diffractive minimum.

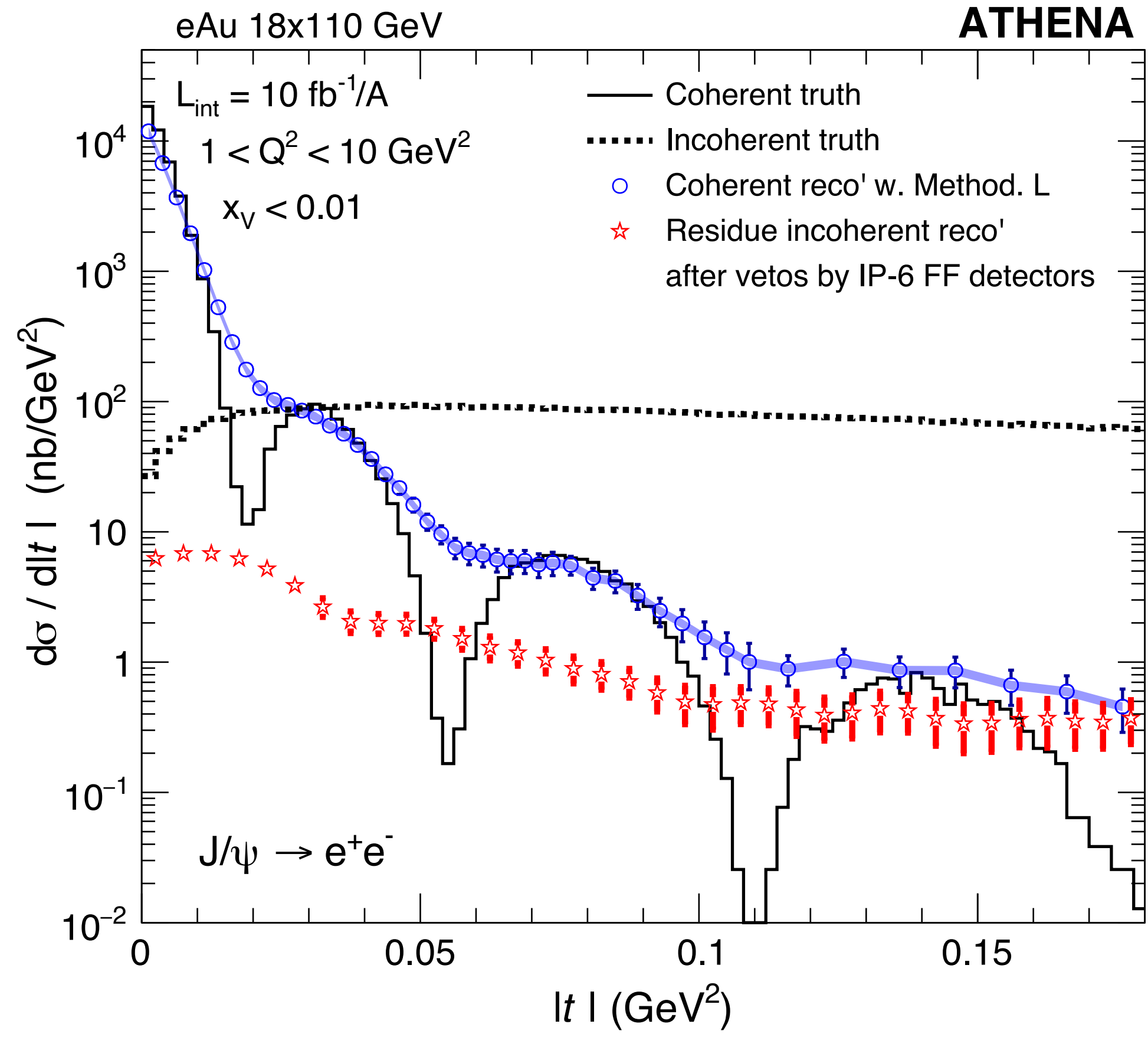
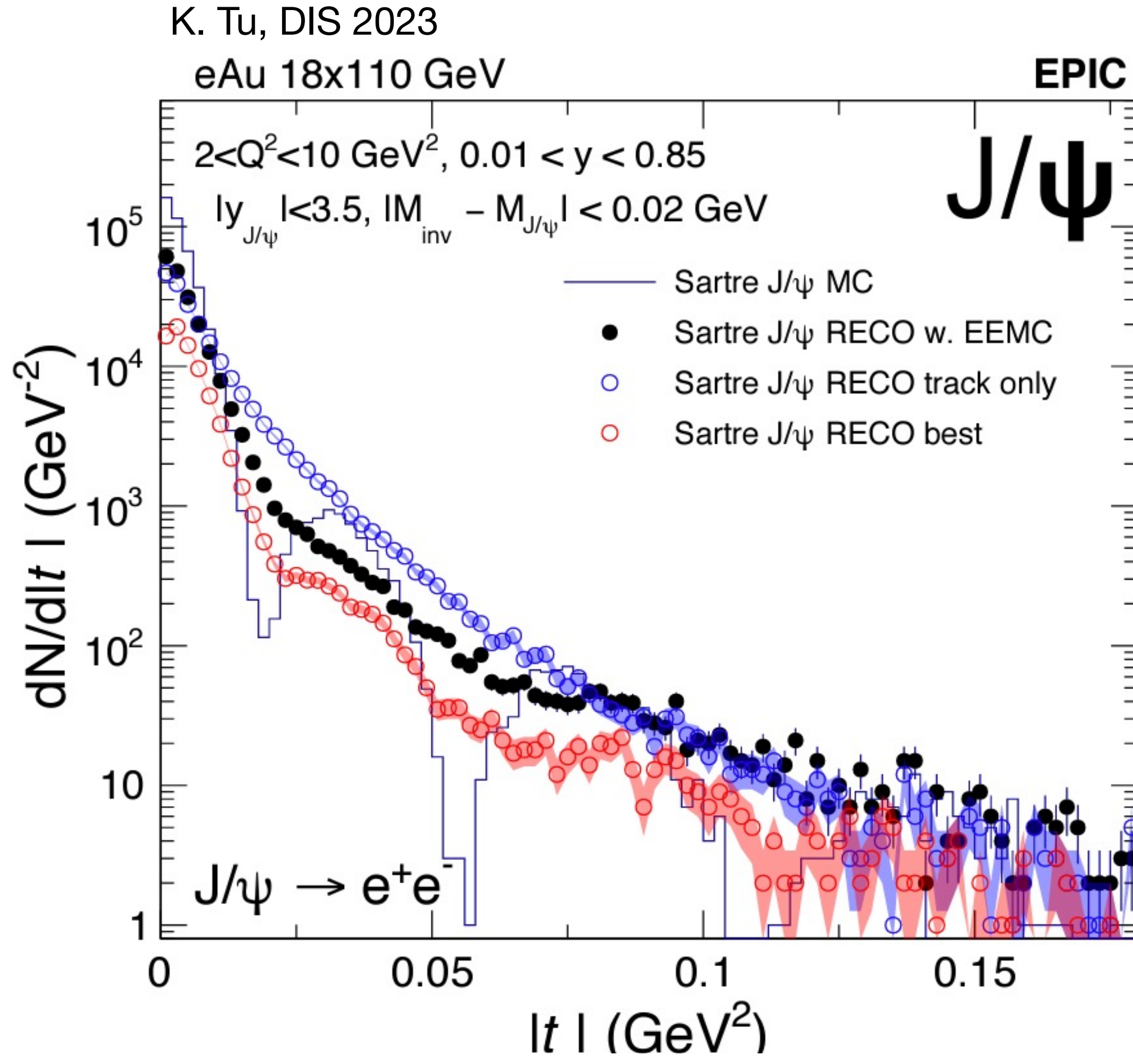
Toll, Ulrich, PRC **87** (13) 0249



→ resolving minima is crucial

- Need 90%, 99%, and > 99.8% veto efficiency for incoherent production, for the respective minima at increasing t.
- veto of events where nuclei break up
 → use entire far-forward detector systems
- Need precise determination of t reconstruction via scattered lepton and exclusively produced vector meson/photon

Exclusive measurements on nuclear targets with the EIC



Summary

EIC with ePIC can address various aspects of the nucleon and nuclear structure through:

- Precise inclusive and semi-inclusive (spin-dependent) DIS measurements via high-resolution EM calorimeters.
- Measurements for 3D (spin-dependent) tomography in momentum space provided by good Cherenkov-based and TOF AC-LGAD hadron PID detectors and tracking.
- Exclusive measurements on protons, using the far-forward detector system.
- Diffractive and exclusive measurements with coherent/incoherent separation via very precise EM calorimeters and far-forward detector system.